G3-1

ASD-TDR-62-792
VOL II

403351

AN EXPERIMENTAL INVESTIGATION OF THE SURFACE PRESSURE AND THE LAMINAR BOUNDARY LAYER ON A BLUNT FLAT PLATE IN HYPERSONIC FLOW

Vol. II. Laminar Boundary Layer Profile on the Flat Plate

TECHNICAL DOCUMENTARY REPORT NO. ASD-TDR-62-792, VOLUME II

March 1963

Flight Dynamics Laboratory
Aeronautical Systems Division
Air Force Systems Command
Wright-Patterson Air Force Base, Ohio

Project No. 1366, Task No. 136606

(Prepared under Contract No. AF 33(616)-7827 by
The Ohio State University, Columbus, Ohio;
G. M. Gregorek, T. C. Nark, J. D. Lee, authors)

NOTICES

When Government drawings, specifications, or other data are used for any purpose other than in connection with a definitely related Government procurement operation, the United States Government thereby incurs no responsibility nor any obligation whatsoever; and the fact that the Government may have formulated, furnished, or in any way supplied the said drawings, specifications, or other data, is not to be regarded by implication or otherwise as in any manner licensing the holder or any other person or corporation, or conveying any rights or permission to manufacture, use, or sell any patented invention that may in any way be related thereto.

Qualified requesters may obtain copies of this report from the Armed Services Technical Information Agency, (ASTIA), Arlington Hall Station, Arlington 12, Virginia.

This report has been released to the Office of Technical Services, U.S. Department of Commerce, Washington 25, D.C., in stock quantities for sale to the general public.

Copies of this report should not be returned to the Aeronautical Systems Division unless return is required by security considerations, contractual obligations, or notice on a specific document.

26-639M, 400, 5-1-

FOREWORD

This report was prepared by the Aerodynamic Laboratory of the Ohio State University, Columbus, Ohio on Air Force Contract AF 33(616)-7827 under Task 136606 "Hypersonic Boundary Layer Properties" on Project No. 1366 "Aerodynamics and Flight Mechanics." This Task and Project are a part of Air Force System Command's Applied Research Program, 750A, "Mechanics of Flight." The work was administered under the direction of Flight Dynamics Laboratory, Aeronautical Systems Division. Captain H. Grubbs and Mr. M. L. Buck were project engineers for the Laboratory.

The study was initiated in January, 1961, and was completed in August, 1962. The final report is in two volumes; Volume I presents the surface pressure distributions on the plate, Volume II presents the laminar boundary layer characteristics of the flat plate.

The authors wish to thank Mr. J. D. Mauersberg of the Aerodynamic Laboratory staff for his aid in the extensive analogue computer work.

This report concludes the work done by the Aerodynamic Laboratory on Contract AF 33(616)-7827.

ABSTRACT

The laminar boundary layer on unswept, 1/2-inch thick, cylindrically-blunted flat plate was examined at Mach numbers of 7, 10, 12 and 14; at Reynolds numbers from 9000 to 21,300, based on the plate thickness; and at angles-of-attack of 0°, 10° (compression) and 15° (expansion). The layer was probed at three stations, S/D = 8, 16 and 22 using a pitot probe and a sonic-pneumatic total temperature probe. The tests were conducted in the 12-inch continuous hypersonic wind tunnel of The Ohio State University Aerodynamic Laboratory.

The two probe outputs, together with the static pressure at the wall, were processed through an analogue computer and the results, i.e., Mach number, velocity, temperature, etc., are tabulated as functions of distance from the surface. Integrations were performed to obtain displacement and momentum thicknesses. Skin friction was also obtained, through the measurement of the velocity gradient at the wall.

The results are presented in tabulated form, while typical data are plotted to illustrate the trends established by Mach number, Reynolds number and angle-of-attack.

This report has been reviewed and is approved.

Philip P. Antonatos

PHILIP P. ANTONATOS
Chief, Flight Branch
Flight Dynamics Laboratory

TABLE OF CONTENTS

		Page
I	INTRODUCTION	1
II	EXPERIMENTAL EQUIPMENT	3
A.	Facility and Model	3
B.	Boundary Layer Probe	3
III	EXPERIMENTAL PROCEDURES	5
A.	Test Procedure	5
B.	Data Reduction	6
IV	RESULTS	8
A.	Boundary Layer Profiles	8
B.	Boundary Layer Thicknesses	8
C.	Skin Friction	9
V	DISCUSSION OF EXPERIMENTAL RESULTS	10
A.	Boundary Layer Profiles	10
B.	Boundary Layer Edge	11
C.	Estimate of Error	12
VI	SUMMARY	14
REFERENCES		16
APPENDIX		17

LIST OF TABLES

		Page
I	Test Conditions for Boundary Layer Surveys	19
II	Boundary Layer Profiles at M = 7	20-28
III	Boundary Layer Profiles at M = 10	29-37
IV	Boundary Layer Profiles at M = 12	38-58
V	Boundary Layer Profiles at M = 14	59-70
VI	Summary of Boundary Layer Thicknesses	71-72
VII	Summary of Skin Friction Data	73-76

LIST OF FIGURES

Figure		Page
1	The Ohio State University 12-inch Hypersonic Wind Tunnel Schematic	77
2	Dimensions of Flat Plate Model	78
3	Flat Plate Mounted in Wind Tunnel	79
4	Side View of Model and Probe in Test Cabin	80
5	Nomenclature of Boundary Layer Probe	81
6	Model and Boundary Layer Probe Dimensions	82
7	Nozzle Calibration at Model Leading Edge	83
8	Effect of Probe on Plate Pressure	84
9	Schematic of the Probe System	85
10	Boundary Layer on Plate at $\alpha = 0^{o}$ for $M_{\infty} = 7$ and $Re_D = 6,900$	86
11	Boundary Layer on Plate at $\alpha = 0^{o}$ for $M_{\infty} = 10$ and $Re_D = 11,000$	87
12	Boundary Layer on Plate at $\alpha = 0^{o}$ for $M_{\infty} = 12$ and $Re_D = 12,650$	88
13	Boundary Layer on Plate at $\alpha = 0^{o}$ for $M_{\infty} = 14$ and $Re_D = 16,100$	89
14	Boundary Layer on Plate at Low Reynolds Number for $M_{\infty} = 12$, $\alpha = 0^{o}$, $Re_D = 8,700$	90
15	Boundary Layer on Plate at High Reynolds Number for $M_{\infty} = 12$ and $Re_D = 19,350$	91
16	Boundary Layer on Plate at Angle of Attack (10^{o} Comp.) for $M_{\infty} = 10$ and $Re_D = 11,000$	92
17	Boundary Layer on Plate at Angle of Attack (15^{o} Exp.) for $M_{\infty} = 10$ and $Re_D = 11,000$	93
18	Effect of Mach Number 7, 10, 12 on Boundary Layer at $\alpha = 0^{o}$ and S/D = 16.4	94

Figure		Page
19	Effect of Mach Number 12, 14 on Boundary Layer ($\alpha = 0^o$) at S/D = 16.4	95
20	Effect of Reynolds Number on Boundary Layer at $M_\infty = 12$, $\alpha = 0^o$ and S/D = 16.4	96
21	Effect of Angle of Attack on Boundary Layer at M = 7, S/D = 16.4 and Re_D = 6,900	97
22	Effect of Angle of Attack on Boundary Layer at M = 14, S/D = 16.4 and Re_D = 16,100	98
23	Boundary Layer Thicknesses, $M_\infty = 7$	99
24	Boundary Layer Thicknesses, $M_\infty = 10$	100
25	Boundary Layer Thicknesses, $M_\infty = 12$	101
26	Boundary Layer Thicknesses, $M_\infty = 14$	102
27	Stagnation Pressure Ratio vs x	103
28	Skin Friction Coefficient vs x	104
29	Error Analysis - Mach No. and Velocity	105
30	Error Analysis - Static and Total Temperature	106
31	Error Analysis - $\rho u/\rho_1 u_1$ and $\rho u^2/\rho_1 {u_1}^2$	107

Figure		Page
19	Effect of Mach Number 12, 14 on Boundary Layer ($\alpha = 0^o$) at S/D = 16.4	95
20	Effect of Reynolds Number on Boundary Layer at $M_\infty = 12$, $\alpha = 0^o$ and S/D = 16.4	96
21	Effect of Angle of Attack on Boundary Layer at M = 7, S/D = 16.4 and $Re_D = 6{,}900$	97
22	Effect of Angle of Attack on Boundary Layer at M = 14, S/D = 16.4 and $Re_D = 16{,}100$	98
23	Boundary Layer Thicknesses, $M_\infty = 7$	99
24	Boundary Layer Thicknesses, $M_\infty = 10$	100
25	Boundary Layer Thicknesses, $M_\infty = 12$	101
26	Boundary Layer Thicknesses, $M_\infty = 14$	102
27	Stagnation Pressure Ratio vs x	103
28	Skin Friction Coefficient vs x	104
29	Error Analysis - Mach No. and Velocity	105
30	Error Analysis - Static and Total Temperature	106
31	Error Analysis - $\rho u/\rho_1 u_1$ and $\rho u^2/\rho_1 u_1{}^2$	107

LIST OF SYMBOLS

Symbols		Dimensions
$\dot{m}$	Mass flow rate	slugs/sec
q	Dynamic pressure	lbs/ft^2
u	Velocity	ft/sec
x	Axial distance from model leading edge	inches
y	Distance above plate	inches
D	Diameter of model leading edge	ft
M	Mach number	--
P	Pressure	mm Hg or lb/ft^2
S	Surface distance from model leading edge	ft
T	Temperature	^oR
Re_D	Reynolds number = $\frac{\rho u D}{\mu}$	--
A_1^*/A_2^*	Ratio of throat areas in sonic probe	--
α	Angle-of-attack	Degrees
δ	Boundary Layer thickness	inches
δ^*	Boundary layer displacement thickness, Eq. (3)	inches
ρ	Density	$slugs/ft^3$
μ	Viscosity	$lb\ sec/ft^2$
θ	Boundary layer momentum thickness, Eq. (4)	inches
τ	Shearing stress, Eq. (5)	lb/ft^2

SUBSCRIPTS

Subscript	
1	Condition at the inviscid surface streamline
2	Condition behind the normal shock
$2n$	Condition behind the normal shock at stagnation point of model
3	Condition at the second throat of sonic probe
0	Condition in the stagnation tank
s	Static condition
t	Total condition
w	Condition at the wall
δ	Condition at outer edge of boundary layer
∞	Condition in the free stream

SECTION I

INTRODUCTION

There is presently a great need for detailed information about the flow fields surrounding blunt bodies moving at hypersonic speeds. A variety of theoretical approaches have been proposed for the prediction of surface pressures, skin friction heat transfer, and flow field temperature but experimental verification is lacking in many instances. This study was undertaken to provide information about the surface pressures and the nature of the boundary layer on an unswept blunt flat plate and the results are reported in two volumes.

The flat plate had a cylindrical leading-edge 1/2-inch in diameter. It was side-mounted, fully spanning the semi-free jet of the wind tunnel in order to depress interference from the support and from the tunnel walls. Pressure orifices were arranged in three streamwise rows and thermocouples were embedded under the surface. No forced cooling was provided, but radiation and conduction maintained the model temperatures well below recovery temperature. In order to obtain more detailed information about the pressures on the leading-edge, separate cylindrical models were also tested.

Experiments were conducted at nominal Mach numbers of 7, 10, 12 and 14 with the Reynolds number (based on the leading-edge diameter) ranging from 9000 to 21,300. Boundary layer data were obtained for angles-of-attack of 0°, 10° (compression) and 15° (expansion) at three stations along the plate centerline. Table I lists the test conditions.

This part of the report (Volume II) deals exclusively with the measurements made throughout the boundary layer on the surface of the flat plate. These were obtained through the use of a pitot probe and a sonic-pneumatic total temperature probe, combined with simultaneous measurements of the surface static pressures and the surface temperatures. On-line data recording and partial reduction were accomplished with an analogue computer. Final data include profiles of velocity, Mach number, total temperatures, static temperature, mass flow rate and momentum flux. The last two were integrated to obtain the displacement thickness and the momentum thickness.

- - - - - - - -

Manuscript released by authors 12 September 1962 for publication as an ASD Technical Documentary Report.

The skin friction was also calculated from the velocity gradient at the surface.

The facility, model, probes and instrumentation are briefly described and the results from the many tests are tabulated. Representative data were selected and plotted to illustrate the effects of Mach number, Reynolds number and angle-of-attack. Since this study was experimental in nature, no analysis of the data is included here. Rather, there is a discussion of the testing techniques and of the possible errors involved. Tunnel interference, especially at high angles-of-attack and at low Reynolds numbers, prevented the acquisition of complete data in some instances.

Volume I describes the surface pressure distributions obtained on the plate and its leading-edge through the angle-of-attack range $\pm 15^{\circ}$.

II EXPERIMENTAL EQUIPMENT

A. Facility and Model

In References 3 and 4, the pertinent features of the wind tunnel used in this study are described. It is a continuous-flow, electrically-heated tunnel having a 12-inch diameter free-jet test region. Axisymmetric, contoured nozzles provide a Mach number range from 6 to 15. Figure 1 is a schematic diagram of the facility and associated equipment.

The flat plate model was fabricated from stainless steel, spanned the jet and was side-mounted for minimum support interference. The basic dimensions of the plate are given in Figure 2. Three streamwise rows of pressure orifices, 0.060" in diameter, and two rows of chromel-alumel thermocouples provided detailed pressure and temperature distributions on the plate. All the pressure leads, of 3/32" OD stainless steel tubing, passed through the hollow side mount to inclined manometers utilizing silicone fluid. The thermocouple leads followed a similar path to multi-point temperature recorders. For angle-of-attack changes, the model could be rotated about its leading-edge; for easing tunnel starts, the model could be retracted from the jet when at zero angle-of-attack.

The model is shown mounted in the wind tunnel in Figure 3, a view from the nozzle end. Surrounding the test region is the cylindrical diffuser scoop. Above the model is the traversing impact probe for Mach number calibration of the nozzle; below the model is the boundary layer probe in its stowed position. Figure 4 is a side view of the test cabin of the tunnel showing the flat plate and the boundary layer probe retracted away from the model.

B. Boundary Layer Probe

The boundary layer probe actually consisted of two probes, a pitot probe to measure total pressure in the boundary layer, and a sonic-pneumatic probe to determine the total temperature in the layer. The pitot probe is a standard device; however, further comments on the total temperature probe are required.

The operation of a sonic-pneumatic total temperature probe may be explained with reference to Figure 5. A sample of the heated gas is taken through the first choked throat, cooled to an acceptable and lower temperature and then

choked again at a second throat. For equality of mass flows at the two throats, in terms of total quantities,

$$\dot{m} = k \frac{P_{t2} A_1^*}{\sqrt{T_{t2}}} = k \frac{P_{t3} A_2^*}{\sqrt{T_{t3}}} \tag{1}$$

where k depends on the ratio of specific heats and the nature of the gas and is considered as a constant here. Solving Eq. (1) for the stream total temperature, T_{t2},

$$T_{t2} = \left[\frac{P_{t2}}{P_{t3}} \frac{A_1^*}{A_2^*} \right]^2 T_{t3} \tag{2}$$

Thus the total temperature can be calculated if the total pressures at the two throats are measured, the total temperature at the second throat determined, and if the ratio of the throat areas is known.

In Reference 5, Welshimer reports a thorough study of the sonic-pneumatic probe for wind-tunnel use and points out that an extensive calibration is generally required when the application is in moderately low density flows. Then the boundary layers in the throats produce sizeable displacements and the "effective" area ratio for equation (2) may be appreciably different from the physical area ratio. Reference 6 reports the details of the development study involved with the probe used here. By using a wide-angle conical inlet, the internal boundary layer effects were resolved to be almost entirely pressure-dependent, a feature which eased the calibration problem considerably.

The dimensions of the probe tips are given in Figure 6. The probe system was mounted on the tunnel attack-mechanism so that it pivoted about the leading-edge of the model. Thus data could be taken for several angles-of-attack during one tunnel run. The position of the probe relative to the plate was determined through the use of a precision potentiometer attached to the probe mount.

III EXPERIMENTAL PROCEDURES

A. Test Procedure

In order to maintain a near-similarity of flow in the boundary layer, the test conditions were selected to maintain equal stagnation temperatures and equal pressures behind the bow shock for different Mach numbers. The exact test conditions are listed in Table I. Prior to each test series, the nozzle flow was calibrated at the position of the model leading edge; typical calibrations are presented in Figure 7.

After the tunnel was started, and the test conditions reached, the model was inserted in the stream and positioned at the desired angle-of-attack. The probe was brought near the plate, but outside the boundary layer, and a check calibration of the temperature probe was made. The probe was then moved to the plate surface and the surface pressure in the vicinity of the probe observed on silicone manometers. If any probe interference was detected, the probe was moved away from the plate until the pressure distribution returned to normal. In general, there was little or no interference on the surveys taken with the plate at zero angle-of-attack or on compression; however, with the plate on expansion the insertion of the probes caused separation of the boundary layer in many cases as the probes approached the plate. In these cases, the first few hundredths of an inch could not be examined. Figure 8 shows typical surface pressure distributions obtained with the boundary layer probe on the plate surface and with it far from the plate; it indicates the moderate pressure disturbance caused by the probe when on the surface.

With the probe in position, the pressures P_{t_2} and P_{t_3} were sensed on variable reluctance pressure transducers and fed into the Laboratory's Electronic Associates analogue computer The position of the probe and T_{t_3} were also fed into the computer which then plotted the total pressure and total temperature at that probe location. The probe was moved to its next position and the process repeated. While a continuous trace of the boundary layer profile might have been desirable, it was not possible because of the low total pressure encountered near the wall. As the response of the P_{t_3} measurement was of the order of one minute, the stepping process was required to allow sufficient time for stabilization of the pressures.

To provide further on-the-line data, an estimate of the plate surface pressure at the probe location, as determined in the previous test reported in Volume I, was also fed into the computer. Under the assumption of a constant static pressure, the Mach number, the static temperature and the velocity were then calculated, printed and plotted simultaneously by the computer. A schematic of the probe data reduction system is presented in Figure 9. For convenience, the basic equations used in the computer program are reviewed in the Appendix and further details of the analogue computer used in the program are available in Reference 7.

During the survey, the wall temperatures were recorded and the surface pressures near the probe were measured on the inclined manometers. A typical boundary layer survey required about 20 minutes to complete; it was possible to examine at least two angles-of-attack for one station during each tunnel run.

B. Data Reduction

After the tunnel run, the raw data was reprocessed through the computer. For this final reduction, small zero shifts in the transducers, which were check calibrated before and after each run, were eliminated and the actual static pressure measured at the probe station during the test was inserted into the computer.

Six important boundary layer quantities were plotted against distance from the plate at this time:

Total temperature	T_t
Mach number	M
Static temperature	T_s
Velocity	u
Mass flow per unit area	ρu
Momentum flow per unit area	ρu^2

The last two items were obtained for integration of their profiles to determine the boundary layer displacement and momentum thicknesses. These six quantities were also recorded on the digitizer along with dimensionless ratios of velocity, density, etc.

For these dimensionless ratios, a question arose as to what reference quantities should be chosen. Since there was a relatively high entropy gradient in the inviscid flow, the edge of the boundary layer was often difficult to determine and, in any case, conditions there were altered by the changes in the boundary layer thickness at different test conditions. The most reasonable reference condition appeared to be that given by the "inviscid surface streamline" i.e., with the measured surface pressure, the stagnation pressure behind the leading edge normal shock wave and the stagnation temperature in the stream. Conditions determined on this basis are designated by the subscript 1 and are used as reference conditions for local boundary layer properties. If other quantities are desired for reference, they can be determined from the tabulated data or from the plotted data. It should be noted that, with the chosen reference conditions, the edge of the boundary layer is no longer defined by, say $u/u_1 = 1$; in fact, the edge is probably best estimated by reference to the total temperature profile.

IV RESULTS

A. Boundary Layer Profiles

The detailed data obtained for each of the boundary layer profiles are grouped by Mach number and presented in Tables II, III, IV and V. Selected profiles, illustrating the nature of the boundary layer on the plate are given in Figures 10 through 22.

The development of the boundary layer on the plate at zero angle-of-attack is shown in Figures 10, 11, 12 and 13 for the four nominal Mach numbers tested. Total conditions behind the normal shock are nearly matched for the nominal Mach numbers of 7 and 10 and are of the same order for nominal Mach numbers of 12 and 14. Figures 14 and 15 show the influence of Reynolds number on the layer at Mach number 12 for the plate at zero angle-of-attack. The effects of angle-of-attack may be seen by comparing Figures 16 and 17 which show data for 10° compression and 15° expansion, respectively, at a Mach number of 10 and a constant Reynolds number. Interference effects previously described prevented the acquisition of data at the downstream station when on expansion. Figure 18 compares profiles at $S/D = 16$ and $\alpha = 0$ for Mach numbers of 7, 10 and 12 while Figure 19 compares similar data for Mach numbers of 12 and 14. The influence of Reynolds number is illustrated in Figure 20 for $M = 12$ and $S/D = 16$. The effects caused by angle-of-attack are shown in Figures 21 and 22 for Mach numbers of 7 and 14 respectively.

B. Boundary Layer Thicknesses

The profiles of ρu and ρu^2 obtained from the data reduction procedure were integrated to determine the boundary layer displacement and momentum thicknesses. Using the inviscid surface streamline as the reference, the displacement thickness is taken as

$$\delta^* = \delta - \int_0^{\delta} \frac{\rho u}{\rho_1 u_1}\, dy \tag{3}$$

and the momentum thickness is taken as

$$\theta = \int_0^{\delta} \frac{\rho u}{\rho_1 u_1}\, dy - \int_0^{\delta} \frac{\rho u^2}{\rho_1 u_1^2}\, dy \tag{4}$$

Inherent in these integrations is the determination of the boundary layer, δ. Because of the rotational field above the layer, the velocity above the layer can have a gradient, which at some conditions and especially at expansion angles, made the estimate of δ difficult. However, since the stream gradients are low compared with those in the boundary layer, the values of δ^* and θ were generally found to be relatively insensitive to the choice of δ.

The results of the integrations are summarized in Table VI. Data from this table, indicating the growth of the boundary layer thicknesses along the plate at the four Mach numbers, are plotted in Figures 23, 24, 25 and 26.

The stagnation pressure at the edge of the boundary layer, Pt_δ, is of interest in many applications; hence, this quantity is also included in Table VI. A summary plot of the stagnation pressure ratio, $Pt_\delta/Pt2_n$, for a portion of the test conditions is given in Figure 27. The determination of this quantity is, of course, subject to the estimate of the location of the boundary layer edge.

C. Skin Friction

An extrapolation of the velocity profiles to zero velocity at the wall was made to allow calculation of the wall skin friction. Measurement of the velocity gradient at the wall gave an estimate of the skin friction, τ , through the expression:

$$\tau_w = \mu_w \left[\frac{du}{dy}\right]_w \tag{5}$$

where μ_w is the viscosity of air at the surface temperature and calculated using Sutherland's relation. The skin friction was non-dimensionalized to coefficient form by dividing by the free stream dynamic pressure, i.e.

$$C_f = \frac{\tau_w}{1/2\ \rho_\infty\ u^2_\infty} \tag{6}$$

Table VII lists the skin friction information. Figure 28 indicates the trends of the skin friction coefficient with angle-of-attack for Mach numbers 7 and 10.

V DISCUSSION OF EXPERIMENTAL RESULTS

A. Boundary Layer Profiles

The profiles presented in Figures 10 to 22 are intended to illustrate the development of the boundary layer under the various test conditions utilized. Two comments are important in the interpretation of these profiles:

(1) The wall temperatures for the three profiles shown along the plate do not necessarily match the wall temperature distributions of the plate at the time of the surveys.

(2) The Mach number distribution shown above the boundary layer is not the true Mach distribution existing above the layer.

The first comment is the result of the testing technique. Because of a tunnel running time limit of approximately 90 minutes, it was not possible to wait for the equilibrium wall temperature to be reached before beginning a survey. Therefore, after a nominal wait for the wall temperature to exceed some value, say 750°R, the survey was begun; upon completion, the angle-of-attack was changed and another survey was started. The wall temperature may have increased to 800°R by the start of the second survey. It is therefore possible, that if the profile at S/D = 8 was the first to be taken during a tunnel run and if the profile at S/D = 16 was the second of a test series, the wall temperatures tabulated might suggest an increase with S/D, when in reality the reverse is true. It is pointed out that the cases where the wall temperature varied more than 150°R are rare; in general, variation of wall temperature during a survey was less than 100°R.

The second comment results from the data reduction procedure in which a constant static pressure normal to the plate was assumed. For the thick boundary layers encountered and the known fact of moderate streamwise pressure gradients, it is likely that the assumption is inexact. Then the Mach number as calculated has some degree of error at the edge of the boundary layer. This difficulty could be resolved only by the measurement of local static pressure at all points within the boundary layer, for which there is no reliable instrumentation at these test conditions.

B. Boundary Layer Edge

For certain test conditions, the estimate of the edge of the boundary layer was difficult. This estimate was chiefly based on the deviation of the total temperature from the temperature of the inviscid stream while also considering the Mach number and velocity profiles. Admittedly, some judgement was required, particularly at expansion angles-of-attack.

As the value of δ, the upper limit of the integrations of Eqs. (3) and (4), determines δ^* and θ as well as the total pressure ratio $P_{t\delta}/P_{t2_n}$, it is prudent to examine the effect of an improper choice of δ. Integration of typical ρu and ρu^2 profiles at different δ indicates that a 10% error in the choice of δ will yield about a 3% error in δ^* and θ. As an error of this magnitude in δ is unlikely, errors in δ^* and θ are probably due to inaccuracies in the layer profiles and not due to a poor estimate of the layer edge.

A similar observation of the ratio $P_{t\delta}/P_{t2_n}$ may be made. the low gradient boundary layers at expansion angles which make estimation of δ difficult also have small variations of P_{t2}; hence, a moderate error in δ does not have a strong effect on the total pressure ratio.

With regard to this ratio, it is interesting to note that even at S/D = 22 and angle-of-attack of 10^o compression, $P_{t\delta}/P_{t2_n}$ remains relatively close to unity. However, at expansion angles $P_{t\delta}/P_{t2_n}$ is appreciably below unity. This surprising result is probably a consequence of the assumption of a constant static pressure through the layer. $P_{t\delta}$ was determined from the normal shock relations at the Mach number calculated from P_w/P_{t2}; therefore, if P at the outer edge of the layer is actually lower than wall pressure, the Mach number at the edge would increase, causing $P_{t\delta}$ to increase.

An estimate was made of the required decrease in static pressure at the boundary layer edge needed to bring $P_{t\delta}/P_{t2_n}$ to unity. For most cases a decrease of but 0.10 mm Hg would suffice. This small pressure change is possible through the thick layers existing at these expansion angles, hence the true value of $P_{t\delta}/P_{t2_n}$ is believed to be close to unity at these angles. The statement indicates that a sizeable amount of the fluid entering the boundary layer has passed through the normal portion of the bow shock.

C. Estimate of Error

In an experimental study, the influence of measuring errors on the data must be considered. As discussed previously, the profiles are generated by measuring P_{t2}, P_{t3}, and T_{t3} and having the A_1^*/A_2^* calibration of the total temperature probe. The calibration of the temperature probe was quite extensive and since a calibration point was taken at the start of each test, the area ratio dependence on Reynolds number was adequately determined. The details of these calibrations are discussed in References 5 and 6; hence, the present discussion will be limited to errors due to improper pressure and temperature measurement.

After passing through the probe's heat exchanger, the inducted gas is near room temperature. Standard thermocouple techniques will indicate the temperature within $\pm$ 2°R. From Eq. (2), this will result in a small error of less than $\pm$ 1/2%.

The greatest possibility for errors occurring in the data comes from the pressure measurements, P_{t2} and P_{t3}. The stagnation pressure at the second throat, P_{t3}, is especially susceptible to error, as its magnitude is lower by a factor of ten from P_{t2}. Some estimates of the pressure experienced by the probe are provided to enable a more complete analysis.

The total pressure behind the normal shock, P_{t2}, varied greatly through the boundary layer, for the conditions tested, ranging from approximately 20 mm Hg to about 0.5 mm Hg. To span this range with the greatest accuracy, two transducers with maximum ranges of 25 mm Hg and of 5 mm Hg were connected in parallel; when P_{t2} dropped below 5 mm Hg, the lower range pressure pickup was used. The variable reluctance type transducers used are accurate to within 1/2% of the full scale; and with proper calibration, have exceeded this performance standard. With the system used, the error in P_{t2} measurement is generally less than 1%; near the wall, however, errors can approach 5% for some selected low pressure conditions.

The pressure drop between the throats of the temperature probe was of the order of 10. Therefore, the range of pressures experienced by P_{t3} was from 2 mm Hg to 0.05 mm Hg. A 5 mm Hg full scale transducer was used to obtain P_{t3} and was calibrated continuously. A dispersion of $\pm$ .020 mm Hg about the linear calibration curve was obtained during these checks. This comparatively small error band on the full scale value of the transducer can create a sizeable error at the low values of P_{t3}.

The influence of these pressure errors is indicated in Figures 29, 30, and 31, for a typical profile at $M = 10$ and $\alpha = 0^o$. Mach number, as determined from the P_{t2} measurement and the static pressure at the wall is known within 1%. The maximum error in the total temperature profile as determined by a 1% error in P_{t2} and a simultaneous opposing .025 mm Hg error in P_{t3} is presented in Figure 30 by the dotted line. As the wall is approached, the low measured pressures drastically influence this maximum error band. A more probable error band is shown shaded, based on the fact that wall temperature was known accurately. The maximum and more probable error bands are also shown for the velocity and static temperature profiles, as well as the ρu and ρu^2 profiles which will be discussed presently.

Of importance in the static temperature profile is the possible variation in the temperature gradient at the wall, $(dT/dy)_w$. With the larger error band in this region, these profiles should not be used for direct heat transfer estimates. However, it may be noted that the velocity profile is not so strongly affected. Consequently, with the knowledge of zero velocity at the wall, the gradient may be determined and skin friction estimated. A maximum error of slightly more than $\pm$ 10% may be expected in this velocity gradient based on pressure and temperature deviations. This velocity gradient at the wall is also a function of the accuracy of the probe location measurement; an estimated precision of $\pm$ .01 inch is used for this quantity. The skin friction, τ, as determined from Eq. (5) is estimated to be within $\pm$ 15%.

Also subject to error, if the profiles are in error, are the boundary layer thicknesses δ^* and θ. Figure 31 presents the maximum errors in $\rho u/\rho_1 u_1$ and $\rho u^2/\rho_1 u_1^2$. When these profiles are integrated, deviations of $\pm$ 15% in δ^* and θ are found.

Summing up this analysis, the probable errors should give tabulated values within the following range of accuracy:

Measured Quantities:	Calculated Quantities
P_{t2} $\pm$ 1% up to 5% near wall	δ^* $\pm$ 15%
P_{t3} $\pm$ 1% up to 20% near wall	θ $\pm$ 15%
T_{t3} $\pm$ 1%	τ $\pm$ 15%
T_t $\pm$ 3% up to 20% near wall	
δ $\pm$ .02 inch	

VI SUMMARY

The results of more than fifty surveys of the boundary layer on a blunted flat plate in hypersonic flow have been presented for a wide range of test conditions. Nominal Mach numbers of 7, 10, 12 and 14 have been examined for free stream Reynolds numbers ranging from 9000 to 21,300 at S/D = 8.3, 16.4, 22.5 and at angles-of-attack of 10° compression, 0°, and 15° expansion. All the results have been tabulated and appropriate summary plots made to illustrate the trends concerning Mach number, Reynolds number, and angle-of-attack effects upon the boundary layer development.

The results of this completely experimental investigation can be summarized as follows:

(1) The surveys indicate a laminar boundary layer existed on the plate at all conditions examined. Moderate velocity gradients above the layer required some degree of judgement in the establishment of the boundary layer edge.

(2) The boundary layer profiles were derived from a total pressure probe and a total temperature probe. The precisior of the profiles near the plate was affected by the accuracy of the total temperature probe. The static temperature profile should not be used to determine heat transfer rates directly; however, the velocity profile is not so strongly influenced by the total temperature error and can be used to estimate skin friction. Values of skin friction are tabulated and a portion of these, plotted.

(3) The generated profiles of ρu and ρu^2 vs location from the plate have been integrated from $y = 0$ to $y = \delta$. Boundary layer displacement thickness, δ^*, and momentum thickness, θ, respectively, have been determined from these integrations with moderate precision. The discrepancies in δ^* and θ are caused by profile deviations, rather than by errors in the estimate of δ.

(4) The ratio of total pressure at the boundary layer edge to total pressure behind the normal shock at the nose has been tabulated. This ratio is approximately unity, at $\alpha = 0$ and at $\alpha = 10^\circ$ compression. For the expansion angles, the assumption of a slight pressure gradient also results in a pressure ratio of unity.

(5) Care must be taken when correlating these data since the wall temperature distribution has a strong influence upon the profiles and this parameter could not be duplicated consistently.

REFERENCES

1. Gregorek, G. M., Nark, T. C., and Lee, J. D., An Experimental Investigation of the Surface Pressure and the Laminar Boundary Layer on a Blunt Plate in Hypersonic Flow: Volume I, ASD-TDR-62-792, September 1962

2. Nark, T. C., Theory of the Compressible Laminar Boundary Layer under Arbitrary Pressure and Temperature Gradients, ASD-TDR-62-962, Aeronautical Systems Division, June 1962

3. Thomas, R. E., and Lee, J. D., The Ohio State University 12-inch Hypersonic Wind Tunnel, TN(ALOSU)559-2; The Ohio State University Research Foundation, Technical Report to WADC on Contract AF 33(616)-5593, July 1959

4. Lee, J. D., Axisymmetric Nozzles for Hypersonic Flow TN(ALOSU)459-1 The Ohio State University Research Foundation, Technical Report to WADC on Contract AF 33(616)-5593, July 1959

5. Welshimer, D. E., The Experimental Application of Sonic-Pneumatic Probe Systems to Temperature Measurement in a Hypersonic Air Stream, ARL 62-364 Aeronautical Research Laboratories, Office of Aerospace Research, USAF, June 1962

6. Lee, J. D., Measurement of Velocity and Temperature in a Hypersonic Laminar Boundary Layer, ASD-TDR-62-914, September 1962

7. Mauersberg, J. D., Thomas, R. E., and Lee, J. D., An Investigation of the Accuracy of the Analog Computer, TN(ALOSU)-759-4; The Ohio State University Research Foundation, Technical Report to Douglas Aircraft Co., on Contract T and M-5637-A, October 1959

APPENDIX

COMPUTER PROGRAM

The analogue computer provided partial on-the-line data reduction during the actual surveys; this monitoring of the raw data helped determine both probe performance and aided detection of any tunnel or probe interference effects. Variable inputs to the computer were Pt_2, Pt_3, and probe position; Tt_3, P, and $A_1{}^*/A_2{}^*$ were relatively constant and were set into the computer manually.

The two key parameters which were immediately determined, were the total temperature and the Mach number. The equation used to obtain the total temperature was the sonic-pneumatic probe relation:

$$T_t = \left[\frac{Pt_2}{Pt_3}\ \frac{A_1{}^*}{A_2{}^*}\right]^2 T_{t_3} \qquad \text{A-1}$$

The Mach number was found from the ratio of Pt_2 and P, the wall surface pressure, from the applicable expression below:

for $1 \leq M \leq 5$

$$M^2 = -\ 0.4026 + 0.7807\ \frac{Pt_2}{P_1} - 0.000\ 2027\left[\frac{Pt_2}{P_1}\right]^2 \qquad \text{A-2}$$

for $0 \leq M \leq 1$

$$M^2 = -\ 1.705 + 2.037\ \frac{Pt_2}{P_1} - 0.3279\left[\frac{Pt_2}{P_1}\right]^2 \qquad \text{A-3}$$

These simple Mach number relations are approximations which were easily handled by the computer, determining M within 1% in the ranges shown.

From Equations A-1 and either A-2 or A-3 the remainder of the required data is obtained from the well known standard equations; i.e.,

$$T = T_t \left[1 + \frac{\gamma-1}{2}\ M^2\right]^{-1} \qquad \text{A-4}$$

$$u = M\sqrt{\gamma RT} \qquad \text{A-5}$$

$$\rho = \frac{P}{RT} \qquad \text{A-6}$$

The ratio of specific heats, γ, is here taken as 1.4 for air at the test temperatures.

The computer then performed the appropriate steps to deliver the final reduced data in terms of the dimensionless ratios $\frac{u}{u_1}$, $\frac{\rho u}{\rho_1 u_1}$, $\frac{\rho u^2}{\rho_1 u_1^2}$. These data were recorded in digitized form.

TABLE I

Test Conditions for Boundary Layer Surveys

M	$T_o \sim {}^oR$	$P_o \sim$ psig	$P_{t_2} \sim$ mm Hg	$Re/\ell \sim$ per ft.	Re_D
6.95	2060	44	45.18	1.657×10^6	0.690×10^4
9.99	2060	292	45.60	2.634×10^6	1.097×10^4
12.08	2060	325	20.50	2.077×10^6	0.865×10^4
12.26	2060	500	29.00	3.037×10^6	1.265×10^4
12.36	2060	800	44.12	4.645×10^6	1.935×10^4
14.20	1910	700	19.93	3.058×10^6	1.274×10^4
14.28	1910	900	24.76	3.858×10^6	1.607×10^4

TABLE II

Boundary Layer Data, M = 7

Test No. 7-1

$M = 6.95$ $Re_D = 6900$ $\alpha = 15^{\circ}$ Exp $S/D = 8.3$ $x = 4.0''$

$T_w = 1072^{\circ}R$ $P_{t_{2n}} = 45.2$ mm Hg $u_1 = 4136$ $\rho_1 u_1 = 7.862 \times 10^{-3}$ $\rho_1 u_1^2 = 32.52$ psf

Y-inches	M	u(fps)	T_t-°R	T_s-°R	$\frac{\rho u}{\rho_1 u_1}$	$\frac{\rho u^2}{\rho_1 u_1^2}$	$\frac{u}{u_1}$	P_{t_2} - mm Hg
.68	3.351	4145	2064	635	1.006	1.010	1.001	11.43
.63	3.335	4138	2066	640	0.998	0.998	0.999	11.31
.58	3.317	4135	2073	646	0.988	0.990	0.999	11.21
.53	3.297	4114	2054	646	0.981	0.977	0.993	11.07
.48	3.259	4079	2044	653	0.965	0.953	0.985	10.81
.43	3.182	4050	2043	673	0.928	0.910	0.978	10.35
.38	3.035	3947	1985	704	0.868	0.828	0.953	9.45
.33	2.789	3732	1888	746	0.775	0.700	0.901	8.05
.28	2.430	3441	1810	835	0.640	0.531	0.830	6.20
.23	1.995	3015	1706	954	0.488	0.357	0.728	4.28
.18	1.526	2472	1583	1090	0.349	0.209	0.597	2.67
.13	1.147	1916	1457	1163	0.255	0.117	0.460	1.66
.08	0.810	1345	1301	1142	0.184	0.060	0.325	1.18
.02	0.651	1054	1179	1086	0.152	0.038	0.254	1.02

TABLE II (CONTINUED)

Test No. 7-2

$M = 6.95$ $Re_D = 6900$ $\alpha = 15^\circ$ Exp $S/D = 16.4$ $x = 8.04$

$T_w = 1057^\circ R$ $P_{t_{en}} = 45.2$ mm Hg $u_1 = 4199$ $\rho_1 u_1 = 6.668 \times 10^{-3}$ $\rho_1 u_1^2 = 28.00$ psf

Y-inches	M	u(fps)	T_t-°R	T_s-°R	$\frac{\rho u}{\rho_1 u_1}$	$\frac{\rho u^2}{\rho_1 u_1^2}$	$\frac{u}{u_1}$	P_{t_2}- mm Hg
.90	3.347	4156	2059	640	0.916	0.907	0.988	8.88
.86	3.326	4155	2070	650	0.906	0.896	0.988	8.78
.81	3.284	4096	2033	649	0.896	0.874	0.974	8.57
.76	3.227	4079	2042	664	0.870	0.844	0.970	8.30
.71	3.125	4013	2012	685	0.832	0.793	0.955	7.81
.66	3.006	3928	1976	710	0.781	0.730	0.934	7.21
.61	2.820	3800	1947	757	0.713	0.644	0.904	6.40
.56	2.604	3632	1901	810	0.637	0.551	0.864	5.50
.51	2.400	3433	1826	855	0.571	0.465	0.819	4.70
.46	2.147	3180	1766	915	0.494	0.374	0.756	3.83
.31	1.428	2353	1583	1135	0.293	0.165	0.560	1.86
.26	1.178	1967	1455	1147	0.242	0.113	0.465	1.37
.21	0.940	1569	1353	1154	0.194	0.072	0.373	1.06
.16	0.748	1199	1192	1070	0.079	0.046	0.285	0.86

TABLE II (CONTINUED)

Test No. 7-3

$M = 6.95$ $Re_D = 6900$ $\alpha = 10^\circ$ Exp $S/D = 22.5$ $x = 11.13$

$T_w = 1060^\circ R$ $P_{t_{2n}} = 45.2$ mm Hg $u_1 = 4219$ $\rho_1 u_1 = 6.388 \times 10^{-3}$ $\rho_1 u_1^2 = 26.95$ psf

Y-inches	M	u(fps)	T_t-°R	T_s-°R	$\frac{\rho u}{\rho_1 u_1}$	$\frac{\rho u^2}{\rho_1 u_1^2}$	$\frac{u}{u_1}$	P_{t_2} - mm Hg
1.09	3.530	4250	2071	602	0.971	0.977	1.007	9.22
1.00	3.499	4250	2088	614	0.951	0.960	1.007	9.04
0.90	3.418	4177	2039	621	0.925	0.917	0.990	8.65
0.80	3.287	4112	2035	653	0.867	0.847	0.974	8.01
0.70	3.054	3949	1959	693	0.781	0.730	0.935	6.95
0.60	2.693	3710	1910	792	0.647	0.570	0.879	5.48
0.55	2.499	3608	1931	870	0.572	0.488	0.854	4.74
0.50	2.264	3421	1892	946	0.497	0.404	0.810	3.96
0.45	2.027	3218	1888	1053	0.422	0.323	0.764	3.22
0.40	1.795	2969	1848	1134	0.358	0.252	0.701	2.59
0.35	1.550	2705	1846	1265	0.294	0.188	0.640	2.00
0.30	1.327	2391	1798	1347	0.240	0.136	0.563	1.53
0.25	1.108	2043	1716	1393	0.200	0.096	0.482	1.16
0.20	0.885	1622	1586	1395	0.161	0.062	0.384	0.92
0.15	0.684	1177	1317	1226	0.134	0.037	0.279	0.70
0.10	0.508	816	1134	1075	0.104	0.020	0.194	0.66

TABLE II (CONTINUED)

Test No. 7-4

$M = 6.95$ $Re_D = 6900$ $\alpha = 0^\circ$ Exp $S/D = 8.3$ $x = 4.0$

$T_w = 1055^\circ R$ $P_{t_2 n} = 45.2$ mm Hg $u_1 = 3853$ $\rho_1 u_1 = 13.99 \times 10^{-3}$ $\rho_1 u_1^2 = 53.89$ psf

Y-inches	M	u(fps)	$T_t - {}^\circ R$	$T_s - {}^\circ R$	$\frac{\rho u}{\rho_1 u_1}$	$\frac{\rho u^2}{\rho_1 u_1^2}$	$\frac{u}{u_1}$	P_{t_2} - mm Hg
0.64	2.986	4010	2076	753	1.165	1.206	1.040	22.61
0.59	2.933	3984	2067	769	1.134	1.165	1.031	21.86
0.54	2.887	3951	2075	780	1.108	1.126	1.023	21.21
0.49	2.851	3899	2048	781	1.092	1.100	1.011	20.69
0.44	2.818	3891	2065	798	1.070	1.075	1.010	20.27
0.39	2.792	3934	2109	823	1.040	1.056	1.019	19.95
0.34	2.750	3868	2058	823	1.029	1.026	1.001	19.42
0.29	2.605	3595	1853	796	0.989	0.920	0.932	17.47
0.24	2.386	3381	1794	838	0.886	0.772	0.878	14.84
0.19	1.934	2853	1573	900	0.688	0.508	0.738	10.08
0.14	1.349	2113	1395	1028	0.448	0.245	0.545	5.36
0.08	0.764	1221	1183	1067	0.250	0.078	0.317	2.77

TABLE II (CONTINUED)

Test No. 7-5

$M = 6.95$ $Re_D = 6900$ $\alpha = 0^\circ$ Exp $S/D = 16.4$ $x = 8.04$

$T_w = 997^\circ R$ $P_{t_{2n}} = 45.2$ mm Hg $u_1 = 3958$ $\rho_1 u_1 = 0.9656 \times 10^{-2}$ $\rho_1 u_1^2 = 46.0$ psf

Y-inches	M	u(fps)	T_t-°R	T_s-°R	$\frac{\rho u}{\rho_1 u_1}$	$\frac{\rho u^2}{\rho_1 u_1^2}$	$\frac{u}{u_1}$	P_{t_2} - mm Hg
0.69	3.107	4039	2059	705	1.096	1.117	1.020	17.91
0.64	3.067	3990	2034	703	1.084	1.092	1.007	17.52
0.59	3.029	3944	2013	707	1.070	1.065	0.997	17.11
0.54	2.978	3916	2009	721	1.043	1.032	0.989	16.58
0.49	2.904	3881	2013	745	0.997	0.978	0.981	15.75
0.44	2.775	3809	1992	782	0.931	0.895	0.961	14.47
0.39	2.577	3622	1924	822	0.843	0.772	0.915	12.57
0.34	2.324	3414	1873	899	0.726	0.622	0.863	10.34
0.28	1.975	2992	1712	958	0.596	0.452	0.755	7.67
0.24	1.641	2602	1619	1049	0.474	0.310	0.655	5.49
0.19	1.262	2040	1415	1086	0.360	0.185	0.516	3.55
0.14	0.919	1546	1365	1180	0.252	0.098	0.390	2.40
0.08	0.623	1012	1173	1100	0.178	0.045	0.256	1.79

TABLE II (CONTINUED)

Test No. 7-6

$M = 6.95$ $Re_D = 6900$ $\alpha = 0^0$ Exp $S/D = 22.5$ $x = 11.13$

$T_w = 910^0R$ $P_{t_{2n}} = 45.2$ mm Hg $u_1 = 4002$ $\rho_1 u_1 = 10.69 \times 10^{-3}$ $\rho_1 u_1^2 = 42.78$ psf

Y-inches	M	u(fps)	T_t-^0R	T_s-^0R	$\frac{\rho u}{\rho_1 u_1}$	$\frac{\rho u^2}{\rho_1 u_1^2}$	$\frac{u}{u_1}$	P_{t_2} - mm Hg
1.13	3.419	4103	1996	598	1.244	1.277	1.023	18.93
1.04	3.312	4082	2032	634	1.173	1.198	1.018	17.79
0.94	3.225	4051	2031	658	1.121	1.135	1.010	16.89
0.84	3.141	4060	2066	694	1.064	1.080	1.013	16.08
0.74	3.072	4022	2065	713	1.027	1.034	1.005	15.41
0.64	3.001	3959	2035	726	0.994	0.983	0.988	14.70
0.59	2.945	3960	2065	752	0.958	0.948	0.988	14.19
0.54	2.873	3865	2007	755	0.934	0.903	0.966	13.54
0.49	2.762	3757	1956	773	0.888	0.833	0.937	12.56
0.44	2.593	3616	1913	812	0.812	0.735	0.902	11.14
0.39	2.386	3397	1823	849	0.732	0.624	0.848	9.55
0.34	2.108	3025	1623	855	0.644	0.488	0.754	7.61
0.29	1.859	2810	1623	958	0.535	0.376	0.702	6.01
0.24	1.262	2464	1536	1007	0.440	0.271	0.614	4.50
0.19	1.230	1983	1391	1075	0.338	0.165	0.493	3.00
0.14	0.870	1468	1363	1187	0.227	0.084	0.366	2.00
0.07	0.551	877	1125	1054	0.152	0.034	0.219	1.49

TABLE II (CONTINUED)

Test No. 7-7

$M = 6.95$ $Re_D = 6900$ $\alpha = 10^\circ$ Comp $S/D = 8.3$ $x = 4.0"$

$T_w = 1158^\circ R$ $P_{t_{sn}} = 45.2$ mm Hg $u_1 = 3526$ $\rho_1 u_1 = 21.83 \times 10^{-3}$ $\rho_1 u_1^2 = 76.99$ psf

Y-inches	M	u(fps)	T_t-°R	T_s-°R	$\frac{\rho u}{\rho_1 u_1}$	$\frac{\rho u^2}{\rho_1 u_1^2}$	$\frac{u}{u_1}$	P_{t_2} - mm Hg
.69	3.006	4004	2064	738	1.586	1.796	1.134	48.04
.64	2.879	3902	2044	767	1.492	1.648	1.106	44.26
.59	2.766	3851	2051	807	1.400	1.526	1.092	41.09
.54	2.669	3810	2059	849	1.317	1.417	1.079	38.31
.49	2.578	3738	2038	876	1.252	1.324	1.060	35.95
.44	2.504	3721	2077	923	1.182	1.248	1.055	33.95
.39	2.430	3636	2043	931	1.144	1.180	1.030	32.16
.34	2.383	3604	2048	954	1.106	1.132	1.021	30.94
.29	2.342	3602	2059	984	1.071	1.094	1.022	29.99
.24	2.285	3510	1996	980	1.049	1.041	0.995	28.61
.19	2.107	3237	1870	986	0.962	0.884	0.918	24.61
.14	1.712	2650	1598	1004	0.769	0.578	0.751	16.81
.08	1.131	1823	1352	1081	0.493	0.256	0.519	8.54

TABLE II (CONTINUED)

Test No. 7-8

$M = 6.95$ $Re_D = 6900$ $\alpha = 10^\circ$ Comp $S/D = 16.4$ $x = 8.04$

$T_w = 883^\circ R$ $P_{t_{2n}} = 45.2$ mm Hg $u_1 = 3589$ $\rho_1 u_1 = 20.44 \times 10^{-3}$ $\rho_1 u_1^2 = 73.35$ psf

Y-inches	M	u(fps)	T_t-°R	T_s-°R	$\frac{\rho u}{\rho_1 u_1}$	$\frac{\rho u^2}{\rho_1 u_1^2}$	$\frac{u}{u_1}$	P_{t_2} - mm Hg
0.74	3.012	4029	2060	744	1.503	1.688	1.122	42.83
0.64	2.790	3907	2059	815	1.335	1.453	1.088	37.10
0.59	2.700	3891	2094	861	1.255	1.362	1.082	34.87
0.54	2.627	3812	2062	876	1.210	1.288	1.061	33.05
0.49	2.557	3771	2057	902	1.162	1.220	1.048	31.42
0.44	2.501	3698	2029	910	1.130	1.168	1.031	30.13
0.39	2.445	3656	2026	932	1.092	1.115	1.019	28.84
0.34	2.385	3643	2050	974	1.040	1.058	1.015	27.46
0.29	2.257	3546	2046	1029	0.958	0.949	0.988	24.85
0.24	1.999	3343	2075	1166	0.797	0.744	0.931	19.83
0.19	1.677	2887	1903	1239	0.646	0.520	0.804	14.43
0.14	1.251	2247	1728	1339	0.466	0.292	0.627	8.85
0.08	0.742	1203	1199	1093	0.306	0.102	0.338	5.05

TABLE II (CONTINUED)

Test No. 7-9

$M = 6.95$ $Re_D = 6900$ $\alpha = 10^\circ$ Comp $S/D = 22.5$ $x = 11.13$

$T_w = 905^\circ R$ $P_{t_{\infty n}} = 45.2$ mm Hg $u_1 = 3654$ $\rho_1 u_1 = 19.02 \times 10^{-3}$ $\rho_1 u_1^2 = 69.49$ psf

Y-inches	M	u(fps)	T_t-°R	T_s-°R	$\frac{\rho u}{\rho_1 u_1}$	$\frac{\rho u^2}{\rho_1 u_1^2}$	$\frac{u}{u_1}$	P_{t_∞} - mm Hg
.69	2.906	3936	2052	766	1.346	1.453	1.077	35.16
.64	2.816	3858	2034	785	1.290	1.365	1.056	33.09
.59	2.727	3795	2021	809	1.236	1.284	1.038	31.22
.54	2.660	3802	2061	851	1.172	1.218	1.038	29.72
.49	2.590	3731	2029	862	1.135	1.160	1.021	28.33
.44	2.535	3716	2056	897	1.088	1.107	1.016	27.14
.39	2.460	3657	2040	922	1.041	1.044	1.000	25.67
.34	2.365	3576	2024	949	0.986	0.964	0.978	23.83
.29	2.192	3415	1997	1013	0.884	0.828	0.934	20.67
.24	1.929	3095	1881	1075	0.755	0.641	0.846	16.37
.19	1.585	2575	1651	1093	0.616	0.432	0.703	11.56
.14	1.235	2000	1433	1095	0.479	0.264	0.550	7.62
.08	0.725	1142	1140	1028	0.290	0.091	0.312	4.38

TABLE III

Boundary Layer Data, M = 10

Test No. 10-1

$M = 9.99$ $Re_D = 10{,}970$ $\alpha = 15^o$ Exp $S/D = 8.3$ $x = 4.0$

$T_w = 1105^oR$ $P_{t_{an}} = 45.6$ mm Hg $u_1 = 4517$ $\rho_1 u_1 = 6.278 \times 10^{-3}$ $\rho_1 u_1^2 = 28.357$ psf

Y-inches	M	u(fps)	T_t-°R	T_s-°R	$\frac{\rho u}{\rho_1 u_1}$	$\frac{\rho u^2}{\rho_1 u_1^2}$	$\frac{u}{u_1}$	P_{t_2} - mm Hg
.78	3.613	4227	2049	568	1.185	1.108	0.935	10.72
.72	3.594	4193	2034	565	1.181	1.100	0.928	10.81
.68	3.570	4196	2041	573	1.164	1.082	0.929	10.68
.63	3.557	4177	2026	572	1.160	1.073	0.924	10.59
.58	3.539	4171	2028	577	1.151	1.064	0.924	10.49
.53	3.511	4166	2027	585	1.135	1.046	0.923	10.33
.48	3.430	4105	1998	595	1.100	1.000	0.909	9.89
.43	3.281	4034	1983	626	1.025	0.916	0.892	9.08
.38	3.035	3862	1925	675	0.914	0.782	0.855	7.80
.35	2.878	3711	1842	690	0.858	0.703	0.822	7.06
.33	2.746	3625	1810	724	0.795	0.639	0.802	6.43
.28	2.304	3279	1726	841	0.620	0.448	0.725	4.62
.25	2.079	3100	1720	928	0.532	0.366	0.688	3.82
.23	1.860	2911	1720	1022	0.452	0.292	0.645	3.11
.20	1.640	2640	1659	1073	0.389	0.228	0.584	2.50
.18	1.450	2363	1576	1112	0.339	0.177	0.524	2.02
.15	1.278	2148	1533	1164	0.290	0.137	0.472	1.64
.13	1.132	1910	1494	1197	0.256	0.108	0.424	1.36
.11	0.982	1705	1486	1259	0.217	0.082	0.378	1.18
.08	0.878	1522	1423	1246	0.196	0.066	0.336	1.04
.04	0.765	1289	1325	1180	0.177	0.050	0.286	0.93

TABLE III (CONTINUED)

Test No. 10-2

$M = 9.99$ $\quad Re_D = 10970$ $\quad \alpha = 15^{\circ}$ Exp $\quad S/D = 16.4$ $\quad x = 8.04$

$T_w = 932^{\circ}R$ $\quad P_{t_{2}n} = 45.6$ mm Hg $\quad u_1 = 4643$ $\quad \rho_1 u_1 = 4.541 \times 10^{-3}$ $\quad \rho_1 u_1^2 = 21.082$ psf

Y-inches	M	u(fps)	T_t-°R	T_s-°R	$\frac{\rho u}{\rho_1 u_1}$	$\frac{\rho u^2}{\rho_1 u_1^2}$	$\frac{u}{u_1}$	P_{t_2} - mm Hg
1.04	3.938	4329	2041	500	1.169	1.090	0.932	7.87
1.00	3.915	4300	2035	501	1.162	1.077	0.926	7.77
.94	3.881	4324	2061	515	1.132	1.057	0.931	7.63
.90	3.818	4250	2023	514	1.119	1.026	0.916	7.41
.84	3.755	4231	2020	527	1.086	0.989	0.912	7.16
.80	3.643	4167	1988	542	1.038	0.933	0.897	6.77
.75	3.495	4077	1953	565	0.974	0.858	0.878	6.22
.70	3.311	3985	1924	599	0.899	0.772	0.856	5.62
.65	3.107	3874	1898	645	0.811	0.677	0.833	4.95
.60	2.879	3734	1864	699	0.724	0.583	0.804	4.29
.55	2.650	3615	1848	773	0.635	0.493	0.778	3.66
.50	2.409	3465	1848	858	0.549	0.408	0.746	3.07
.45	2.175	3281	1832	947	0.471	0.333	0.707	2.53
.40	1.940	3073	1822	1041	0.400	0.264	0.661	2.05
.35	1.710	2794	1750	1112	0.340	0.206	0.604	1.63
.30	1.480	2518	1716	1201	0.284	0.154	0.543	1.28
.26	1.320	2302	1728	1275	0.244	0.122	0.496	1.05
.20	1.093	1873	1506	1223	0.208	0.083	0.240	0.78
.15	0.904	1566	1465	1246	0.170	0.057	0.337	0.65
.10	0.760	1251	1238	1119	0.152	0.040	0.269	0.56
.06	0.700	1110	1145	1047	0.143	0.035	0.239	0.53

TABLE III (CONTINUED)

Test No. 10-3

$M = 9.99$ $Re_D = 10970$ $\alpha = 10^{\circ}$ Exp $S/D = 22.5$ $x = 11.13$

$T_w = 862^{\circ}R$ $P_{t_2 n} = 45.6$ mm Hg $u_1 = 4624$ $\rho_1 u_1 = 4.791 \times 10^{-3}$ $\rho_1 u_1^2 = 22.155$ psf

Y-inches	M	u(fps)	T_t-°R	T_s-°R	$\frac{\rho u}{\rho_1 u_1}$	$\frac{\rho u^2}{\rho_1 u_1^2}$	$\frac{u}{u_1}$	P_{t_2} - mm Hg
1.13	3.789	4280	2044	529	1.117	1.036	0.925	7.98
1.04	3.728	4275	2052	545	1.085	1.003	0.924	7.73
0.98	3.676	4246	2049	552	1.062	0.976	0.918	7.52
0.93	3.618	4214	2041	563	1.036	0.944	0.910	7.28
0.89	3.535	4164	2008	573	1.004	0.904	0.899	6.98
0.78	3.295	4051	1994	627	0.894	0.783	0.876	6.08
0.74	3.139	3960	1967	662	0.828	0.711	0.857	5.53
0.69	2.966	3886	1965	713	0.758	0.636	0.841	4.97
0.64	2.790	3755	1929	751	0.692	0.563	0.809	4.42
0.59	2.579	3582	1875	801	0.621	0.482	0.774	3.81
0.54	2.370	3375	1787	845	0.554	0.406	0.732	3.24
0.49	2.185	3170	1717	879	0.506	0.347	0.686	2.80
0.44	1.968	2930	1650	932	0.440	0.280	0.633	2.29
0.39	1.746	2629	1504	942	0.386	0.220	0.566	1.86
0.34	1.533	2350	1431	982	0.331	0.170	0.510	1.48
0.29	1.290	2044	1380	1033	0.270	0.121	0.440	1.12
0.19	0.875	1362	1148	1009	0.188	0.056	0.294	0.69
0.16	0.781	1170	1036	934	0.176	0.044	0.254	0.63
0.14	0.660	990	1000	929	0.148	0.032	0.213	0.56
0.11	0.565	775	834	778	0.138	0.024	0.166	0.52
0.08	0.665	871	774	709	0.170	0.032	0.189	0.56

TABLE III (CONTINUED)

Test No. 10-4

$M = 9.99$ $Re_D = 10,970$ $\alpha = 0^o$ Exp $S/D = 8.3$ $x = 4.0$

$T_w = 940^oR$ $P_{t_2n} = 45.6$ mm Hg $u_1 = 4177.8$ $\rho_1 u_1 = 11.849 \times 10^{-2}$ $\rho_1 u_1^2 = 49.505$ psf

Y-inches	M	u(fps)	T_t-°R	T_s-°R	$\frac{\rho u}{\rho_1 u_1}$	$\frac{\rho u^2}{\rho_1 u_1^2}$	$\frac{u}{u_1}$	P_{t_2} - mm Hg
1.61	2.999	3987	2048.5	734	1.209	1.154	.954	30.26
0.48	2.960	3963	2058.8	745	1.186	1.124	.948	38.87
0.42	2.928	3927	2035.0	747	1.172	1.102	.939	38.14
0.37	2.886	3919	2056.8	769	1.141	1.070	.937	37.10
0.34	2.863	3910	2053.5	777	1.124	1.052	.934	36.48
0.32	2.828	3900	2068.8	793	1.100	1.028	.933	35.66
0.29	2.763	3859	2057.8	812	1.060	0.980	.922	34.08
0.27	2.652	3786	2046.5	848	0.996	0.902	.905	31.55
0.24	2.512	3650	1996.3	878	0.928	0.812	.873	28.52
0.22	2.326	3440	1909.3	913	0.842	0.693	.824	24.60
0.19	2.101	3136	1741.3	928	0.755	0.568	.752	20.44
0.17	1.824	2725	1545.3	928	0.654	0.427	.651	15.80
0.14	1.541	2354	1411.0	970	0.540	0.304	.564	11.74
0.12	1.283	1933	1263.8	955	0.451	0.208	.464	8.59
0.08	0.944	1459	1167.5	992	0.330	0.116	.349	5.89
0.06	0.782	1142	1001.8	885	0.292	0.080	.273	4.93

TABLE III (CONTINUED)

Test No. 10-5

$M = 9.99$ $Re_D = 10{,}970$ $\alpha = 0^\circ$ Exp $S/D = 16.4$ $x = 8.04$

$T_w = 907^\circ R$ $P_{t_{e}n} = 45.6$ mm Hg $u_1 = 4337.7$ $\rho_1 u_1 = 9.092 \times 10^{-3}$ $\rho_1 u_1^2 = 39.438$ psf

Y-inches	M	u(fps)	T_t-°R	T_s-°R	$\frac{\rho u}{\rho_1 u_1}$	$\frac{\rho u^2}{\rho_1 u_1^2}$	$\frac{u}{u_1}$	P_{t_e} - mm Hg
1.04	3.585	4235.5	2060.8	579	1.414	1.381	.975	37.68
0.99	3.533	4229.5	2079.0	595	1.370	1.370	.974	36.54
0.94	3.479	4194.5	2060.3	603	1.342	1.300	.966	35.51
	3.438	4214.0	2092.8	624	1.303	1.268	.971	34.65
0.84	3.395	4204.5	2066.0	636	1.274	1.235	.968	33.79
0.79	3.354	4159.5	2055.3	638	1.258	1.163	.957	33.06
0.74	3.325	4177.0	2083.8	655	1.229	1.184	.961	32.04
0.69	3.290	4132.0	2075.8	654	1.219	1.163	.950	31.85
0.64	3.255	4110.0	2070.3	661	1.201	1.140	.947	31.22
0.59	3.215	4089.5	2070.0	672	1.176	1.111	.942	30.46
0.54	3.155	4066.5	2070.8	691	1.136	1.068	.937	29.33
0.49	3.063	4007.0	2055.0	712	1.089	1.006	.924	27.71
0.44	2.900	3857.0	1977.3	734	1.015	0.903	.888	25.00
0.39	2.690	3620.0	1850.8	754	0.930	0.777	.834	21.64
0.34	2.407	3326.0	1720.5	782	0.812	0.622	.766	17.59
0.29	2.141	3031.5	1608.8	836	0.702	0.493	.700	14.14
0.24	1.808	2599.5	1434.8	864	0.583	0.352	.601	10.41
0.19	1.515	2226.5	1324.0	909	0.473	0.245	.515	7.58

TABLE III (CONTINUED)

Test No. 10-6

$M = 9.99$ $Re_D = 10,970$ $\alpha = 0^\circ$ Exp $S/D = 22.5$ $x = 11.13$

$T_w = 1030^\circ R$ $P_{t_{2n}} = 45.6$ mm Hg $u_1 = 4412$ $\rho_1 u_1 = 7.927 \times 10^{-3}$ $\rho_1 u_1^2 = 34.97$ psf

Y-inches	M	u(fps)	T_t-°R	T_s-°R	$\frac{\rho u}{\rho_1 u_1}$	$\frac{\rho u^2}{\rho_1 u_1^2}$	$\frac{u}{u_1}$	P_{t_2} - mm Hg
1.03	3.585	4247	2059	581	1.309	1.259	0.962	15.28
0.93	3.499	4175	2036	589	1.272	1.202	0.946	14.60
0.89	3.467	4174	2056	602	1.246	1.179	0.946	14.32
0.84	3.435	4156	2041	606	1.226	1.155	0.941	14.04
0.79	3.402	4147	2049	616	1.206	1.133	0.939	13.79
0.74	3.364	4135	2058	629	1.182	1.108	0.937	13.48
0.69	3.318	4122	2058	641	1.156	1.080	0.933	13.14
0.64	3.257	4090	2051	655	1.120	1.039	0.926	12.66
0.59	3.170	4052	2040	678	1.071	0.984	0.918	12.01
0.54	3.042	3955	2008	702	1.013	0.909	0.896	11.13
0.49	2.877	3800	1936	727	0.942	0.811	0.861	9.99
0.44	2.812	3600	1843	756	0.858	0.700	0.815	8.69
0.39	2.419	3306	1696	777	0.766	0.575	0.749	7.20
0.34	2.128	2995	1573	820	0.657	0.447	0.677	5.69
0.29	1.840	2618	1418	842	0.558	0.332	0.592	4.35
0.19	1.170	1810	1265	1000	0.325	0.132	0.409	2.07
0.14	0.882	1385	1185	1027	0.245	0.076	0.314	1.49

TABLE III (CONTINUED)

Test No. 10-7

$M = 9.99$ $Re_D = 10{,}970$ $\alpha = 10^oC$ $S/D = 8.3$ $x = 4.0$

$T_w = 1137^oR$ $P_{t_{a_n}} = 45.6$ mm Hg $u_1 = 3836.8$ $\rho_1 u_1 = 13.834 \times 10^{-3}$ $\rho_1 u_1^2 = 72.263$ psf

Y-inches	M	u(fps)	T_t-^oR	T_s-^oR	$\frac{\rho u}{\rho_1 u_1}$	$\frac{\rho u^2}{\rho_1 u_1^2}$	$\frac{u}{u_1}$	P_{t_s} - mm Hg
.60	2.918	3933	2039.0	755.8	1.544	1.583	1.025	39.68
.50	2.713	3846	2068.3	835.8	1.369	1.372	1.001	34.61
.40	2.561	3708	2026.5	872.8	1.260	1.219	0.966	30.93
.35	2.504	3667	2018.5	890.5	1.223	1.169	0.954	29.72
.30	2.457	3613	1999.8	901.0	1.191	1.122	0.940	28.61
.25	2.381	3540	1975.5	922.0	1.142	1.054	0.923	26.98
.22	2.292	3425	1912.3	928.0	1.095	0.977	0.891	25.14
.20	2.190	3328	1891.5	959.3	1.031	0.892	0.866	23.11
.15	1.940	3006	1761.0	998.8	0.891	0.699	0.783	18.50
.13	1.735	2707	1635.8	1015.5	0.789	0.557	0.707	15.11
.12	1.323	2106	1426.5	1047.5	0.596	0.327	0.549	9.61
.09	1.066	1687	1285.5	1042.5	0.476	0.211	0.783	6.79
.65	3.036	4006	2042.8	723.0	1.641	1.715	1.043	42.89
.55	2.805	3873	2052.5	795.5	1.445	1.462	1.009	36.76
.45	2.624	3777	2057.5	861.3	1.302	1.282	0.983	32.44
.35	2.500	3665	2027.5	896.8	1.216	1.161	0.955	29.55
.30	2.446	3616	2008.3	907.8	1.184	1.116	0.943	28.45
.25	2.379	3545	1973.8	922.0	1.138	1.051	0.922	26.92
.20	2.176	3326	1909.8	976.3	1.014	0.880	0.867	22.80
.17	1.972	2995	1725.8	965.3	0.922	0.720	0.783	19.01
.15	1.695	2623	1574.0	1001.3	0.777	0.532	0.685	14.49
.12	1.345	2075	1362.5	1000.0	0.616	0.334	0.543	9.76
.09	1.042	1583	1179.5	963.3	0.485	0.202	0.412	6.59

TABLE III (CONTINUED)

Test No. 10-8

$M = 9.99$ $Re_D = 10970$ $\alpha = 10^\circ$ Comp $S/D = 16.4$ $x = 8.04$

$T_w = 865^\circ R$ $P_{t_{2n}} = 45.6$ mm Hg $u_1 = 3911$ $\rho_1 u_1 = 17.235 \times 10^{-3}$ $\rho_1 u_1^2 = 67.402$ psf

Y-inches	M	u(fps)	T_t-°R	T_s-°R	$\frac{\rho u}{\rho_1 u_1}$	$\frac{\rho u^2}{\rho_1 u_1^2}$	$\frac{u}{u_1}$	P_{t_2} - mm Hg
.86	3.470	4180	2046	603	1.920	2.056	1.069	47.60
.80	3.295	4105	2048	645	1.764	1.853	1.048	43.02
.75	3.174	4042	2039	674	1.664	1.719	1.033	40.05
.70	3.054	4001	2051	712	1.559	1.596	1.021	37.22
.65	2.953	3951	2046	745	1.472	1.489	1.010	34.81
.60	2.850	3902	2052	780	1.392	1.388	0.997	32.58
.55	2.775	3839	2035	800	1.338	1.314	0.982	30.95
.50	2.696	3811	2050	834	1.273	1.243	0.974	29.30
.45	2.638	3787	2059	857	1.229	1.191	0.968	28.15
.40	2.575	3765	2073	889	1.176	1.134	0.961	26.85
.35	2.501	3757	2119	941	1.112	1.069	0.961	25.41
.30	2.386	3647	2089	974	1.042	0.972	0.932	23.24
.25	2.131	3401	2010	1063	0.893	0.777	0.869	18.89
.20	1.758	2762	1675	1032	0.742	0.525	0.707	13.27
.15	1.300	1980	1277	957	0.572	0.289	0.504	7.98
.09	0.885	1330	1080	931	0.392	0.132	0.340	4.50

TABLE III (CONTINUED)

Test No. 10-9

$M = 9.99$ $Re_D = 10{,}970$ $\alpha = 10^\circ C$ $S/D = 22.5$ $x = 11.13$

$T_w = 965^\circ R$ $P_{t_2 n} = 45.6$ mm Hg $u_1 = 3971.9$ $\rho_1 u_1 = 15.751 \times 10^{-3}$ $\rho_1 u_1^2 = 62.56$ psf

Y-inches	M	u(fps)	T_t-°R	T_s-°R	$\frac{\rho u}{\rho_1 u_1}$	$\frac{\rho u^2}{\rho_1 u_1^2}$	$\frac{u}{u_1}$	P_{t_2} - mm Hg
.65	3.000	3971.5	2057.3	731	1.443	1.440	1.000	32.76
.55	2.837	3919.5	2080.5	792	1.311	1.292	0.986	28.18
.45	2.694	3819.0	2057.3	835	1.213	1.166	0.960	25.54
.35	2.525	3712.0	2043.3	899	1.094	1.022	0.934	22.56
.30	2.329	3530.5	1991.0	952	0.983	0.873	0.888	19.46
.27	2.202	3284.5	1838.8	929	0.939	0.776	0.827	17.45
.25	2.071	3113.0	1752.3	934	0.884	0.690	0.782	15.68
.22	1.880	2822.0	1607.8	937	0.798	0.566	0.710	13.08
.20	1.666	2519.5	1485.3	951	0.702	0.445	0.634	10.54
.17	1.455	2202.0	1358.5	951	0.610	0.338	0.551	8.34
.12	1.247	1835.5	1184.8	907	0.536	0.247	0.462	6.45

TABLE IV

Boundary Layer Data, M = 12

Test No. 12-1

M = 12.26 Re_D = 12700 α = 15° Exp   S/D = 8.3   x = 4.0

T_w = 1048°R $P_{t_2 n}$ = 29 mm Hg u_1 = 4126 $\rho_1 u_1$ = 5.252 x 10^{-3} $\rho_1 u_1^2$ = 21.67 psf

Y-inches	M	u(fps)	T_t-°R	T_s-°R	$\frac{\rho u}{\rho_1 u_1}$	$\frac{\rho u^2}{\rho_1 u_1^2}$	$\frac{u}{u_1}$	P_{t_2} - mm Hg
.80	2.978	3883	1953	706	0.868	0.818	0.941	6.16
.70	2.939	3870	1972	719	0.849	0.796	0.938	6.01
.65	2.916	3821	1942	715	0.845	0.783	0.926	5.91
.60	2.870	3798	1937	729	0.823	0.758	0.920	5.73
.55	2.792	3691	1871	728	0.802	0.717	0.894	5.43
.50	2.668	3597	1824	757	0.750	0.655	0.871	4.99
.45	2.482	3385	1723	776	0.691	0.568	0.820	4.36
.40	2.253	3156	1633	815	0.613	0.468	0.764	3.64
.35	1.991	2815	1489	837	0.532	0.364	0.682	2.89
.30	1.711	2510	1412	897	0.442	0.269	0.609	2.20
.25	1.425	2165	1356	964	0.354	0.186	0.524	1.60
.20	1.160	1812	1298	1025	0.278	0.124	0.438	1.15
.15	0.892	1446	1259	1092	0.208	0.073	0.350	0.87
.10	0.647	1038	1159	1068	0.154	0.040	0.251	0.68

TABLE IV (CONTINUED)

Test No. 12-2

$M = 12.36$ $\quad Re_D = 19400$ $\quad \alpha = 10^\circ$ Exp $\quad S/D = 22.5$ $\quad x = 11.13$

$T_w = 1060^\circ R$ $\quad P_{t_2 n} = 44.1$ mm Hg $\quad u_1 = 4224$ $\quad \rho_1 u_1 = 4.018 \times 10^{-3}$ $\quad \rho_1 u_1^2 = 16.97$ psf

Y-inches	M	u(fps)	T_t-°R	T_s-°R	$\frac{\rho u}{\rho_1 u_1}$	$\frac{\rho u^2}{\rho_1 u_1^2}$	$\frac{u}{u_1}$	P_{t_2} - mm Hg
1.00	3.633	4242	2055	568	1.024	1.029	1.003	6.03
0.90	3.466	4149	2028	597	0.956	0.940	0.981	5.51
0.80	3.216	4070	2042	667	0.837	0.807	0.962	4.76
0.70	2.881	3889	2007	760	0.703	0.647	0.920	3.85
0.65	2.697	3792	2018	823	0.633	0.569	0.896	3.40
0.60	2.500	3592	1917	860	0.575	0.488	0.849	2.95
0.55	2.302	3403	1859	908	0.484	0.416	0.806	2.53
0.50	2.109	3202	1808	964	0.457	0.348	0.759	2.14
0.45	1.900	2941	1708	1000	0.405	0.282	0.696	1.78
0.40	1.705	2688	1629	1041	0.354	0.226	0.639	1.46
0.35	1.505	2386	1517	1056	0.309	0.176	0.564	1.17
0.30	1.310	2111	1452	1089	0.265	0.133	0.498	0.93
0.25	1.137	1850	1396	1112	0.228	0.100	0.434	0.74
0.20	0.952	1589	1369	1155	0.188	0.072	0.376	0.62
0.15	0.857	1412	1294	1128	0.172	0.058	0.334	0.56

TABLE IV (CONTINUED)

Test No. 12-3

$M = 12.26$ $Re_D = 12700$ $\alpha = 10^\circ$ Exp $S/D = 16.4$ $x = 8.04$

$T_w = 1040^\circ R$ $P_{t_{2n}} = 29$ mm Hg $u_1 = 4224$ $\rho_1 u_1 = 4.048 \times 10^{-3}$ $\rho_1 u_1^2 = 17.0984$ psf

Y-inches	M	u(fps)	T_t-°R	T_s-°R	$\frac{\rho u}{\rho_1 u_1}$	$\frac{\rho u^2}{\rho_1 u_1^2}$	$\frac{u}{u_1}$	P_{t_2} - mm Hg
.90	3.288	4129	2065	654	0.862	0.843	0.977	5.03
.80	3.124	4031	2036	689	0.802	0.764	0.952	4.57
.70	2.885	3852	1973	740	0.715	0.650	0.909	3.92
.65	2.714	3691	1897	764	0.666	0.579	0.869	3.51
.60	2.539	3509	1824	795	0.607	0.504	0.828	3.08
.55	2.355	3319	1756	830	0.550	0.434	0.786	2.67
.50	2.144	3099	1684	874	0.491	0.360	0.735	2.26
.45	1.948	2889	1604	909	0.434	0.298	0.680	1.89
.40	1.749	2612	1517	943	0.381	0.238	0.623	1.54
.35	1.535	2394	1484	1005	0.327	0.184	0.567	1.24
.30	1.350	2174	1475	1080	0.275	0.142	0.512	0.99
.25	1.156	1915	1433	1129	0.234	0.102	0.450	0.78
.15	0.747	1232	1250	1121	0.152	0.043	0.291	0.50
.10	0.564	969	1315	1232	0.109	0.024	0.230	0.43

TABLE IV (CONTINUED)

Test No. 12-4

$M = 12.26$ $Re_D = 12700$ $\alpha = 10^\circ$ Exp $S/D = 22.5$ $x = 11.13$

$T_w = 927^\circ R$ $P_{t_2 n} = 29$ mm Hg $u_1 = 4133$ $\rho_1 u_1 = 5.129 \times 10^{-3}$ $\rho_1 u_1^2 = 21.20$ psf

Y-inches	M	u(fps)	T_t-°R	T_s-°R	$\frac{\rho u}{\rho_1 u_1}$	$\frac{\rho u^2}{\rho_1 u_1^2}$	$\frac{u}{u_1}$	P_{t_2} - mm Hg
1.00	2.422	3636	2033	940	0.604	0.533	0.879	4.01
0.95	2.350	3565	1998	958	0.581	0.502	0.860	3.80
0.90	2.279	3535	2050	1002	0.550	0.472	0.855	3.59
0.85	2.188	3494	2078	1057	0.516	0.436	0.844	3.34
0.80	2.134	3482	2105	1114	0.491	0.414	0.843	3.18
0.75	1.998	3261	1980	1113	0.458	0.361	0.788	2.80
0.70	1.874	3065	1898	1117	0.429	0.320	0.742	2.50
0.65	1.765	2966	1900	1183	0.391	0.281	0.719	2.24
0.60	1.636	2780	1830	1204	0.360	0.244	0.674	1.97
0.55	1.521	2638	1816	1257	0.326	0.209	0.637	1.73
0.50	1.386	2402	1713	1250	0.300	0.174	0.580	
0.45	1.246	2127	1570	1213	0.272	0.141	0.514	1.25
0.40	1.096	1817	1420	1160	0.245	0.108	0.440	1.02
0.35	0.904	1528	1366	1188	0.202	0.075	0.370	0.85
0.30	0.716	1191	1257	1153	0.161	0.047	0.288	0.70
0.25	0.437	705	1128	1086	0.102	0.018	0.171	0.57

TABLE IV (CONTINUED)

Test No. 12-5

$M = 12.08$ $Re_D = 8700$ $\alpha = 10^{\circ}$ Exp $S/D = 8.3$ $x = 4.0$

$T_w = 1013^{\circ}R$ $P_{t_{2}n} = 20.5$ mm Hg $u_1 = 4102$ $\rho_1 u_1 = 4.096 \times 10^{-3}$ $\rho_1 u_1^2 = 16.80$ psf

Y-inches	M	u(fps)	T_t-$^{\circ}R$	T_s-$^{\circ}R$	$\frac{\rho u}{\rho_1 u_1}$	$\frac{\rho u^2}{\rho_1 u_1^2}$	$\frac{u}{u_1}$	P_{t_2} - mm Hg
1.00	3.264	4111	2057	661	1.008	1.010	1.002	5.88
0.90	3.187	4042	2033	668	0.982	0.966	0.984	5.63
0.80	3.130	4046	2056	694	0.944	0.929	0.984	5.43
0.75	3.105	3996	2024	689	0.940	0.915	0.974	5.35
0.70	3.083	3996	2014	698	0.928	0.902	0.972	5.28
0.65	3.046	3951	2002	700	0.916	0.880	0.962	5.15
0.60	2.984	3901	1981	710	0.892	0.848	0.949	4.97
0.55	2.911	3824	1937	718	0.862	0.804	0.932	4.72
0.50	2.795	3726	1902	740	0.817	0.742	0.908	4.37
0.45	2.641	3545	1783	750	0.768	0.664	0.864	3.93
0.40	2.467	3437	1784	809	0.692	0.580	0.836	3.46
0.35	2.213	3159	1675	851	0.604	0.466	0.771	2.82
0.30	1.946	2852	1572	894	0.516	0.358	0.695	2.22
0.25	1.641	2430	1392	914	0.431	0.255	0.593	1.64
0.20	1.350	2055	1305	966	0.344	0.172	0.501	1.17
0.15	1.106	1738	1268	1024	0.275	0.116	0.423	0.86
0.10	0.801	1276	1184	1054	0.195	0.080	0.311	0.63

TABLE IV (CONTINUED)

Test No. 12-6

$M = 12.08$ $Re_D = 8700$ $\alpha = 10^\circ$ Exp $S/D = 16.4$ $x = 8.04$

$T_w = 1010^\circ R$ $P_{t_{2n}} = 20.5$ mm Hg $u_1 = 4177$ $\rho_1 u_1 = 3.138 \times 10^{-3}$ $\rho_1 u_1^2 = 13.10$ psf

Y-inches	M	u(fps)	T_t-°R	T_s-°R	$\frac{\rho u}{\rho_1 u_1}$	$\frac{\rho u^2}{\rho_1 u_1^2}$	$\frac{u}{u_1}$	P_{t_2} - mm Hg
.90	2.932	3951	2052	756	0.764	0.724	0.945	3.36
.80	2.691	3781	1998	815	0.678	0.613	0.903	2.86
.65	2.262	3393	1893	939	0.531	0.432	0.811	2.06
.55	1.950	3050	1787	1018	0.438	0.320	0.728	1.57
.45	1.629	2560	1576	1035	0.362	0.222	0.612	1.13
.35	1.306	2100	1417	1060	0.288	0.145	0.503	0.79
.30	1.160	1867	1341	1058	0.260	0.114	0.446	0.65
.20	0.831	1332	1213	1066	0.184	0.060	0.319	0.46

TABLE IV (CONTINUED)

Test No. 12-7

$M = 12.08$ Re_D 8700 $\alpha = 10^\circ$ Exp $S/D = 22.5$ $x = 11.13$

$T_w = 853^\circ R$ $P_{t_{2n}} = 20.5$ mm Hg $u_1 = 4170$ $\rho_1 u_1 = 3.206 \times 10^{-3}$ $\rho_1 u_1^2 = 13.37$ psf

Y-inches	M	u(fps)	T_t-°R	T_s-°R	$\frac{\rho u}{\rho_1 u_1}$	$\frac{\rho u^2}{\rho_1 u_1^2}$	$\frac{u}{u_1}$	P_{t_2} - mm Hg
	2.941	4000	1984	731	0.796	0.744	0.934	3.48
1.15	2.766	3765	1939	733	0.727	0.657	0.903	3.09
1.05	2.629	3820	2076	878	0.649	0.596	0.917	2.82
1.00	2.526	3706	2023	894	0.618	0.550	0.888	2.61
0.95	2.380	3404	1806	852	0.596	0.486	0.816	2.33
0.90	2.303	3269	1727	839	0.584	0.457	0.783	2.20
0.80	2.048	2922	1544	845	0.516	0.362	0.700	1.77
0.70	1.806	2605	1423	867	0.447	0.280	0.624	1.40
0.65	1.676	2400	1332	859	0.417	0.241	0.576	1.23
0.60	1.555	2235	1268	864	0.385	0.208	0.536	1.08
0.55	1.431	2105	1261	904	0.346	0.176	0.504	0.93
0.50	1.300	1885	1161	877	0.319	0.145	0.452	0.80
0.45	1.188	1735	1133	890	0.292	0.122	0.415	0.69
	1.081	1559	1063	870	0.264	0.010	0.372	0.60

TABLE IV (CONTINUED)

Test No. 12-8

$M = 12.36$ $Re_D = 19400$ $\alpha = 0^\circ$ Exp $S/D = 8.3$ $x = 4.0$

$T_w = 1050^\circ R$ $P_{t_{2}n} = 44.1$ mm Hg $u_1 = 3937$ $\rho_1 u_1 = 11.95 \times 10^{-3}$ $\rho_1 u_1^2 = 47.04$ psf

Y-inches	M	u(fps)	T_t-°R	T_s-°R	$\frac{\rho u}{\rho_1 u_1}$	$\frac{\rho u^2}{\rho_1 u_1^2}$	$\frac{u}{u_1}$	P_{t_2} - mm Hg
.82	3.086	4053	2074	717	1.112	1.146	1.030	18.68
.77	3.016	4012	2067	735	1.073	1.095	1.020	17.87
.72	2.950	3950	2044	744	1.044	1.048	1.004	17.14
.67	2.903	3903	2023	751	1.024	1.016	0.992	16.62
.62	2.858	3882	2028	768	0.997	0.984	0.986	16.15
.57	2.820	3869	2038	786	0.974	0.957	0.983	15.72
.52	2.788	3870	2019	799	0.953	0.937	0.981	15.38
.47	2.761	3825	2015	797	0.946	0.920	0.972	15.12
.42	2.736	3813	2018	808	0.932	0.903	0.970	14.87
.37	2.699	3768	2000	813	0.918	0.878	0.958	14.48
.32	2.616	3725	2085	848	0.868	0.823	0.948	13.60
.27	2.406	3547	1961	906	0.771	0.698	0.903	11.64
.22	2.026	3247	1927	1066	0.601	0.495	0.825	8.48
.17	1.535	2687	1857	1274	0.414	0.283	0.681	5.15
.12	1.095	1917	1592	1288	0.295	0.144	0.487	2.98
.06	0.642	1070	1243	1149	0.183	0.050	0.271	1.92

TABLE IV (CONTINUED)

Test No. 12-9

$M = 12.36$ $Re_D = 19400$ $\alpha = 0^\circ$ Exp $S/D = 16.4$ $x = 8.04$

$T_w = 899^\circ R$ $P_{t_{e_n}} = 44.1$ mm Hg $u_1 = 4064$ $\rho_1 u_1 = 9.097 \times 10^{-3}$ $\rho_1 u_1^2 = 36.97$ psf

Y-inches	M	u(fps)	T_t-°R	T_s-°R	$\frac{\rho u}{\rho_1 u_1}$	$\frac{\rho u^2}{\rho_1 u_1^2}$	$\frac{u}{u_1}$	P_{t_e} - mm Hg
.90	3.264	4095	2044	652	1.072	1.078	1.007	13.76
.80	3.184	4002	1988	656	1.043	1.025	0.984	13.12
.70	3.110	4005	2019	687	0.995	0.977	0.985	12.54
.60	3.030	3953	2003	705	0.959	0.929	0.972	11.94
.55	2.974	3900	1970	712	0.931	0.890	0.959	11.47
.50	2.851	3800	1937	737	0.881	0.822	0.935	10.61
.45	2.696	3694	1922	782	0.813	0.737	0.908	9.56
.40	2.482	3499	1845	824	0.728	0.626	0.858	8.19
.35	2.227	3310	1836	920	0.620	0.502	0.814	6.68
.30	1.938	3028	1790	1023	0.508	0.379	0.745	5.16
.25	1.649	2586	1597	1033	0.431	0.274	0.638	3.86
.20	1.327	2090	1398	1033	0.346	0.176	0.515	2.68
.15	1.069	1636	1214	988	0.286	0.115	0.406	1.92
:10	0.745	1140	1080	972	0.101	0.027	0.280	1.39
.04	0.551	835	1012	957	0.074	0.015	0.205	1.19

TABLE IV (CONTINUED)

Test No. 12-10

$M = 12.36$ $Re_D = 19400$ $\alpha = 0^\circ$ Exp $S/D = 22.5$ $x = 11.13$

$T_w = 885^\circ R$ $P_{t_{2n}} = 44.1$ mm Hg $u_1 = 4133$ $\rho_1 u_1 = 7.784 \times 10^{-3}$ $\rho_1 u_1^2 = 32.17$ psf

Y-inches	M	u(fps)	$T_s - ^\circ R$	$T_t - ^\circ R$	$\frac{\rho u}{\rho_1 u_1}$	$\frac{\rho u^2}{\rho_1 u_1^2}$	$\frac{u}{u_1}$	P_{t_2} - mm Hg
0.91	3.362	4146	633	2049	1.022	1.026	1.002	11.41
0.81	3.297	4114	648	2051	0.990	0.986	0.995	10.98
0.71	3.216	4078	668	2046	0.952	0.938	0.986	10.47
0.66	3.147	4011	676	2007	0.927	0.898	0.969	10.03
0.61	3.060	3932	687	1968	0.892	0.849	0.950	9.50
0.56	2.937	3807	699	1894	0.852	0.783	0.919	8.80
0.51	2.787	3696	731	1853	0.789	0.705	0.894	7.96
0.46	2.610	3531	761	1784	0.726	0.619	0.853	7.04
0.41	2.395	3336	806	1720	0.647	0.522	0.806	5.99
0.36	2.160	3054	837	1602	0.571	0.423	0.740	4.92
0.31	1.896	2765	886	1517	0.486	0.326	0.669	3.88
0.26	1.625	2386	904	1366	0.411	0.238	0.580	2.94
0.21	1.319	1965	919	1239	0.332	0.158	0.473	2.07
0.16	0.986	1492	951	1126	0.246	0.088	0.361	1.43
0.11	0.738	1117	952	1055	0.184	0.050	0.270	1.09

TABLE IV (CONTINUED)

Test No. 12-11

$M = 12.26$ $Re_D = 12700$ $\alpha = 0^{\circ}$ Exp $S/D = 8.3$ $x = 4.0$

$T_w = 1025^{\circ}R$ $P_{t_{e}n} = 29$ mm Hg $u_1 = 3854$ $\rho_1 u_1 = 9.097 \times 10^{-3}$ $\rho_1 u_1^2 = 35.06$ psf

Y-inches	M	u(fps)	T_t-°R	T_s-°R	$\frac{\rho u}{\rho_1 u_1}$	$\frac{\rho u^2}{\rho_1 u_1^2}$	$\frac{u}{u_1}$	P_{t_e} - mm Hg
0.72	2.743	3906	2109	846	1.002	1.014	1.012	12.47
0.67	2.690	3814	2055	836	0.989	0.978	0.990	12.04
0.62	2.653	3788	2050	848	0.967	0.950	0.981	11.70
0.57	2.613	3735	2018	850	0.951	0.921	0.968	11.38
0.52	2.579	3733	2043	874	0.926	0.897	0.968	11.09
0.47	2.548	3702	2029	880	0.911	0.876	0.959	10.83
0.42	2.505	3708	2063	914	0.880	0.847	0.962	10.51
0.37	2.426	3557	1961	896	0.860	0.794	0.923	9.89
0.32	2.275	3371	1850	914	0.798	0.700	0.875	8.77
0.27	2.041	3070	1714	938	0.708	0.564	0.797	7.19
0.22	1.706	2660	1601	1021	0.563	0.391	0.694	5.17
0.17	1.315	2109	1439	1081	0.423	0.231	0.549	3.31
0.12	0.911	1509	1315	1138	0.287	0.112	0.392	2.11
0.06	0.479	777	1138	1091	0.154	0.032	0.201	1.43

TABLE IV (CONTINUED)

Test No. 12-12

$M = 12.26$ $Re_D = 12700$ $\alpha = 0^\circ$ Exp $S/D = 16.4$ $x = 8.04$

$T_w = 950^\circ R$ $P_{t_{2n}} = 29$ mm Hg $u_1 = 3921$ $\rho_1 u_1 = 6.357 \times 10^{-3}$ $\rho_1 u_1^2 = 24.92$ psf

Y-inches	M	u(fps)	T_t-°R	T_s-°R	$\frac{\rho u}{\rho_1 u_1}$	$\frac{\rho u^2}{\rho_1 u_1^2}$	$\frac{u}{u_1}$	P_{t_2} - mm Hg
.93	3.303	4128	2054	646	1.015	1.066	1.051	9.19
.83	3.233	4086	2050	664	0.980	1.021	1.043	8.82
.73	3.150	4083	2075	696	0.932	0.968	1.041	8.37
.68	3.094	4027	2053	704	0.910	0.935	1.028	8.10
.63	3.008	3971	2038	723	0.876	0.886	1.012	7.69
.58	2.913	3926	2040	756	0.829	0.829	1.001	7.22
.53	2.785	3851	2028	794	0.776	0.759	0.980	6.63
.48	2.602	3784	2074	881	0.687	0.663	0.966	5.83
.43	2.382	3586	2011	940	0.609	0.555	0.914	4.94
.38	2.136	3257	1858	968	0.537	0.448	0.829	4.04
.33	1.880	2921	1704	994	0.467	0.346	0.741	3.20
.28	1.600	2470	1506	994	0.395	0.250	0.628	2.41
.23	1.338	2092	1374	1011	0.332	0.174	0.531	1.78
.18	1.076	1679	1261	1024	0.262	0.112	0.427	1.26
.13	0.811	1283	1179	1039	0.098	0.031	0.326	0.97
.07	0.569	904	1116	1044	0.069	0.015	0.230	0.78

TABLE IV (CONTINUED)

Test No. 12-13

$M = 12.26$ $Re_D = 12700$ $\alpha = 0^0$ Exp $S/D = 22.5$ $x = 11.13$

$T_w = 900^0R$ $P_{t_{2n}} = 29$ mm Hg $u_1 = 4116$ $\rho_1 u_1 = 5.35 \times 10^{-3}$ $\rho_1 u_1^2 = 22.02$ psf

Y-inches	M	u(fps)	T_t-^0R	T_s-^0R	$\frac{\rho u}{\rho_1 u_1}$	$\frac{\rho u^2}{\rho_1 u_1^2}$	$\frac{u}{u_1}$	P_{t_2} - mm Hg
0.91	3.234	4102	2071	669	0.977	0.974	0.995	7.47
0.81	3.143	4068	2080	698	0.930	0.918	0.987	7.06
0.71	3.008	3945	2018	717	0.880	0.843	0.958	6.50
0.66	2.918	3945	2043	761	0.828	0.793	0.957	6.13
0.61	2.802	3841	1998	782	0.784	0.732	0.932	5.67
0.56	2.665	3705	1941	806	0.736	0.662	0.900	5.16
0.51	2.503	3574	1903	850	0.670	0.584	0.867	4.58
0.46	2.316	3385	1830	890	0.607	0.498	0.821	3.95
0.41	2.116	3160	1752	930	0.542	0.417	0.767	3.35
0.36	1.903	2903	1660	970	0.478	0.338	0.706	2.76
0.31	1.672	2601	1565	1012	0.411	0.260	0.635	2.19
0.26	1.410	2235	1452	1040	0.341	0.185	0.542	1.64
0.21	1.187	1900	1371	1079	0.280	0.130	0.460	1.23
0.16	0.900	1450	1240	1079	0.214	0.076	0.352	0.91
0.11	0.641	1033	1153	1081	0.153	0.039	0.251	0.70
0.05	0.440	667	992	957	0.109	0.018	0.162	0.61

TABLE IV (CONTINUED)

Test No. 12-14

$M = 12.08$ $Re_D = 8700$ $\alpha = 0^\circ$ Exp $S/D = 8.3$ $x = 4.0$

$T_w = 1060^\circ R$ $P_{t_{2n}} = 20.5$ mm Hg $u_1 = 3923$ $\rho_1 u_1 = 5.942 \times 10^{-3}$ $\rho_1 u_1^2 = 23.31$ psf

Y-inches	M	u(fps)	T_t-°R	T_s-°R	$\frac{\rho u}{\rho_1 u_1}$	$\frac{\rho u^2}{\rho_1 u_1^2}$	$\frac{u}{u_1}$	P_{t_2} - mm Hg
1.00	3.392	4172	2068	628	1.327	1.415	1.062	11.41
0.92	3.241	4097	2062	666	1.234	1.290	1.043	10.43
0.82	3.085	4008	2041	702	1.143	1.170	1.020	9.49
0.72	2.956	3988	2087	758	1.055	1.076	1.016	8.74
0.67	2.902	3955	2084	776	1.024	1.034	1.007	8.43
0.62	2.854	3932	2066	792	0.997	1.001	1.000	8.16
0.57	2.808	3878	2052	797	0.977	0.969	0.988	7.92
0.52	2.768	3872	2069	818	0.951	0.942	0.986	7.71
0.47	2.707	3860	2093	848	0.914	0.900	0.982	7.39
0.42	2.611	3746	2031	858	0.876	0.838	0.954	6.91
0.37	2.456	3577	1930	881	0.813	0.742	0.911	6.15
0.32	2.243	3356	1856	933	0.721	0.618	0.853	5.19

TABLE IV (CONTINUED)

Test No. 12-15

$M = 12.08$ $Re_D = 8700$ $\alpha = 0^0$ Exp $S/D = 16.4$ $x = 8.04$

$T_w = 780^oR$ $P_{t_{2n}} = 20.5$ mm Hg $u_1 = 4024$ $\rho_1 u_1 = 4.481 \times 10^{-3}$ $\rho_1 u_1^2 = 18.03$ psf

Y-inches	M	u(fps)	T_t-^oR	T_s-^oR	$\frac{\rho u}{\rho_1 u_1}$	$\frac{\rho u^2}{\rho_1 u_1^2}$	$\frac{u}{u_1}$	P_{t_2} - mm Hg
.94	3.120	4046	2048	698	1.039	1.040	1.005	6.56
.84	3.017	4000	2044	729	0.983	0.974	0.993	6.15
.74	2.891	3955	2085	783	0.910	0.894	0.982	5.66
.64	2.686	3791	2032	831	0.821	0.771	0.940	4.93
.59	2.555	3725	2041	886	0.754	0.697	0.924	4.47
.54	2.380	3556	1969	927	0.689	0.610	0.883	3.93
.49	2.201	3335	1881	958	0.624	0.518	0.828	3.39
.44	2.012	3205	1906	1056	0.544	0.431	0.795	2.86
.39	1.808	2855	1713	1043	0.494	0.351	0.712	2.37
.34	1.590	2550	1602	1074	0.426	0.271	0.634	1.89
.29	1.351	2211	1509	1113	0.357	0.197	0.552	1.44
.24	1.170	1904	1401	1107	0.309	0.145	0.472	1.14
.19	0.914	1470	1253	1078	0.244	0.090	0.366	0.87

TABLE IV (CONTINUED)

Test No. 12-16

$M = 12.08$ $\quad Re_D = 8700$ $\quad \alpha = 0^\circ$ Exp $\quad S/D = 22.5$ $\quad x = 11.13$

$T_w = 820^\circ R$ $\quad P_{t_{2n}} = 20.5$ mm Hg $\quad u_1 = 4094$ $\quad \rho_1 u_1 = 3.867 \times 10^{-3}$ $\quad \rho_1 u_1^2 = 15.83$ psf

Y-inches	M	u(fps)	T_t-°R	T_s-°R	$\frac{\rho u}{\rho_1 u_1}$	$\frac{\rho u^2}{\rho_1 u_1^2}$	$\frac{u}{u_1}$	P_{t_2} - mm Hg
.87	3.100	4043	2055	707	0.937	0.926	0.987	5.10
.82	3.000	3970	2032	728	0.894	0.866	0.969	4.78
.77	2.891	3860	1965	742	0.857	0.809	0.942	4.47
.72	2.766	3785	1964	781	0.798	0.738	0.923	4.10
.67	2.625	3630	1879	795	0.753	0.668	0.887	3.73
.62	2.486	3516	1849	836	0.694	0.597	0.858	3.35
.57	2.318	3310	1745	849	0.645	0.523	0.809	2.95
.52	2.155	3120	1663	870	0.592	0.450	0.761	2.58
.47	1.991	2910	1579	890	0.538	0.383	0.712	2.22
.42	1.810	2665	1480	907	0.482	0.316	0.650	1.86
.37	1.564	2205	1226	835	0.434	0.236	0.540	1.44
.32	1.428	2160	1328	953	0.373	0.197	0.530	1.24
.27	1.256	1925	1299	994	0.320	0.152	0.471	1.00
.22	1.080	1650	1207	986	0.279	0.114	0.404	0.80
.17	0.812	1222	1057	939	0.216	0.064	0.298	0.61
.12	0.653	963	975	901	0.176	0.042	0.235	0.53

TABLE IV (CONTINUED)

Test No. 12-17

$M = 12.36$ $Re_D = 19400$ $\alpha = 5^o$ Comp $S/D = 22.5$ $x = 11.13$

$T_w = 847^oR$ $P_{t_2n} = 44.1$ mm Hg $u_1 = 3988$ $\rho_1 u_1 = 10.656 \times 10^{-3}$ $\rho_1 u_1^2 = 42.50$ psf

Y-inches	M	u(fps)	T_t-°R	T_s-°R	$\frac{\rho u}{\rho_1 u_1}$	$\frac{\rho u^2}{\rho_1 u_1^2}$	$\frac{u}{u_1}$	P_{t_2} - mm Hg
.80	3.193	4078	2048	678	1.120	1.142	1.022	16.81
.70	3.089	4035	2054	707	1.060	1.072	1.010	15.81
	3.048	4001	2047	718	1.040	1.044	1.003	15.39
.60	2.997	3966	2040	729	1.014	1.008	0.993	14.89
.55	2.927	3914	2024	743	0.982	0.969	0.981	14.27
.50	2.842	3823	1976	753	0.949	0.908	0.958	13.49
.45	2.726	3690	1899	761	0.904	0.837	0.924	12.46
.40	2.559	3496	1803	778	0.839	0.736	0.877	11.03
.35	2.348	3290	1710	820	0.749	0.620	0.825	9.37
.30	2.102	2974	1559	836	0.664	0.497	0.747	7.63
.25	1.795	2549	1368	842	0.563	0.384	0.638	5.70
.20	1.447	2056	1183	839	0.457	0.236	0.516	3.95
.15	1.110	1597	1066	865	0.344	0.138	0.400	2.57
.10	0.724	1016	901	816	0.232	0.059	0.254	1.74

TABLE IV (CONTINUED)

Test No. 12-18

$M = 12.26$ $Re_D = 12700$ $\alpha = 5^0$ Comp $S/D = 16.4$ $x = 8.04$

$T_w = 870^0 R$ $P_{t_2 n} = 29$ mm Hg $u_1 = 3906$ $\rho_1 u_1 = 8.259 \times 10^{-3}$ $\rho_1 u_1^2 = 32.26$ psf

Y-inches	M	u(fps)	T_t-^{0}R	T_s-^{0}R	$\frac{\rho u}{\rho_1 u_1}$	$\frac{\rho u^2}{\rho_1 u_1^2}$	$\frac{u}{u_1}$	P_{t_2} - mm Hg
.92	3.179	4088	2070	688	1.215	1.273	1.045	14.22
.82	3.042	4006	2063	723	1.136	1.164	1.025	13.05
.72	2.929	3985	2085	770	1.061	1.082	1.020	12.16
.67	2.876	3920	2060	774	1.037	1.042	1.002	11.73
.62	2.825	3905	2066	796	1.005	1.005	0.999	11.33
.57	2.768	3868	2052	814	0.973	0.965	0.989	10.89
.52	2.684	3800	2041	835	0.934	0.908	0.972	10.29
.47	2.595	3720	2011	856	0.890	0.848	0.952	9.63
.42	2.447	3553	1934	876	0.830	0.757	0.910	8.65
.37	2.267	3343	1830	909	0.752	0.646	0.856	7.47
.32	2.005	3058	1742	965	0.649	0.509	0.783	6.00
.27	1.735	2699	1597	1004	0.548	0.379	0.690	4.60
.22	1.438	2210	1396	983	0.460	0.260	0.566	3.33
.17	1.138	1760	1243	994	0.364	0.164	0.451	2.29
.12	0.819	1267	1127	994	0.262	0.085	0.324	1.63
.06	0.525	781	961	910	0.175	0.035	0.199	1.27

TABLE IV (CONTINUED)

Test No. 12-19

$M = 12.26$ $\qquad Re_D = 12700$ $\qquad \alpha = 5^{o}$ Comp $\qquad S/D = 22.5$ $\qquad x = 11.13$

$T_w = 1067^{o}R$ $\qquad P_{t_2 n} = 29$ mm Hg $\qquad u_1 = 3957$ $\qquad \rho_1 u_1 = 7.511 \times 10^{-3}$ $\qquad \rho_1 u_1^2 = 29.72$ psf

Y-inches	M	u(fps)	T_t-°R	T_s-°R	$\frac{\rho u}{\rho_1 u_1}$	$\frac{\rho u^2}{\rho_1 u_1^2}$	$\frac{u}{u_1}$	P_{t_2} - mm Hg
.90	3.183	4077	2055	681	1.155	1.192	1.030	12.25
.80	3.077	4019	2059	711	1.092	1.110	1.016	11.44
.70	2.975	3974	2059	744	1.036	1.038	1.003	10.74
.65	2.913	3923	2044	757	1.001	0.994	0.991	10.29
.60	2.828	3903	2062	793	0.952	0.938	0.985	9.75
.55	2.722	3792	2018	810	0.908	0.871	0.957	9.08
.50	2.580	3627	1916	821	0.856	0.783	0.916	8.20
.45	2.411	3486	1874	871	0.776	0.682	0.879	7.22
.40	2.170	3200	1745	903	0.688	0.555	0.808	5.96
.35	1.953	2945	1659	949	0.600	0.444	0.743	4.88
.30	1.677	2575	1533	987	0.507	0.330	0.651	3.73
.25	1.388	2190	1412	1024	0.411	0.228	0.554	2.70
.20	1.127	1812	1357	1079	0.326	0.150	0.462	1.94
.15	0.863	1422	1288	1133	0.244	0.088	0.359	1.47
.10	0.635	1043	1207	1120	0.182	0.048	0.264	1.18

TABLE IV (CONTINUED)

Test No. 12-20

$M = 12.36$ $Re_D = 19400$ $\alpha = 10^{\circ}$ Comp $S/D = 16.4$ $x = 8.04$

$T_w = 912^{\circ}R$ $P_{t_{2n}} = 44.1$ mm Hg $u_1 = 3680$ $\rho_1 u_1 = 17.69 \times 10^{-3}$ $\rho_1 u_1^2 = 65.11$ psf

Y-inches	M	u(fps)	T_t-°R	T_s-°R	$\frac{\rho u}{\rho_1 u_1}$	$\frac{\rho u^2}{\rho_1 u_1^2}$	$\frac{u}{u_1}$	P_{t_2} - mm Hg
.32	2.186	3293	1848	945	0.892	0.798	0.895	18.71
.27	2.037	3137	1800	989	0.809	0.692	0.852	16.38
.22	1.779	2786	1678	1023	0.693	0.524	0.755	12.79
.17	1.481	2361	1539	1066	0.564	0.364	0.642	9.29
.12	1.086	1718	1277	1024	0.426	0.197	0.463	5.71
.06	0.567	867	1025	969	0.228	0.055	0.235	3.49

TABLE IV (CONTINUED)

Test No. 12-21

$M = 12.26$ $Re_D = 12700$ $\alpha = 10^\circ$ Comp $S/D = 8.3$ $x = 4.0$

$T_w = 1000^\circ R$ $P_{t_2 n} = 29$ mm Hg $u_1 = 3609$ $\rho_1 u_1 = 12.85 \times 10^{-3}$ $\rho_1 u_1^2 = 46.39$ psf

Y-inches	M	u(fps)	T_t-°R	T_s-°R	$\frac{\rho u}{\rho_1 u_1}$	$\frac{\rho u^2}{\rho_1 u_1^2}$	$\frac{u}{u_1}$	P_{t_2} - mm Hg
.47	2.517	3726	2053	911	1.104	1.138	1.031	18.73
.42	2.442	3631	2033	924	1.066	1.073	1.007	17.73
.37	2.371	3577	2026	947	1.025	1.014	0.991	16.81
.27	2.226	3457	1995	1006	0.934	0.894	0.958	14.94
.22	2.029	3207	1903	1040	0.836	0.742	0.889	12.58
.17	1.686	2790	1770	1138	0.658	0.508	0.772	8.98
.12	1.243	2100	1548	1192	0.474	0.276	0.582	5.38
.06	0.746	1183	1162	1046	0.308	0.101	0.327	3.14

TABLE V

Boundary Layer Data, M = 14

Test No. 14-1

$M = 14.28$ $Re_D = 16100$ $\alpha = 5^{\circ}$ Exp $S/D = 8.3$ $x = 4.0$

$T_w = 1100^{\circ}R$ $P_{t_{2n}} = 24.8$ mm Hg $u_1 = 3956.2$ $\rho_1 u_1 = 5.935 \times 10^{-3}$ $\rho_1 u_1^2 = 23.48$ psf

Y-inches	M	u(fps)	T_t-°R	T_s-°R	$\frac{\rho u}{\rho_1 u_1}$	$\frac{\rho u^2}{\rho_1 u_1^2}$	$\frac{u}{u_1}$	P_{t_2} - mm Hg
1.14	3.991	4183	1899	456.8	1.282	1.356	1.056	11.05
1.04	3.823	4156	1904	489.5	1.187	1.246	1.049	10.17
0.95	3.696	4106	1906	512.8	1.120	1.161	1.036	9.51
0.85	3.586	4097	1915	542.8	1.057	1.093	1.035	8.97
0.75	3.496	4037	1914	555.3	1.022	1.042	1.021	8.55
0.70	3.466	4034	1910	562.8	1.006	1.025	1.018	8.41
0.65	3.431	4016	1893	570.3	0.988	1.002	1.014	8.24
0.60	3.411	3999	1898	571.8	0.981	0.990	1.010	8.15
0.55	3.382	4004	1905	581.3	0.964	0.975	1.012	8.02
0.50	3.343	3986	1898	590.3	0.944	0.950	1.006	7.83
0.45	3.265	3925	1873	600.5	0.915	0.908	0.992	7.48
0.40	3.121	3803	1814	617.8	0.862	0.828	0.960	6.85
0.35	2.906	3592	1693	634.5	0.792	0.720	0.907	5.98
0.30	2.611	3341	1592	677.5	0.689	0.584	0.844	4.89
0.25	2.237	2900	1386	699.0	0.581	0.427	0.734	3.65
0.20	1.850	2510	1285	775.3	0.456	0.290	0.636	2.57
0.15	1.500	2135	1184	833.0	0.356	0.192	0.536	1.80

TABLE V (CONTINUED)

Test No. 14-2

$M = 14.28$ $Re_D = 16100$ $\alpha = 5^\circ$ Exp $S/D = 16.4$ $x = 8.04$

$T_w = 920^\circ R$ $P_{ten} = 24.8$ mm Hg $u_1 = 4051.4$ $\rho_1 u_1 = 4.966 \times 10^{-3}$ $\rho_1 u_1^2 = 20.12$ psf

Y-inches	M	u(fps)	T_t-°R	T_s-°R	$\frac{\rho u}{\rho_1 u_1}$	$\frac{\rho u^2}{\rho_1 u_1^2}$	$\frac{u}{u_1}$	P_{t2} - mm Hg
1.13	3.125	3917	1911	650.8	0.950	0.918	0.965	6.44
1.04	3.067	3887	1904	664.8	0.919	0.882	0.956	6.20
0.94	3.016	3858	1906	680.3	0.896	0.852	0.951	6.01
0.84	2.953	3816	1889	691.3	0.870	0.818	0.940	5.77
0.79	2.916	3795	1877	704.0	0.850	0.796	0.935	5.62
0.74	2.846	3785	1893	737.0	0.812	0.756	0.932	5.36
0.69	2.760	3739	1888	763.0	0.774	0.715	0.923	5.08
0.64	2.656	3628	1836	776.3	0.740	0.664	0.894	4.73
0.59	2.550	3563	1818	814.5	0.692	0.609	0.878	4.37
0.54	2.385	3425	1785	855.3	0.635	0.535	0.845	3.86
0.49	2.222	3296	1743	916.0	0.568	0.463	0.815	3.37
0.44	2.050	3095	1658	941.8	0.518	0.395	0.762	2.92
0.39	1.853	2840	1574	972.8	0.460	0.321	0.700	2.43
0.34	1.631	2578	1521	1042.0	0.391	0.248	0.638	1.93
0.29	1.436	2304	1459	1082.0	0.338	0.192	0.569	1.55
0.24	1.180	1885	1315	1075.0	0.279	0.130	0.465	1.13
0.19	0.933	1552	1289	1149.0	0.210	0.081	0.382	0.87
0.14	0.668	1076	1118	1077.0	0.156	0.041	0.265	0.66
0.11	0.544	860	1065	1038.0	0.132	0.028	0.213	0.60

TABLE V (CONTINUED)

Test No. 14-3

$M = 14.28$ $Re_D = 16100$ $\alpha = 5^{\circ}$ Exp $S/D = 22.5$ $x = 11.13$

$T_w = 850^{\circ}R$ $P_{t_2 n} = 24.8$ mm Hg $u_1 = 4048$ $\rho_1 u_1 = 4.797 \times 10^{-3}$ $\rho_1 u_1^2 = 19.42$ psf

Y-inches	M	u(fps)	T_t-°R	T_s-°R	$\frac{\rho u}{\rho_1 u_1}$	$\frac{\rho u^2}{\rho_1 u_1^2}$	$\frac{u}{u_1}$	P_{t_2} - mm Hg
1.25	2.882	3781	1896	715	0.851	0.802	0.933	5.39
1.15	2.833	3750	1899	731	0.827	0.775	0.926	5.21
1.05	2.776	3731	1899	751	0.780	0.744	0.922	5.01
0.95	2.703	3710	1909	782	0.763	0.706	0.915	4.76
0.89	2.649	3697	1911	811	0.734	0.675	0.912	4.58
0.85	2.592	3646	1898	825	0.713	0.648	0.901	4.40
0.80	2.519	3552	1838	824	0.692	0.611	0.875	4.16
0.75	2.413	3506	1858	879	0.644	0.562	0.865	3.85
0.70	2.311	3418	1844	909	0.605	0.516	0.843	3.55
0.65	2.193	3316	1829	951	0.561	0.464	0.818	3.22
0.60	2.055	3160	1780	983	0.517	0.407	0.781	2.85
0.55	1.915	2985	1728	1017	0.472	0.353	0.739	2.50
0.50	1.735	2697	1578	1003	0.430	0.290	0.664	2.10
0.45	1.580	2506	1552	1055	0.382	0.240	0.618	1.78
0.40	1.424	2310	1524	1104	0.337	0.196	0.572	1.49
0.35	1.232	2027	1463	1141	0.288	0.147	0.504	1.18
0.30	1.076	1713	1288	1054	0.259	0.111	0.420	0.95
0.25	0.925	1500	1263	1092	0.220	0.082	0.370	0.84
0.22	0.863	1360	1175	1027	0.212	0.071	0.335	0.78

TABLE V (CONTINUED)

Test No. 14-4

$M = 14.28$ $Re_D = 16100$ $\alpha = 0^{\circ}$ Exp $S/D = 8.3$ $x = 4.0$

$T_w = 900^{\circ}R$ $P_{t_2 n} = 24.8$ mm Hg $u_1 = 3839$ $\rho_1 u_1 = 7.386 \times 10^{-3}$ $\rho_1 u_1^2 = 28.358$ psf

Y-inches	M	u(fps)	T_t-°R	T_s-°R	$\frac{\rho u}{\rho_1 u_1}$	$\frac{\rho u^2}{\rho_1 u_1^2}$	$\frac{u}{u_1}$	P_{t_2} - mm Hg
.75	2.950	3781	1917	703	1.128	1.111	0.984	11.05
.70	2.899	3682	1862	691	1.118	1.073	0.958	10.69
.65	2.855	3631	1825	692	1.100	1.040	0.944	10.39
.60	2.818	3707	1903	741	1.050	1.014	0.964	10.12
.55	2.785	3675	1884	743	1.037	0.993	0.956	9.93
.50	2.755	3653	1886	755	1.019	0.970	0.951	9.71
.45	2.706	3609	1889	761	0.999	0.940	0.939	9.42
.40	2.645	3480	1782	738	0.990	0.898	0.904	9.02
.35	2.524	3530	1912	839	0.885	0.813	0.918	8.23
.30	2.318	3259	1772	848	0.810	0.688	0.849	7.03
.25	2.040	2952	1658	901	0.688	0.530	0.768	5.53
.20	1.662	2415	1411	906	0.556	0.352	0.628	3.82
.15	1.245	1713	1068	810	0.444	0.198	0.444	2.36
.12	1.052	1300	814	661	0.416	0.141	0.339	1.82
.09	0.814	908	601	530	0.359	0.086	0.236	1.46

TABLE V (CONTINUED)

Test No. 14-5

$M = 14.28$ $Re_D = 16100$ $\alpha = 0^{\circ}$ Exp $S/D = 16.4$ $x = 8.04$

$T_W = 700^{\circ}R$ $P_{t_2 n} = 24.8$ mm Hg $u_1 = 3958.17$ $\rho_1 u_1 = 5.704 \times 10^{-3}$ $\rho_1 u_1^2 = 22.57$ psf

Y-inches	M	u(fps)	T_t-$^{\circ}$R	T_s-$^{\circ}$R	$\frac{\rho u}{\rho_1 u_1}$	$\frac{\rho u^2}{\rho_1 u_1^2}$	$\frac{u}{u_1}$	P_{t_2} - mm Hg
.75	3.011	3852	1912	682.5	1.003	0.977	0.973	7.68
.70	2.965	3844	1929	697.3	0.975	0.949	0.971	7.46
.65	2.896	3780	1900	707.5	0.948	0.905	0.954	7.13
.60	2.816	3764	1931	743.0	0.901	0.858	0.950	6.77
.55	2.709	3691	1915	773.3	0.850	0.792	0.931	6.28
.50	2.565	3510	1820	781.0	0.802	0.710	0.886	5.67
.45	2.395	3336	1735	807.3	0.736	0.620	0.843	4.99
.40	2.184	3084	1636	832.3	0.660	0.516	0.781	4.20
.35	1.963	2810	1523	855.0	0.584	0.415	0.710	3.44
.30	1.712	2471	1387	870.3	0.504	0.315	0.625	2.69
.25	1.430	2095	1260	893.0	0.415	0.219	0.527	1.98
.20	1.180	1691	1103	862.3	0.347	0.148	0.427	1.44
.15	0.932	1326	982.3	841.8	0.281	0.094	0.335	1.11

TABLE V (CONTINUED)

Test No. 14-6

$M = 14.28$ $Re_D = 16100$ $\alpha = 0^\circ$ Exp $S/D = 22.5$ $x = 11.13$

$T_w = 950^\circ R$ $P_{t_2 n} = 24.8$ mm Hg $u_1 = 4043$ $\rho_1 u_1 = 5.049 \times 10^{-3}$ $\rho_1 u_1^2 = 20.41$ psf

Y-inches	M	u(fps)	T_t-°R	T_s-°R	$\frac{\rho u}{\rho_1 u_1}$	$\frac{\rho u^2}{\rho_1 u_1^2}$	$\frac{u}{u_1}$	P_{t_2} - mm Hg
.94	3.178	3921	1895	630.8	0.991	0.960	0.968	6.78
.84	3.096	3887	1914	653.3	0.946	0.910	0.960	6.44
.74	2.977	4062	2155	774.0	0.841	0.844	1.003	5.99
.69	2.903	3862	1985	735.5	0.838	0.780	0.954	5.69
.64	2.807	3772	1947	752.8	0.802	0.749	0.933	5.34
.59	2.678	3671	1907	780.8	0.751	0.682	0.907	4.88
.54	2.539	3522	1847	802.3	0.704	0.612	0.871	4.41
.49	2.369	3316	1742	817.8	0.648	0.532	0.819	3.87
.44	2.177	3119	1666	850.3	0.586	0.452	0.771	3.32
.39	1.967	2915	1626	914.8	0.509	0.368	0.721	2.75
.34	1.753	2705	1603	990.8	0.435	0.290	0.667	2.23
.29	1.474	2315	1483	1027.0	0.358	0.205	0.571	1.65
.24	1.226	1935	1339	1021.0	0.302	0.143	0.474	1.23
.19	0.924	1481	1242	1069.0	0.222	0.081	0.366	0.87
.14	0.707	1164	1230	1128.0	0.164	0.048	0.288	0.70
.11	0.602	1008	1254	1167.0	0.138	0.034	0.249	0.64

TABLE V (CONTINUED)

Test No. 14-7

$M = 14.28$ $Re_D = 16100$ $\alpha = 5^{\circ}$ Comp $S/D = 8.3$ $x = 4.0$

$T_w = 1020^{\circ}R$ $P_{t_2 n} = 24.8$ mm Hg $u_1 = 3700$ $\rho_1 u_1 = 9.346 \times 10^{-3}$ $\rho_1 u_1^2 = 34.58$ psf

Y-inches	M	u(fps)	T_t-°R	T_s-°R	$\frac{\rho u}{\rho_1 u_1}$	$\frac{\rho u^2}{\rho_1 u_1^2}$	$\frac{u}{u_1}$	P_{t_2} - mm Hg
.94	3.348	3999	1911	591.8	1.594	1.721	1.080	20.66
.89	3.208	3947	1927	628.5	1.485	1.583	1.068	19.04
.84	3.089	3901	1916	660.5	1.391	1.467	1.052	17.69
.79	2.983	3841	1917	687.3	1.318	1.370	1.037	16.56
.73	2.895	3800	1911	716.8	1.251	1.283	1.026	15.58
.69	2.813	3761	1919	743.8	1.194	1.214	1.017	14.75
.64	2.746	3723	1918	766.0	1.149	1.158	1.006	14.09
.59	2.683	3667	1893	776.0	1.120	1.108	0.990	13.54
.54	2.633	3652	1902	801.0	1.079	1.064	0.984	13.02
.49	2.585	3603	1882	807.8	1.052	1.026	0.972	12.58
.44	2.550	3604	1903	833.8	1.021	0.995	0.974	12.22
.39	2.500	3580	1918	850.5	0.992	0.960	0.965	11.80
.34	2.427	3552	1893	889.8	0.943	0.906	0.958	11.18
.29	2.278	3405	1900	929.0	0.866	0.798	0.921	9.93
.24	2.015	3039	1710	943.0	0.760	0.624	0.821	7.93
.19	1.649	2628	1627	1065.0	0.584	0.414	0.712	5.51
.14	1.241	2053	1463	1140.0	0.423	0.234	0.554	3.42
.11	0.9798	1583	1289	1087.0	0.346	0.148	0.427	2.58
.04	0.7694	1193	1123	999.3	0.286	0.092	0.322	2.04

TABLE V (CONTINUED)

Test No. 14-8

$M = 14.28$ $Re_D = 16100$ $\alpha = 5^o$ Comp $S/D = 16.4$ $x = 8.04$

$T_w = 950^oR$ $P_{t_2n} = 24.8$ mm Hg $u_1 = 3833.6$ $\rho_1 u_1 = 7.499 \times 10^{-3}$ $\rho_1 u_1^2 = 28.746$ psf

Y-inches	M	u(fps)	T_t-°R	T_s-°R	$\frac{\rho u}{\rho_1 u_1}$	$\frac{\rho u^2}{\rho_1 u_1^2}$	$\frac{u}{u_1}$	P_{t_2} - mm Hg
.84	2.978	3853	1893	693.8	1.149	1.154	1.003	11.52
.75	2.876	3806	1908	727.0	1.088	1.079	0.991	10.81
.65	2.797	3745	1914	745.0	1.042	1.019	0.977	10.23
.60	2.750	3721	1914	761.8	1.014	0.984	0.970	9.89
.55	2.687	3692	1920	785.8	0.977	0.941	0.962	9.48
.50	2.593	3606	1891	807.5	0.929	0.875	0.942	8.85
.45	2.483	3500	1851	827.8	0.880	0.804	0.912	8.18
.40	2.326	3320	1756	843.5	0.816	0.706	0.864	7.24
.35	2.122	3080	1665	879.3	0.730	0.586	0.805	6.10
.30	1.865	2791	1576	937.0	0.618	0.450	0.729	4.80
.26	1.591	2445	1465	985.8	0.51[illegible]	0.326	0.636	3.61
.20	1.270	1964	1289	991.3	0.409	0.208	0.510	2.49
.15	1.013	1595	1222	1039.0	0.317	0.133	0.416	1.76
.12	0.8239	1262	1084	975.3	0.270	0.088	0.329	1.51

TABLE V (CONTINUED)

Test No. 14-9

$M = 14.28$ $Re_D = 16100$ $\alpha = 5^{0}$ Comp $S/D = 22.5$ $x = 11.13$

$T_w = 1050^{o}R$ $P_{t_2 n} = 24.8$ mm Hg $u_1 = 3875.3$ $\rho_1 u_1 = 6.94 \times 10^{-3}$ $\rho_1 u_1^2 = 26.91$ psf

Y-inches	M	u(fps)	T_t-^{o}R	T_s-^{o}R	$\frac{\rho u}{\rho_1 u_1}$	$\frac{\rho u^2}{\rho_1 u_1^2}$	$\frac{u}{u_1}$	P_{t_2} - mm Hg
.64	2.925	3858	1924	723.8	1.048	1.045	0.995	9.76
.54	2.699	3727	1916	792.3	0.928	0.893	0.961	8.40
.49	2.561	3625	1929	832.3	0.858	0.802	0.934	7.59
.44	2.426	3565	1923	896.5	0.784	0.721	0.918	6.87
.39	2.181	3263	1771	933.8	0.689	0.581	0.842	5.62
.34	1.928	3042	1754	1036.0	0.578	0.453	0.783	4.48
.29	1.664	2761	1738	1150.0	0.472	0.337	0.714	3.44
.24	1.373	2311	1586	1183.0	0.387	0.231	0.598	2.49
.19	1.121	1882	1438	1164.0	0.318	0.154	0.484	1.81
.14	0.940	1526	1260	1085.0	0.278	0.108	0.392	1.41
.11	0.800	1286	1206	1072.0	0.235	0.078	0.331	1.29

TABLE V (CONTINUED)

Test No. 14-10

$M = 14.2$ $Re_D = 12700$ $\alpha = 5^{\circ}$ Exp $S/D = 16.4$ $x = 8.04$

$T_w = 840^{\circ}R$ $P_{t_2 n} = 19.9$ mm Hg $u_1 = 4037.88$ $\rho_1 u_1 = 4.02 \times 10^{-3}$ $\rho_1 u_1^2 = 16.233$ psf

Y-inches	M	u(fps)	T_t-°R	T_s-°R	$\frac{\rho u}{\rho_1 u_1}$	$\frac{\rho u^2}{\rho_1 u_1^2}$	$\frac{u}{u_1}$	P_{t_2} - mm Hg
1.14	3.237	3950	1917	619.5	1.032	1.012	0.978	5.69
1.04	3.180	3921	1905	632.3	1.004	0.977	0.971	5.50
0.94	3.108	3875	1895	644.3	0.972	0.933	0.958	5.26
0.84	2.997	3835	1912	682.8	0.909	0.866	0.949	4.90
0.74	2.828	3716	1868	718.0	0.839	0.771	0.920	4.39
0.69	2.711	3626	1849	745.3	0.792	0.712	0.897	4.06
0.64	2.586	3520	1821	776.3	0.737	0.646	0.873	3.70
0.59	2.429	3385	1770	807.8	0.681	0.571	0.838	3.30
0.54	2.266	3181	1651	818.5	0.630	0.496	0.787	2.89
0.49	2.091	2986	1603	849.0	0.572	0.424	0.740	2.50
0.44	1.907	2780	1515	885.3	0.510	0.351	0.686	2.10
0.39	1.721	2545	1446	916.3	0.443	0.284	0.630	1.74
0.34	1.511	2326	1423	918.0	0.384	0.221	0.575	1.40
0.29	1.336	2102	1405	1046.0	0.328	0.172	0.522	1.14
0.24	1.146	1750	1221	971.0	0.292	0.126	0.432	0.89
0.19	0.918	1400	1129	967.0	0.232	0.081	0.346	0.71

TABLE V (CONTINUED)

Test No. 14-11

$M = 14.2$ $\quad Re_D = 12700$ $\quad \alpha = 0^\circ$ Exp $\quad S/D = 16.4$ $\quad x = 8.04$

$T_w = 850^\circ R$ $\quad P_{t_{2n}} = 19.9$ mm Hg $\quad u_1 = 3934.2$ $\quad \rho_1 u_1 = 5.079 \times 10^{-3}$ $\quad \rho_1 u_1^2 = 19.98$ psf

Y-inches	M	u(fps)	T_t-°R	T_s-°R	$\frac{\rho u}{\rho_1 u_1}$	$\frac{\rho u^2}{\rho_1 u_1^2}$	$\frac{u}{u_1}$	P_{t_2} - mm Hg
.94	3.061	3869	1905	665.3	1.068	1.052	0.983	7.29
.84	2.985	3796	1876	672.5	1.039	1.003	0.965	6.96
.79	2.937	3787	1890	690.5	1.008	0.971	0.962	6.74
.74	2.882	3776	1912	716.0	0.973	0.935	0.960	6.51
.69	2.811	3738	1900	735.3	0.936	0.890	0.949	6.20
.64	2.730	3720	1937	773.8	0.889	0.840	0.945	5.88
.59	2.586	3493	1781	760.8	0.847	0.753	0.888	5.29
.54	2.452	3381	1748	789.0	0.789	0.677	0.858	4.80
.49	2.308	3251	1710	829.3	0.724	0.600	0.826	4.27
.39	1.943	2800	1528	866.8	0.594	0.425	0.712	3.11
.34	1.742	2602	1508	935.3	0.510	0.340	0.662	2.54
.29	1.521	2386	1509	1028.0	0.425	0.259	0.605	2.01
.24	1.250	2000	1409	1070.0	0.344	0.176	0.506	1.45
.19	1.045	1673	1311	1069.0	0.288	0.122	0.423	1.10
.14	0.726	1118	1087	985.3	0.210	0.059	0.284	0.82

TABLE V (CONTINUED)

Test No. 14-12

$M = 14.2$ $Re_D = 12700$ $\alpha = 5^{\circ}$ Comp $S/D = 16.4$ $x = 8.04$

$T_w = 900^{\circ}R$ $P_{t_2 n} = 19.9$ mm Hg $u_1 = 3750$ $\rho_1 u_1 = 7.073 \times 10^{-3}$ $\rho_1 u_1^2 = 26.522$ psf

Y-inches	M	u(fps)	T_t-$^{\circ}$R	T_s-$^{\circ}$R	$\frac{\rho u}{\rho_1 u_1}$	$\frac{\rho u^2}{\rho_1 u_1^2}$	$\frac{u}{u_1}$	P_{t_2} - mm Hg
.70	2.691	3685	1906	778.8	1.068	1.048	0.981	9.71
.60	2.572	3601	1902	815.8	0.994	0.953	0.959	8.89
.50	2.397	3480	1898	879.5	0.893	0.828	0.928	7.78
.45	2.273	3307	1801	881.5	0.845	0.744	0.880	7.04
.40	2.125	3190	1773	940.3	0.767	0.651	0.851	6.22
.35	1.938	3000	1732	996.5	0.678	0.543	0.800	5.26
.30	1.744	2745	1645	1032.0	0.596	0.436	0.732	4.32
.25	1.505	2413	1544	1072.0	0.506	0.325	0.644	3.36
.20	1.259	2067	1477	1129.0	0.412	0.230	0.552	2.50
.15	0.969	1603	1337	1136.0	0.316	0.135	0.427	1.82
.10	0.656	1029	1107	1020.0	0.225	0.063	0.274	1.31

TABLE VI

Summary of Boundary Layer Thicknesses

Test No.	α	S/D	$\delta \sim$ in	$\delta^* \sim$ in	$\theta \sim$ in	$P_{t_\delta}/P_{t_{an}}$	$P_{t_{an}} \sim$ mm Hg
				Mach 7			
7-1	15E	8.3	.42	.26	.04	.77	45.18
7-2	15E	16.4	.72	.50	.05	.62	45.18
7-3	10E	22.5	.80	.47	.07	.73	45.18
7-4	0	8.3	.34	.14	.04	1.16	45.18
7-5	0	16.4	.48	.24	.06	1.07	45.18
7-6	0	22.5	.57	.27	.06	1.00	45.18
7-7	10C	8.3	.24	.09	.03	1.10	45.18
7-8	10C	16.4	.32	.17	.03	1.11	45.18
7-9	10C	22.5	.35	.16	.04	1.15	45.18
				Mach 10			
10-1	15E	8.3	.48	.22	.06	.96	45.6
10-2	15E	16.4	.85	.42	.10	.98	45.6
10-3	10E	22.5	.80	.47	.10	.59	45.6
10-4	0	8.3	.30	.15	.04	1.05	45.6
10-5	0	16.4	.52	.19	.08	1.14	45.6
10-6	0	22.5	.60	.26	.09	1.10	45.6
10-7	10C	8.3	.25	.08	.04	1.13	45.6
10-8	10C	16.4	.35	.13	.05	1.19	45.6
10-9	10C	22.5	.38	.13	.06	1.26	45.6

TABLE VI (CONTINUED)

Test No.	α	S/D	$\delta \sim$ in	$\delta^* \sim$ in	$\theta \sim$ in	$P_{t_\delta}/P_{t_{\infty n}}$	$P_{t_{\infty n}} \sim$ mm Hg
				Mach 12			
12-1	15E	8.3	.60	.33	.07	.57	29.0
12-2	10E	22.5	1.04	.50	.06		29.0
12-3	10E	16.4	.90	.51	.10	.70	29.0
12-4	10E	22.5	1.04	.74	.09	.29	29.0
12-5	10E	8.3	.62	.29	.07	.81	20.5
12-6	10E	16.4	1.00	.57	.10	.69	20.5
12-7	10E	22.5	1.25	.75	.14	.26	20.5
12-8	0	8.3	.32	.18	.03	.73	44.12
12-9	0	16.4	.55	.27	.07	.81	44.12
12-10	0	22.5	.71	.32	.07	.94	44.12
12-11	0	8.3	.42	.20	.05	.76	29.0
12-12	0	16.4	.63	.34	.05	.85	29.0
12-13	0	22.5	.69	.37	.07	.[illegible]	29.0
12-14	0	8.3	.47	.23	.04	.90	20.5
12-15	0	16.4	.70	.39	.07	.72	20.5
12-16	0	22.5	.90	.44	.09	.92	20.5
12-17	5C	22.5	.50	.22	.08	.87	44.12
12-18	5C	16.4	.47	.24	.06	.75	29.0
12-19	5C	22.5	.60	.29	.07	.93	29.0
12-20	10C	16.4	.34	.15	.05	.81	44.12
12-21	10C	8.3	.34	.13	.03	1.03	29.0
				Mach 14			
14-1	5E	8.3	.43	.21	.05	1.21	24.8
14-2	5E	16.4	.69	.41	.07	.60	24.8
14-3	5E	22.5	.89	.55	.09	.41	24.8
14-4	0	8.3	.40	.17	.06	.93	24.8
14-5	0	16.4	.65	.30	.08	.91	24.8
14-6	0	22.5	.80	.39	.08	.89	24.8
14-7	5C	8.3	.34	.16	.04	.90	24.8
14-8	5C	16.4	.58	.24	.07	.82	24.8
14-9	5C	22.5	.64	.29	.05	.85	24.8
14-10	5E	16.4	.70	.42	.08	.53	19.9
14-11	0	16.4	.64	.33	.08	.76	19.9
14-12	5C	16.4	.45	.25	.06	.62	19.9

TABLE VII

Summary of Skin Friction Data

Test No.	$x \sim$ in.	α	$(du/dy)_w \sim$ ft/sec ft	$T_w \sim {}^{o}R$	$\tau_w \sim lbf/ft^2$	$\tau_w/q_\infty = C_f$
7-1	4	15^oE	18.75×10^4	1072	11.74×10^{-2}	17.42×10^{-4}
7-2	8	15^oE	9.09×10^4	1057	5.63×10^{-2}	8.35×10^{-4}
7-3	11	10^oE	10.14×10^4	1060	6.29×10^{-2}	9.34×10^{-4}
7-4	4	0^o	19.48×10^4	1055	12.04×10^{-2}	17.86×10^{-4}
7-5	8	0^o	14.63×10^4	997	8.72×10^{-2}	12.94×10^{-4}
7-6	11	0^o	12.82×10^4	910	7.21×10^{-2}	10.69×10^{-4}
7-7	4	10^oC	40.54×10^4	1158	26.68×10^{-2}	39.59×10^{-4}
7-8	8	10^oC	22.73×10^4	883	12.50×10^{-2}	18.54×10^{-4}
7-9	11	10^oC	18.46×10^4	905	10.34×10^{-2}	15.34×10^{-4}

TABLE VII (CONTINUED)

Test No.	x ~ in.	α	$(du/dy)_w$ ~ ft/sec ft	T_W ~ °R	τ_w ~ lbf/ft²	$\tau_w/q_\infty = C_f$
10-1	4	15°E	13.33×10^4	1105	8.49×10^{-2}	12.44×10^{-4}
10-2	8	15°E	13.04×10^4	932	7.45×10^{-2}	10.91×10^{-4}
10-3	11	10°E	8.62×10^4	862	4.67×10^{-2}	6.85×10^{-4}
10-4	4	0°	21.51×10^4	940	12.37×10^{-2}	18.12×10^{-4}
10-5	8	0°	15.39×10^4	1005	9.23×10^{-2}	13.52×10^{-4}
10-6	11	0°	12.47×10^4	1030	7.61×10^{-2}	11.15×10^{-4}
10-7	4	10°C	22.22×10^4	1137	14.44×10^{-2}	21.16×10^{-4}
10-8	8	10°C	17.99×10^4	865	9.77×10^{-2}	14.32×10^{-4}
10-9	11	10°C	15.08×10^4	965	8.80×10^{-2}	12.90×10^{-4}

TABLE VII (CONTINUED)

Test No.	$x \sim$ in.	α	$(du/dy)_w \sim$ ft/sec ft	$T_w \sim {}^\circ R$	$\tau_w \sim lbf/ft^2$	$\tau_w/q_\infty = C_f$
12-1	4	15°E	11.81×10^4	1048	7.26×10^{-2}	16.73×10^{-4}
12-2	11	10°E	9.52×10^4	1060	5.91×10^{-2}	8.95×10^{-4}
12-3	8	10°E	10.53×10^4	1040	6.46×10^{-2}	14.88×10^{-4}
12-4	11	10°E	6.59×10^4	927	3.74×10^{-2}	8.62×10^{-4}
12-5	4	10°E	12.37×10^4	1013	7.47×10^{-2}	24.29×10^{-4}
12-6	8	10°E	9.09×10^4	1010	5.48×10^{-2}	17.81×10^{-4}
12-7	11	10°E	4.65×10^4	853	2.50×10^{-2}	8.12×10^{-4}
12-8	4	0°	21.43×10^4	1050	13.22×10^{-2}	20.00×10^{-4}
12-9	8	0°	12.74×10^4	899	7.10×10^{-2}	10.73×10^{-4}
12-10	11	0°	11.77×10^4	885	6.48×10^{-2}	9.81×10^{-4}
12-11	4	0°	16.58×10^4	1025	10.07×10^{-2}	23.19×10^{-4}
12-12	8	0°	10.91×10^4	950	6.31×10^{-2}	14.52×10^{-4}
12-13	11	0°	10.73×10^4	900	5.98×10^{-2}	13.78×10^{-4}
12-14	4	0°	14.46×10^4	1060	8.98×10^{-2}	29.19×10^{-4}
12-15	8	0°	9.38×10^4	780	4.74×10^{-2}	15.42×10^{-4}
12-16	11	0°	9.45×10^4	820	4.94×10^{-2}	16.07×10^{-4}
12-17	11	5°C	13.27×10^4	847	7.09×10^{-2}	10.72×10^{-4}
12-18	8	5°C	15.58×10^4	870	8.49×10^{-2}	19.56×10^{-4}
12-19	11	5°C	11.43×10^4	1067	7.12×10^{-2}	16.40×10^{-4}
12-20	8	10°C	25.53×10^4	912	14.38×10^{-2}	21.74×10^{-4}
12-21	4	10°C	22.81×10^4	1000	13.64×10^{-2}	31.42×10^{-4}

TABLE VII (CONTINUED)

Test No.	x ~ in.	α	$(du/dy)_w$ ~ ft/sec ft	T_w ~ ^{o}R	τ_w ~ lbf/ft^2	$\tau_w/q_\infty = C_f$
14-1	4	5^{o} E	17.65×10^{4}	1100	11.24×10^{-2}	30.33×10^{-4}
14-2	8	5^{o} E	9.89×10^{4}	920	5.59×10^{-2}	15.07×10^{-4}
14-3	11	5^{o} E	7.40×10^{4}	850	3.97×10^{-2}	10.70×10^{-4}
14-4	4	0^{o}	22.06×10^{4}	900	12.30×10^{-2}	33.19×10^{-4}
14-5	8	0	10.68×10^{4}	700	4.99×10^{-2}	13.47×10^{-4}
14-6	11	0	10.14×10^{4}	950	5.86×10^{-2}	15.807×10^{-4}
14-7	4	5 C	17.49×10^{4}	1020	10.60×10^{-2}	28.60×10^{-4}
14-8	8	5 C	13.54×10^{4}	950	7.83×10^{-2}	21.12×10^{-4}
14-9	11	5 C	13.04×10^{4}	1050	8.05×10^{-2}	21.72×10^{-4}
14-10	8	5 E	9.85×10^{4}	840	5.25×10^{-2}	17.64×10^{-4}
14-11	8	0	12.27×10^{4}	850	6.58×10^{-2}	22.09×10^{-4}
14-12	8	5 C	14.78×10^{4}	900	8.24×10^{-2}	27.68×10^{-4}

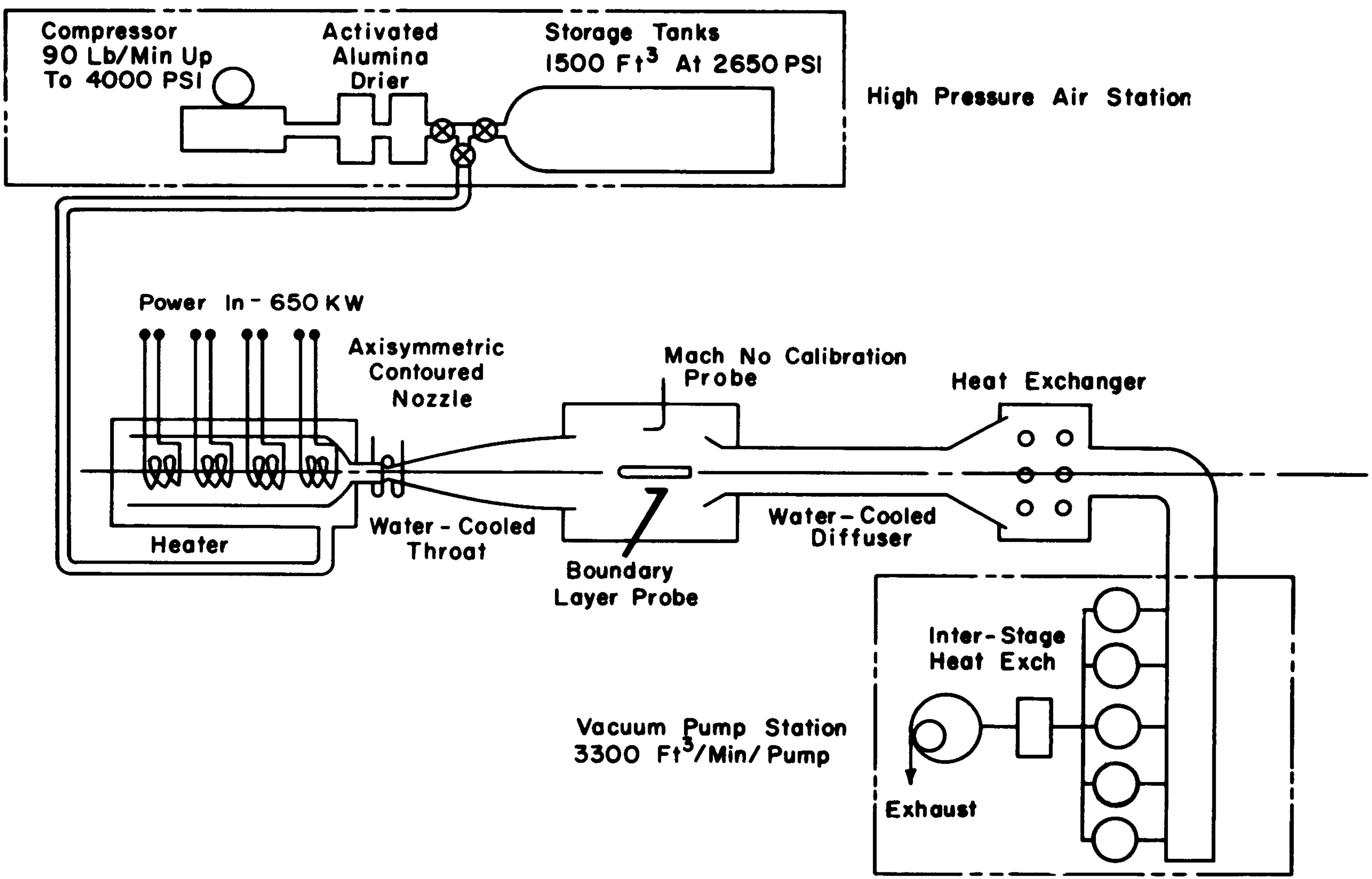

Figure 1 The Ohio State University 12 Inch Hypersonic Wind Tunnel Schematic

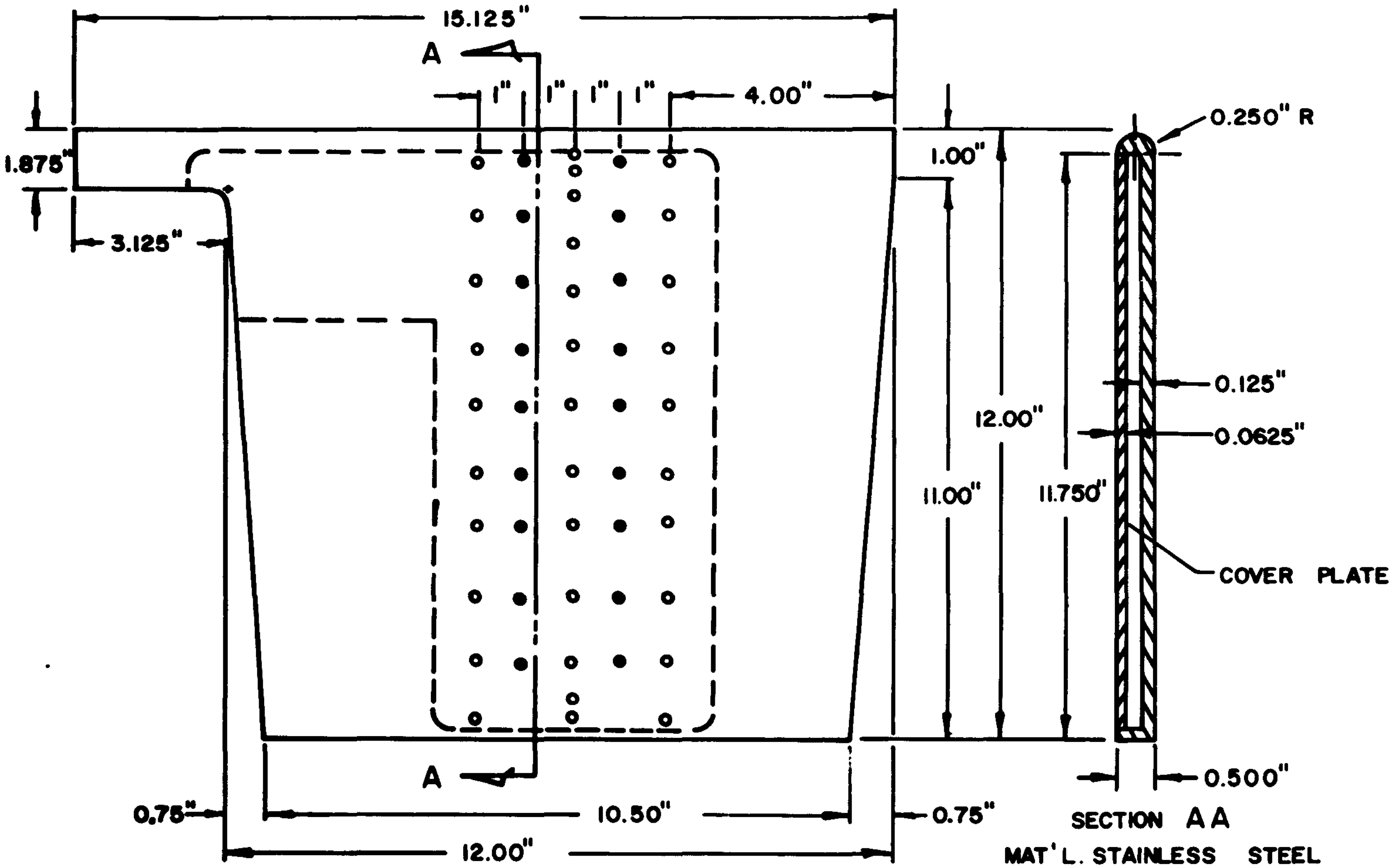

FIG. 2.. DIMENSIONS OF FLAT PLATE MODEL

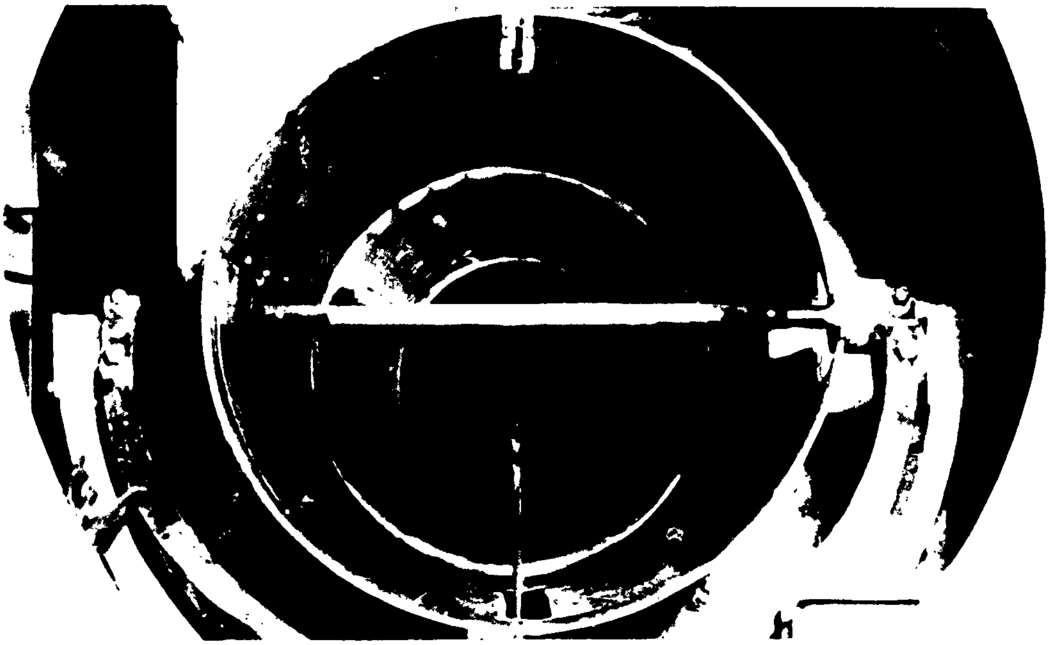

FIG. 3. FLAT PLATE MOUNTED IN WIND TUNNEL

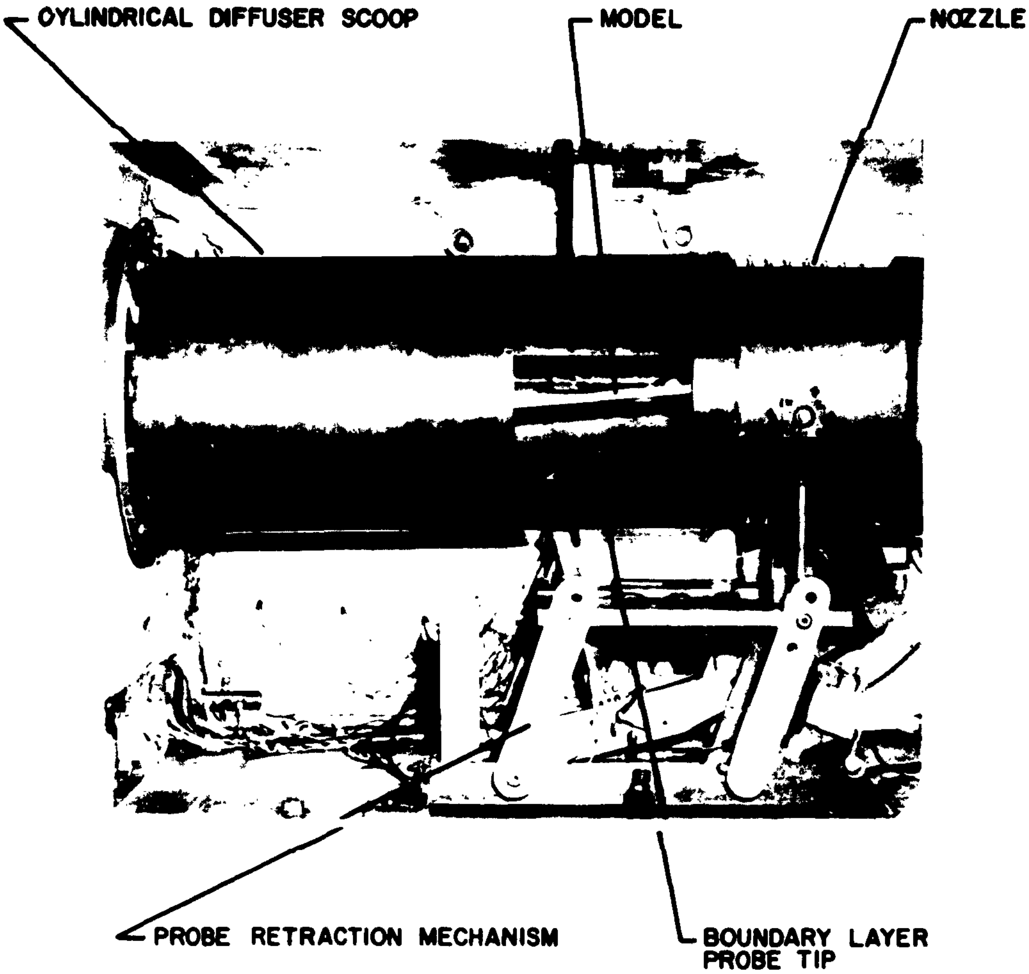

FIG. 4. SIDE VIEW OF MODEL AND PROBE IN TEST CABIN

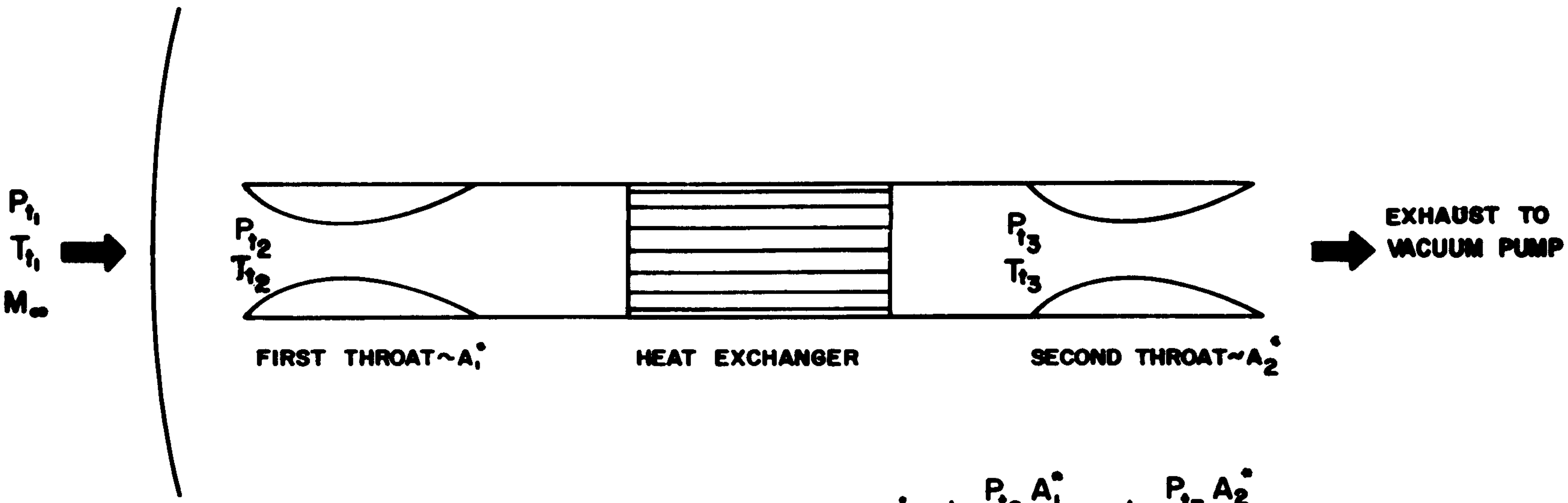

MASS FLOW RATE, BOTH NOZZLES CHOKED= $\dot{m} = k \dfrac{P_{t_2} A_1^*}{\sqrt{T_{t_2}}} = k \dfrac{P_{t_3} A_2^*}{\sqrt{T_{t_3}}}$

FIG. 5. NOMENCLATURE OF BOUNDARY LAYER PROBE

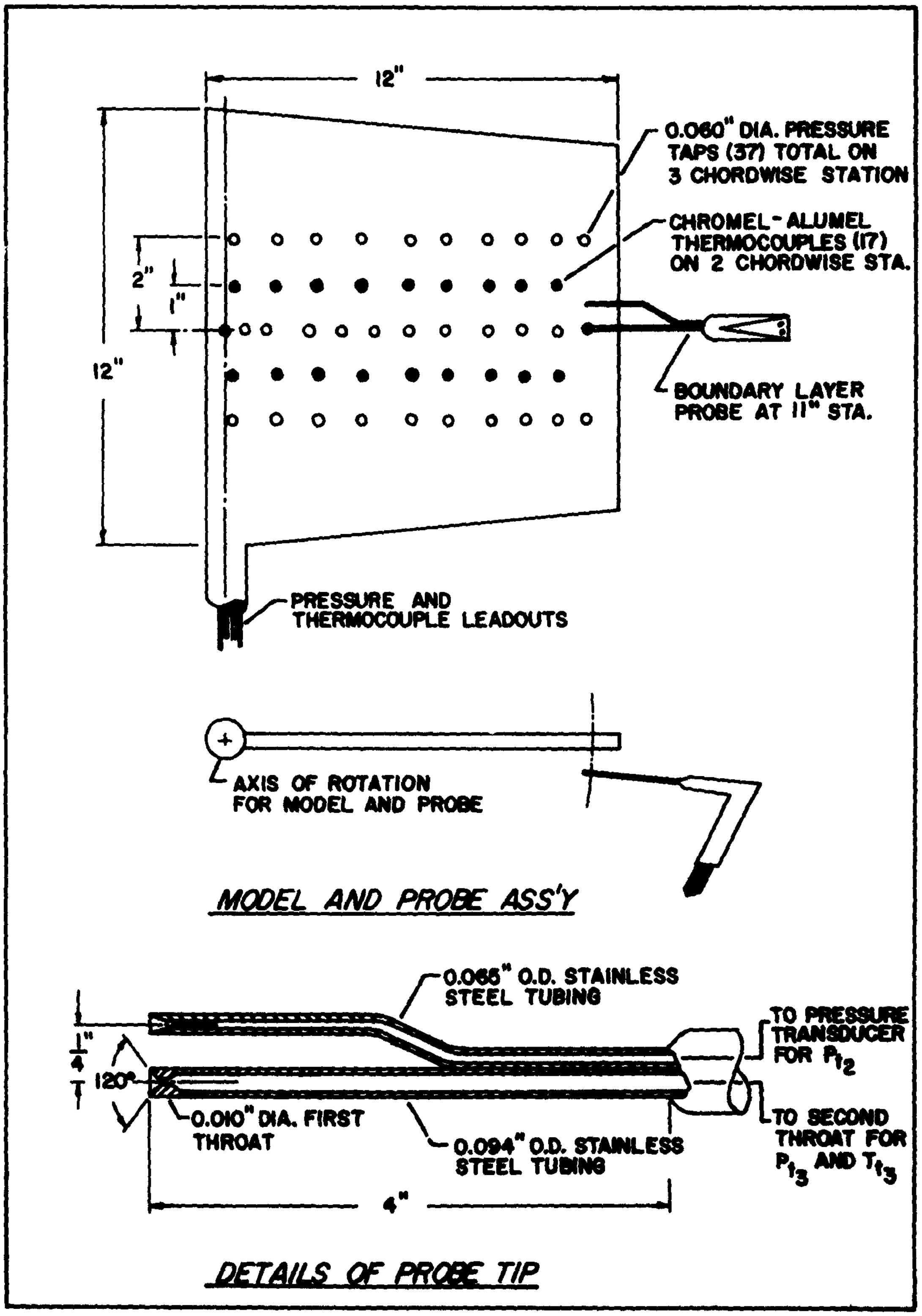

FIG. 6. MODEL AND BOUNDARY LAYER PROBE DIMENSIONS.

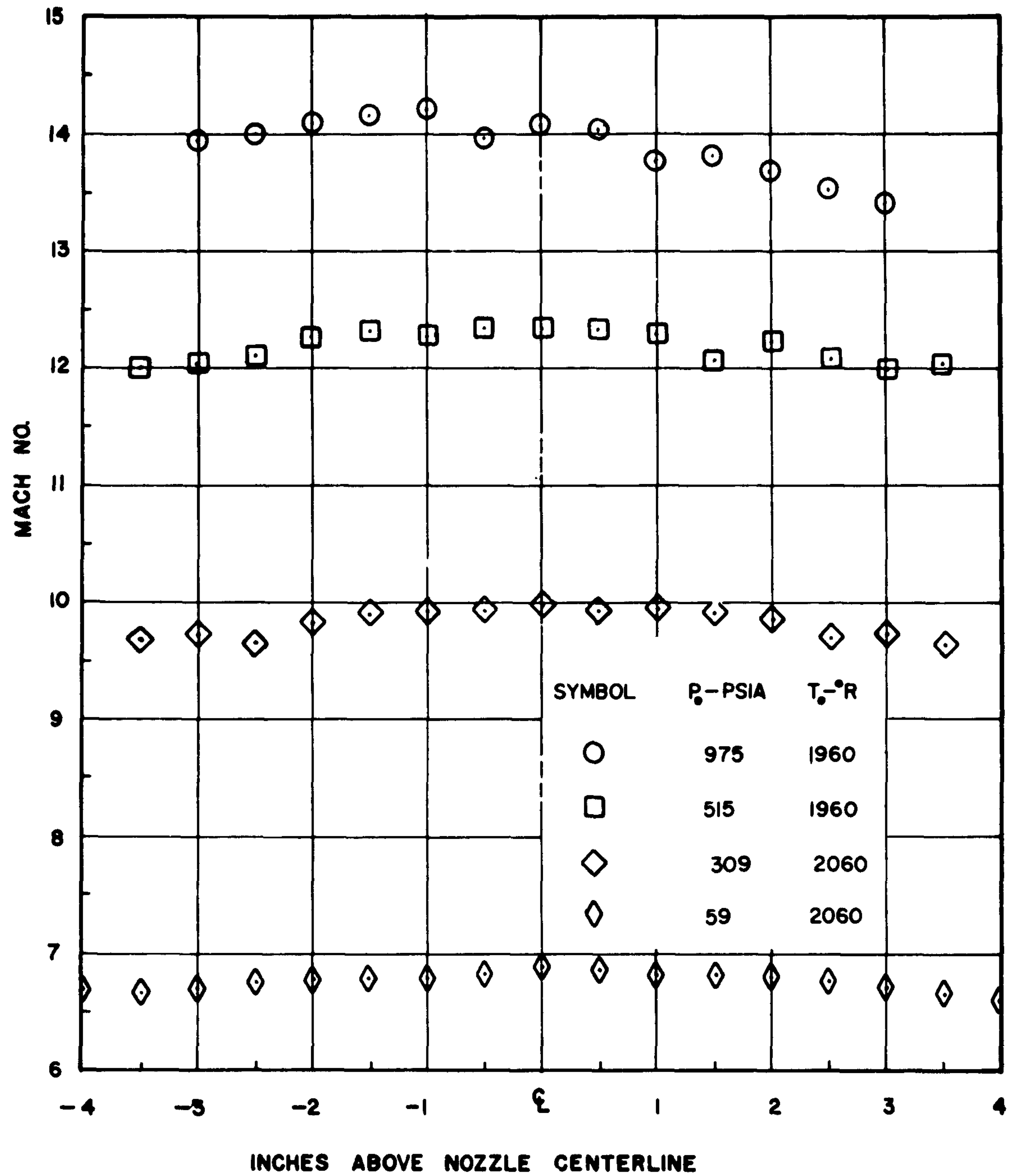

FIG. 7. NOZZLE CALIBRATION AT MODEL LEADING EDGE

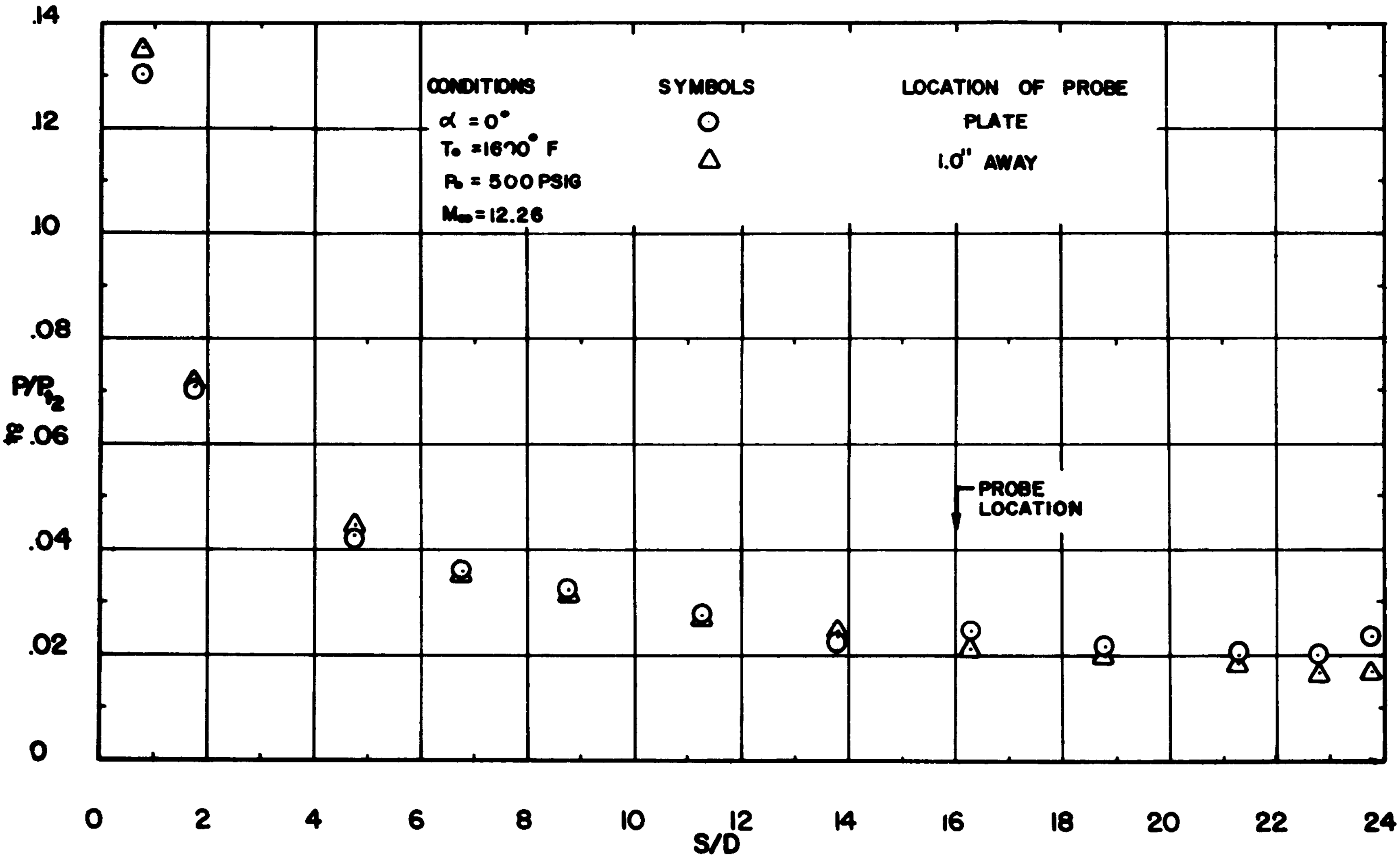

FIG. 8. EFFECT OF PROBE ON PLATE PRESSURE

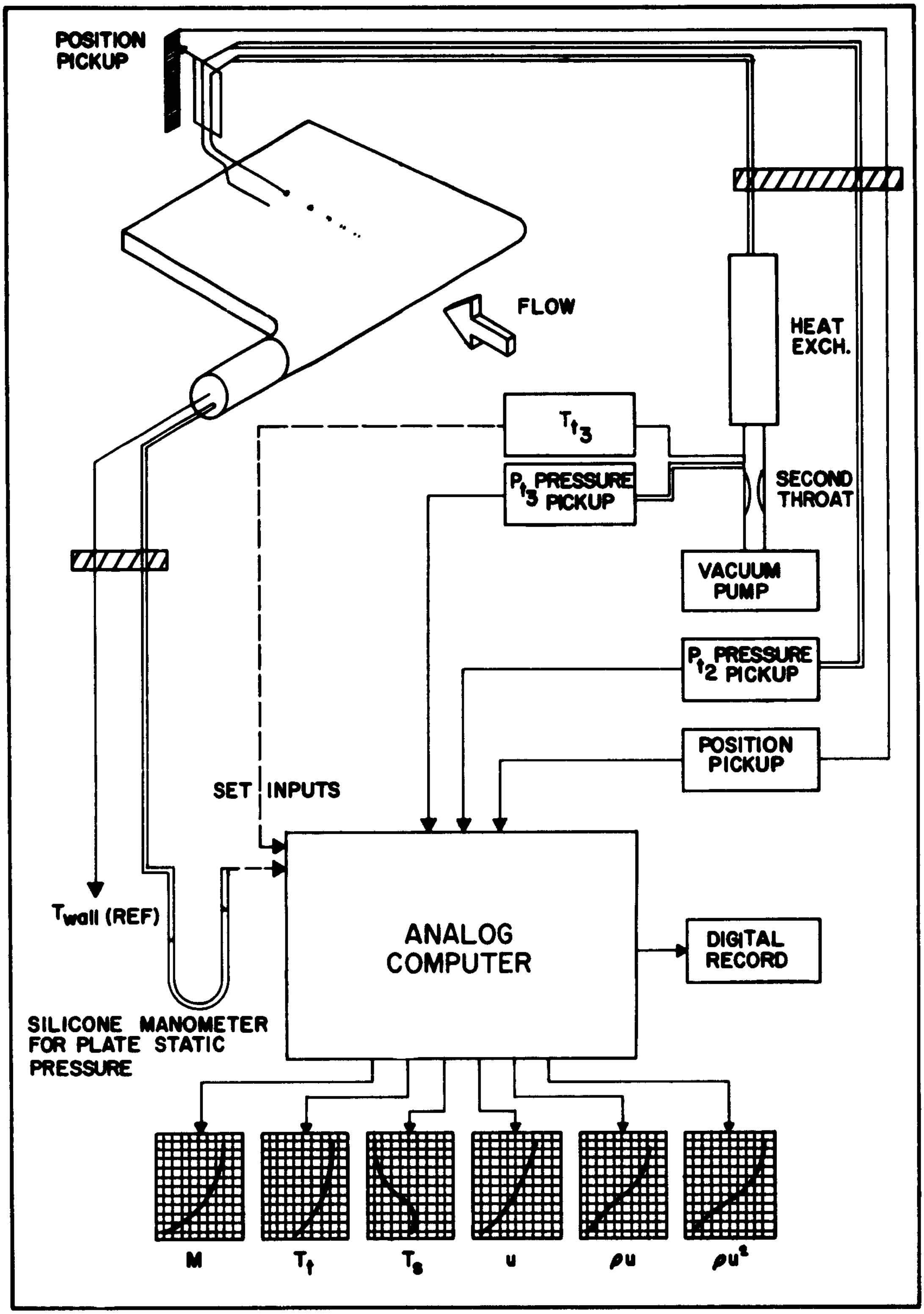

FIG. 9. SCHEMATIC OF THE PROBE SYSTEM

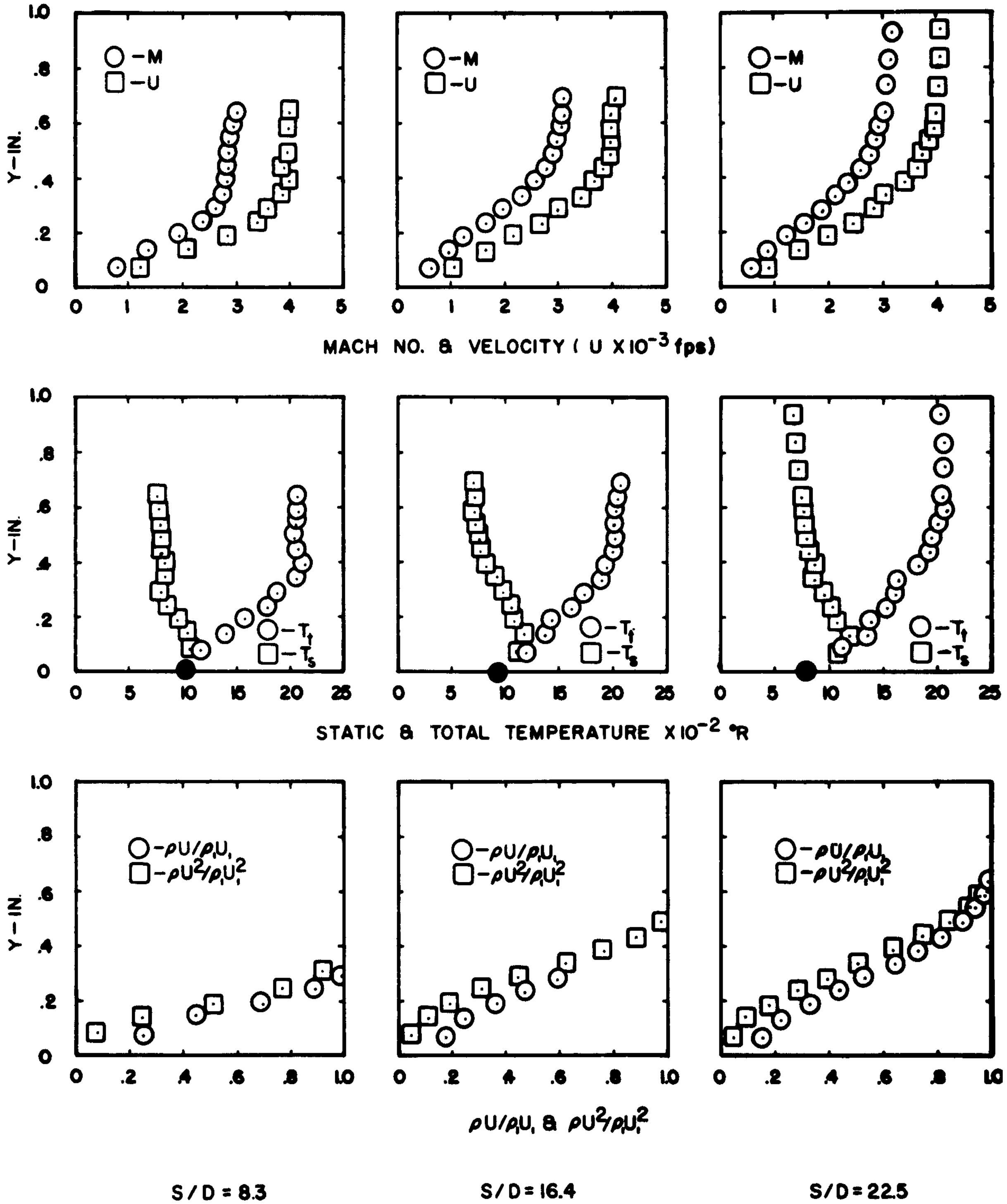

FIG. 10. BOUNDARY LAYER ON PLATE AT $\alpha = 0°$ FOR $M_\infty = 7$ AND $Re_D = 6,900$

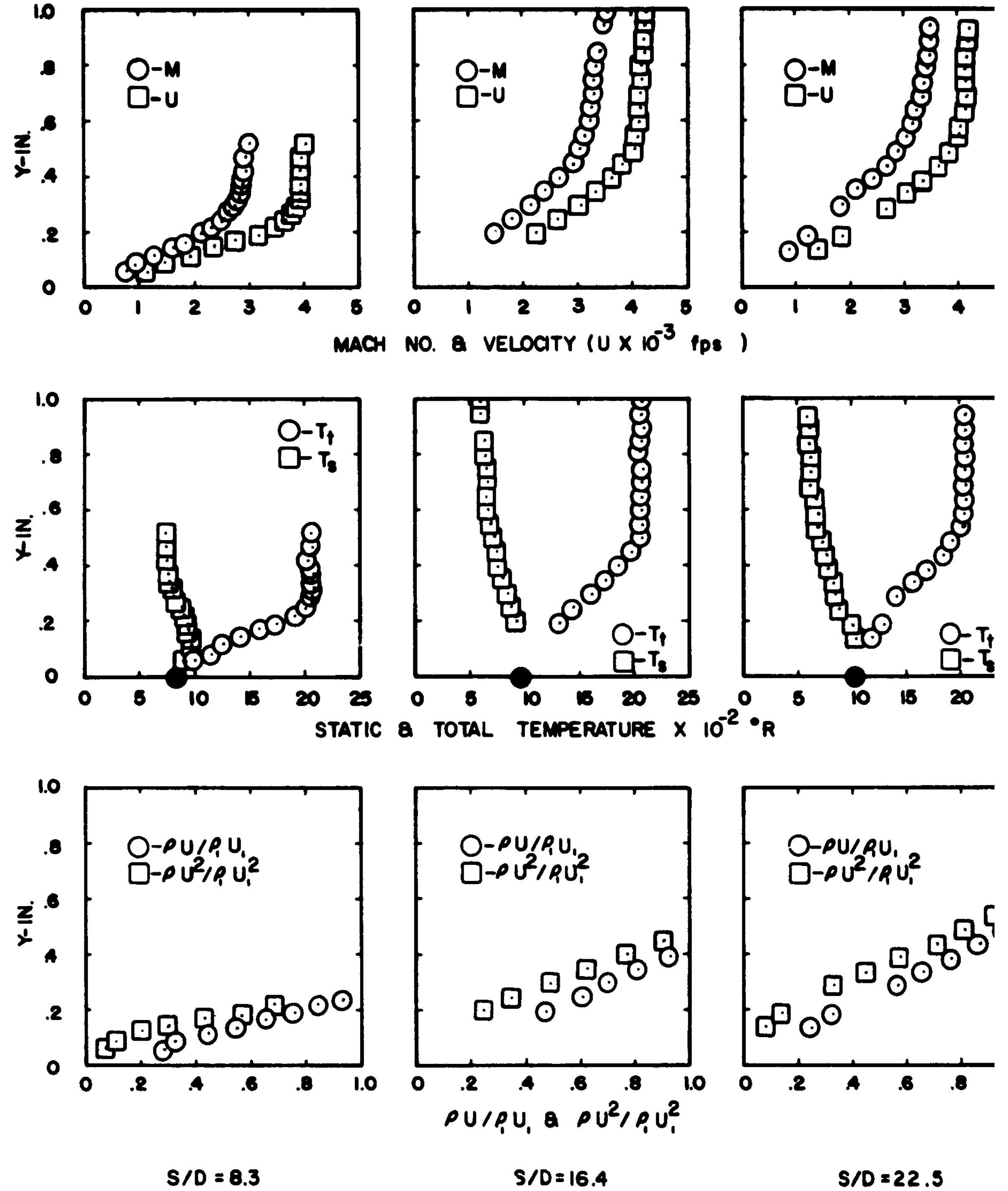

FIG. 11. BOUNDARY LAYER ON PLATE AT $\alpha = 0^\circ$ FOR $M_\infty = 10$ AND $Re_D = 11{,}000$

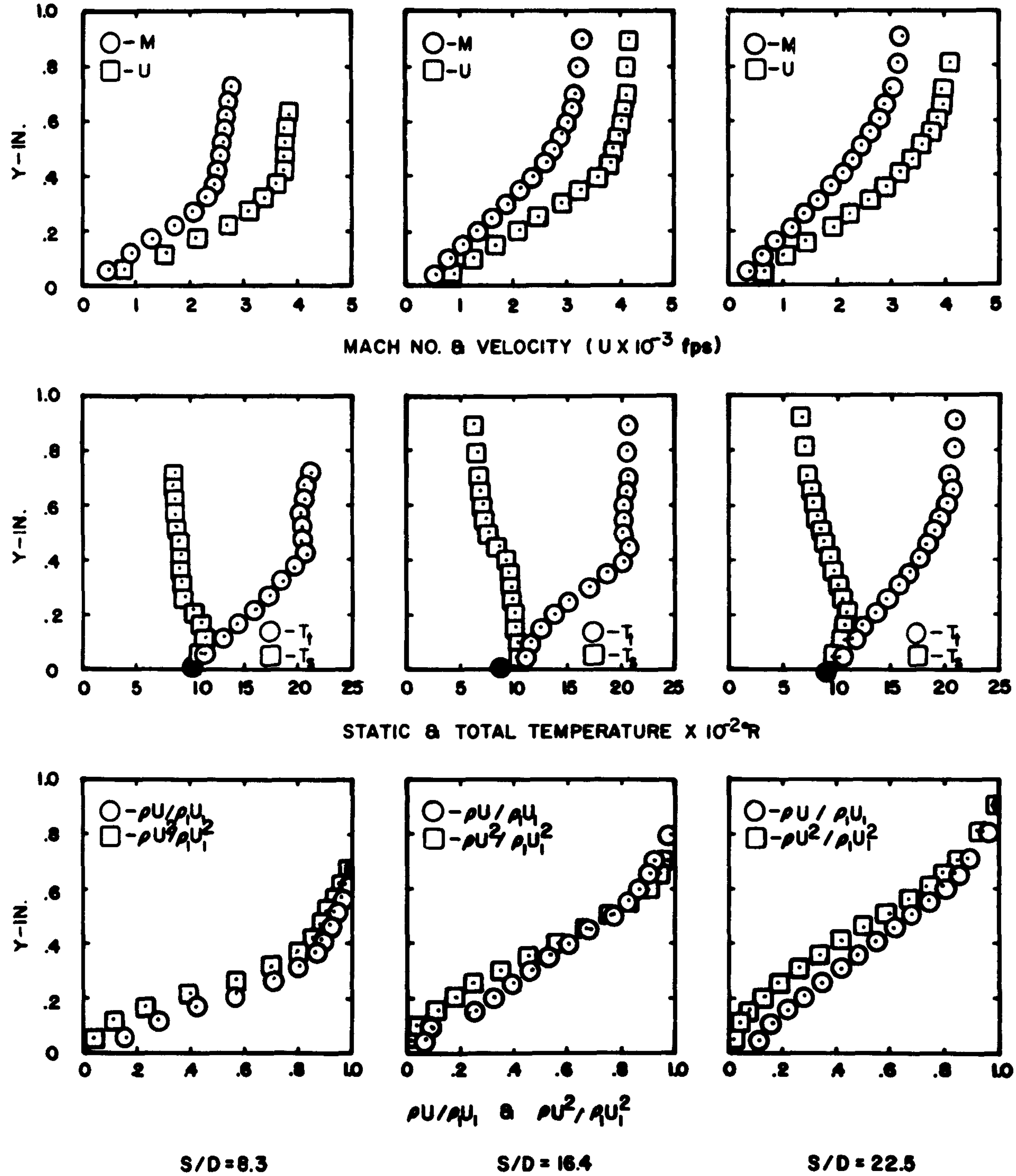

FIG. 12. BOUNDARY LAYER ON PLATE AT $\alpha = 0°$ FOR $M_\infty = 12$ AND $Re_D = 12{,}650$

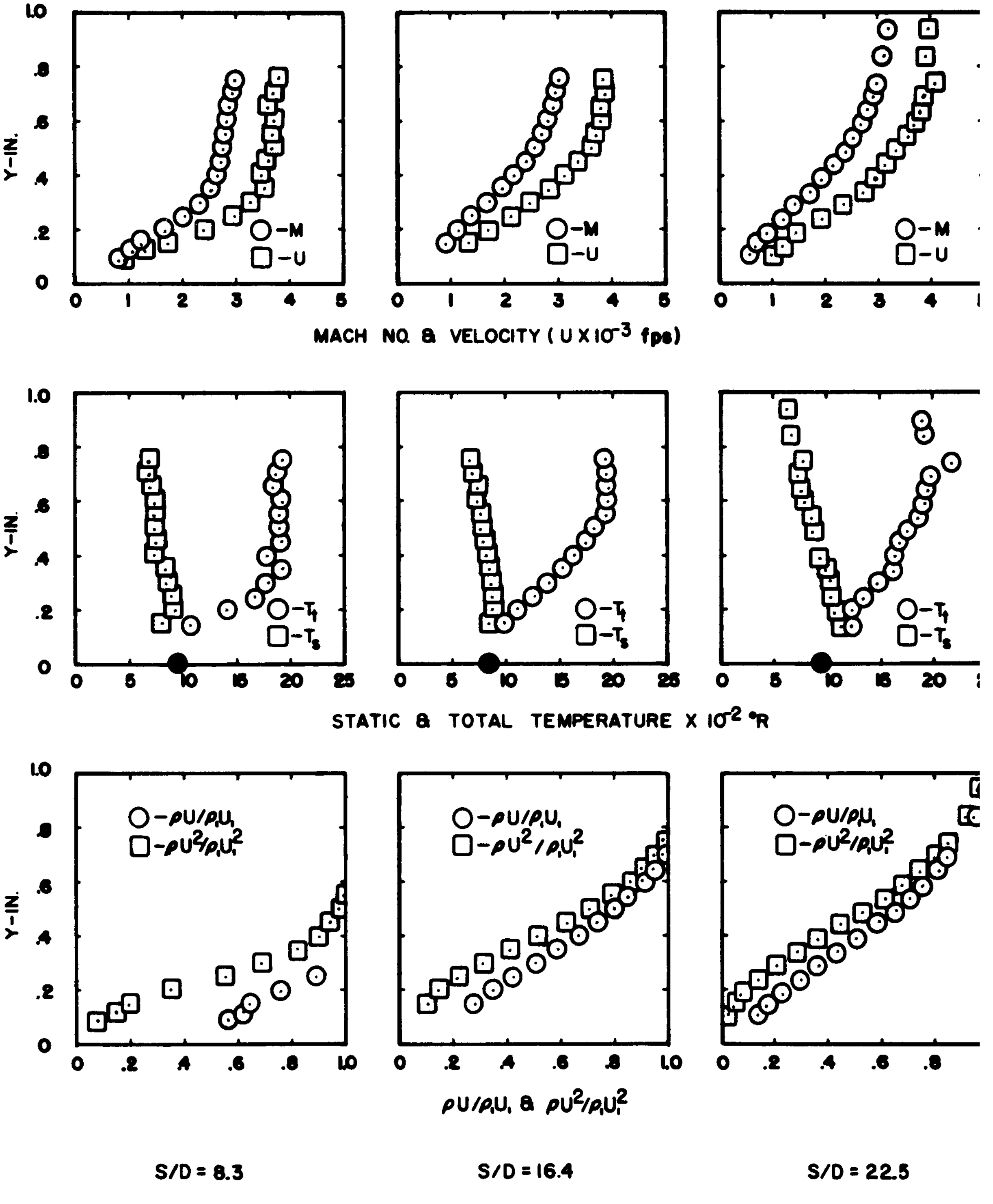

FIG. 13. BOUNDARY LAYER ON PLATE AT $\alpha = 0°$ FOR $M_\infty = 14$ AND $Re_D = 16,100$

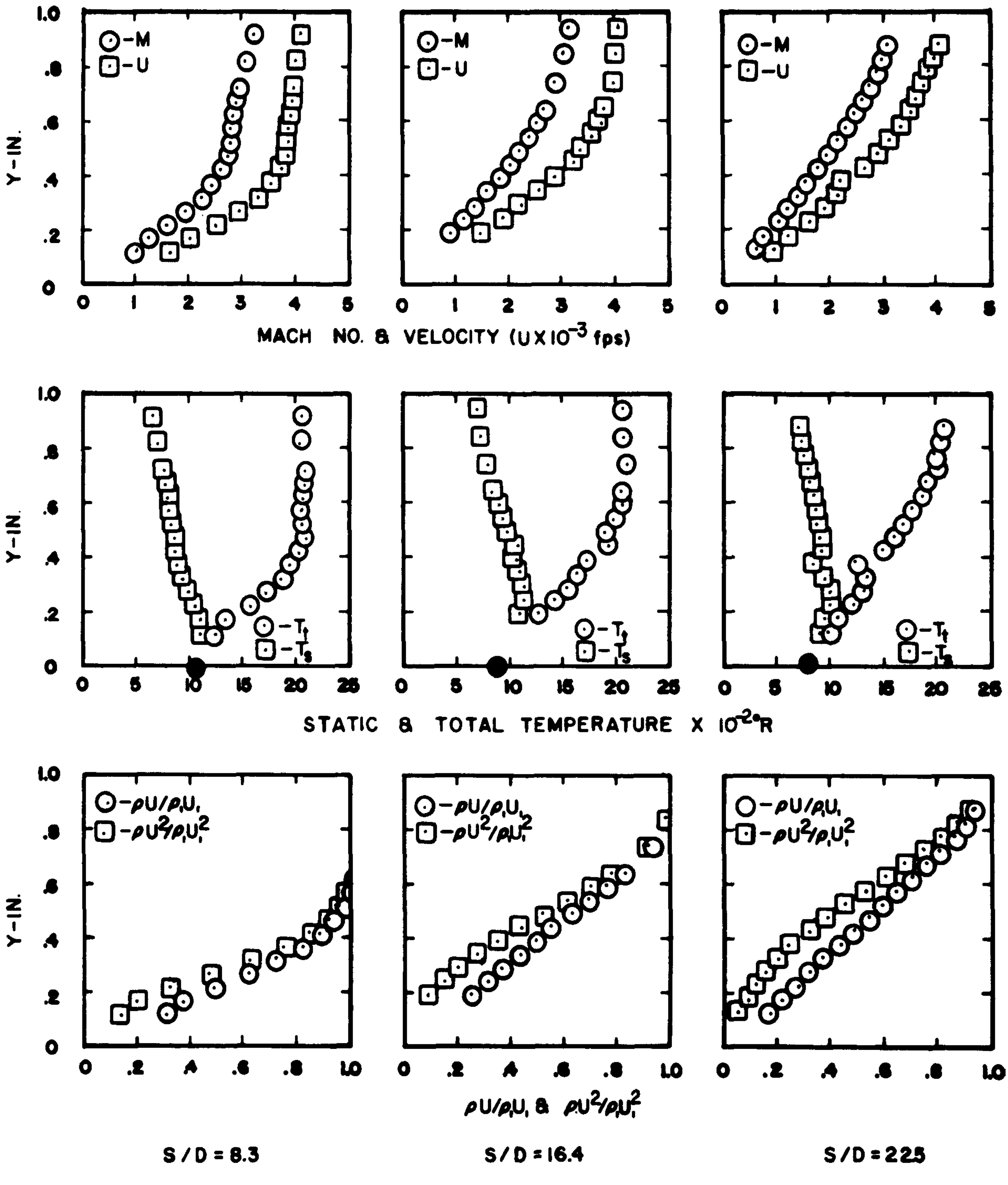

FIG. 14. BOUNDARY LAYER ON PLATE AT LOW REYNOLDS NUMBER FOR $M_\infty = 12, \alpha = 0°$, $Re_D = 8,700$

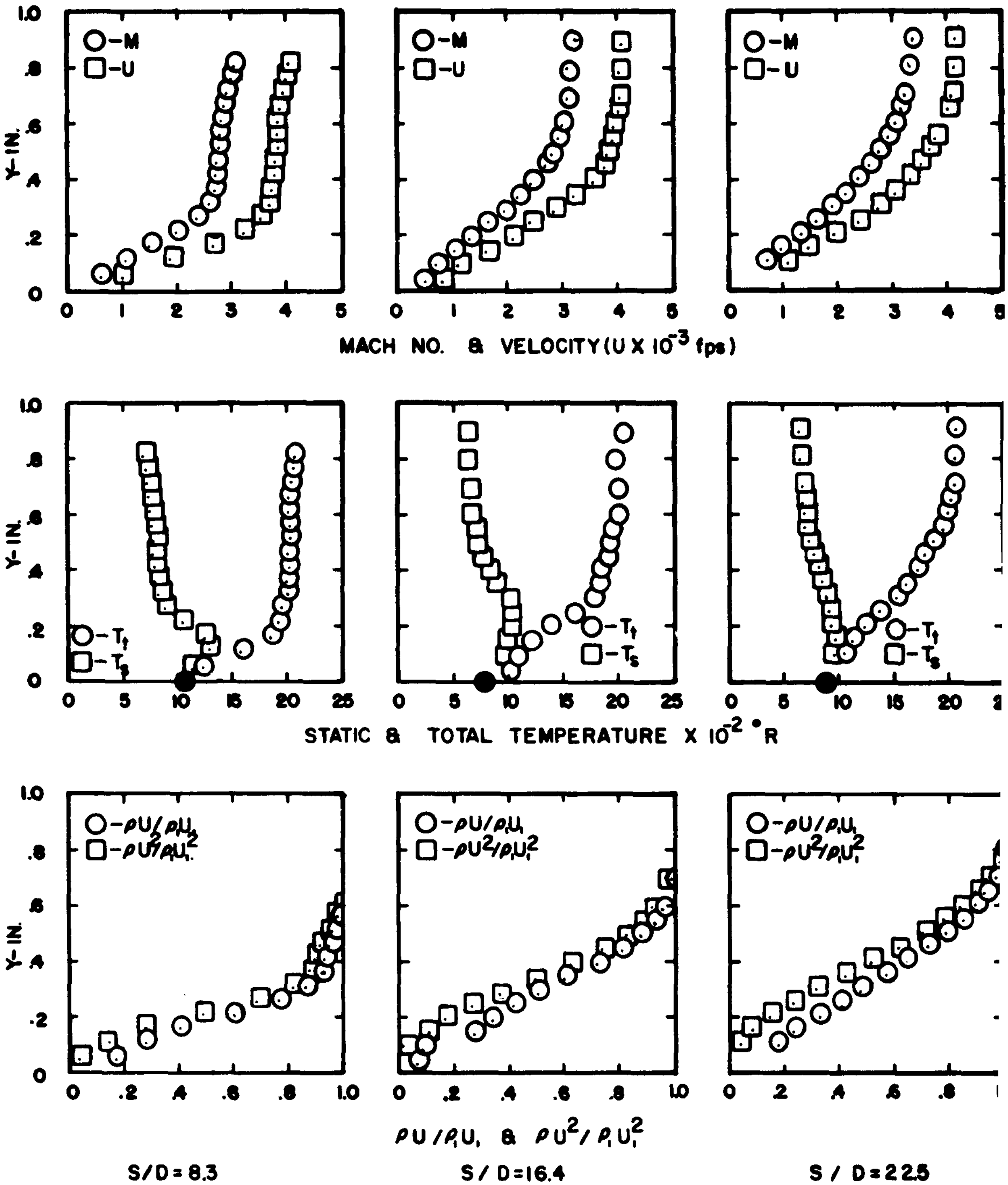

FIG. 15. BOUNDARY LAYER ON PLATE AT HIGH REYNOLDS NUMBER FOR M_∞ = 12 AND Re_D = 19,350

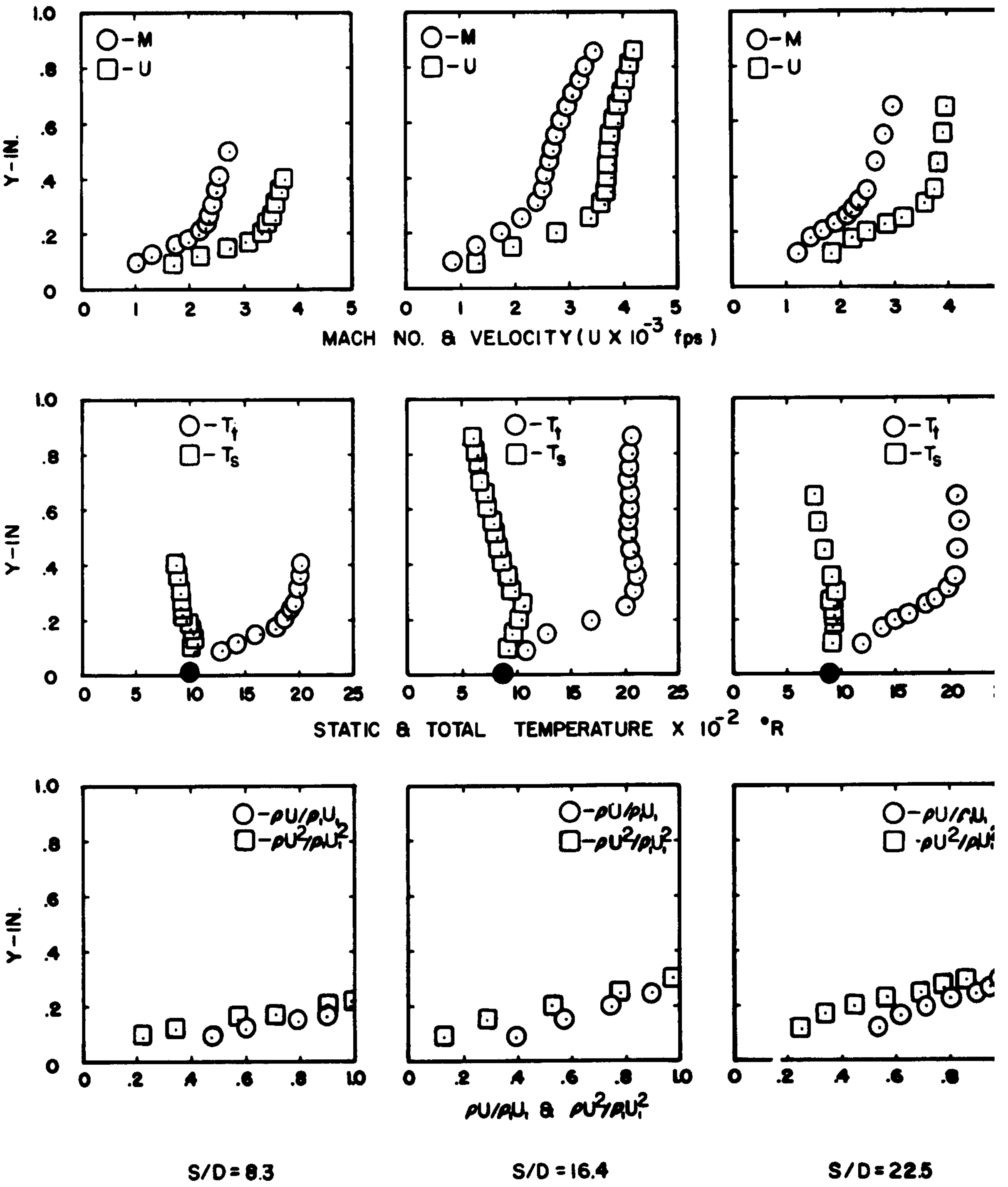

FIG. 16. BOUNDARY LAYER ON PLATE AT ANGLE OF ATTACK (10° COMP.) FOR $M_\infty = 10$ AND $Re_D = 11,000$

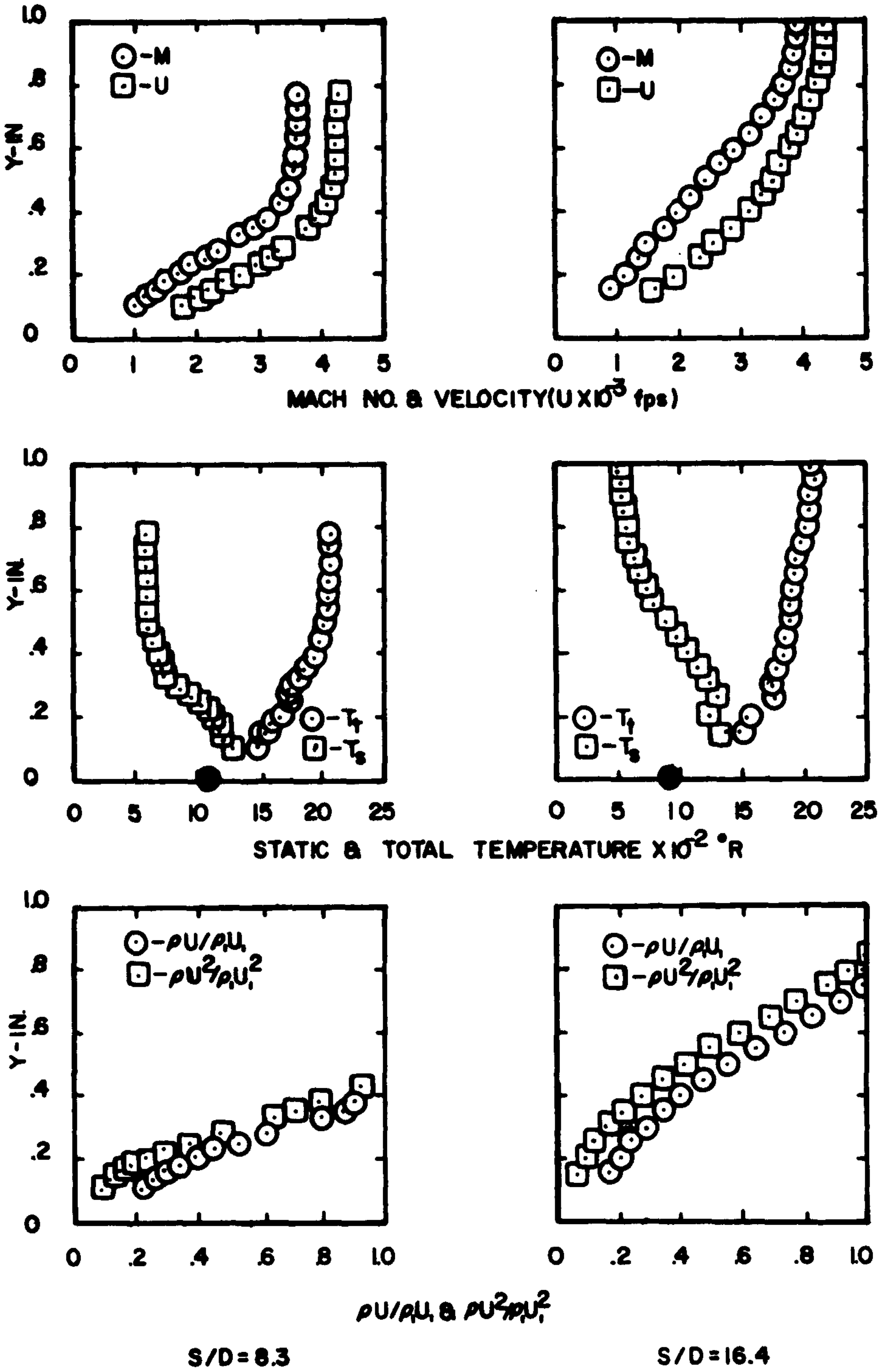

FIG. 17 BOUNDARY LAYER ON PLATE AT ANGLE OF ATTACK (15° EXP.) FOR $M_\infty = 10$ AND $Re_D = 11,000$

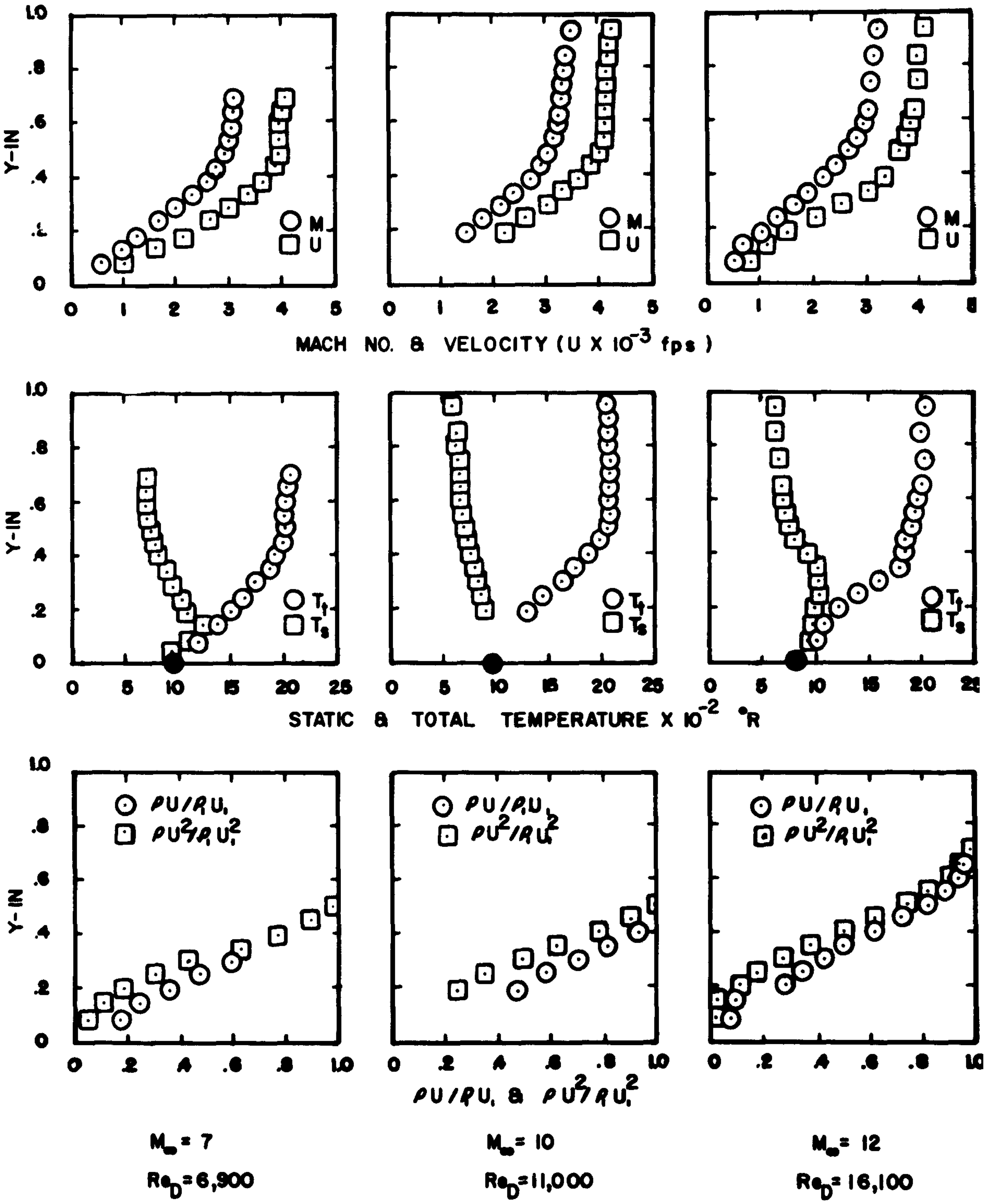

FIG. 18. EFFECT OF MACH NUMBER 7, 10, 12. ON BOUNDARY LAYER AT $\alpha = 0°$ AND S/D = 16.4

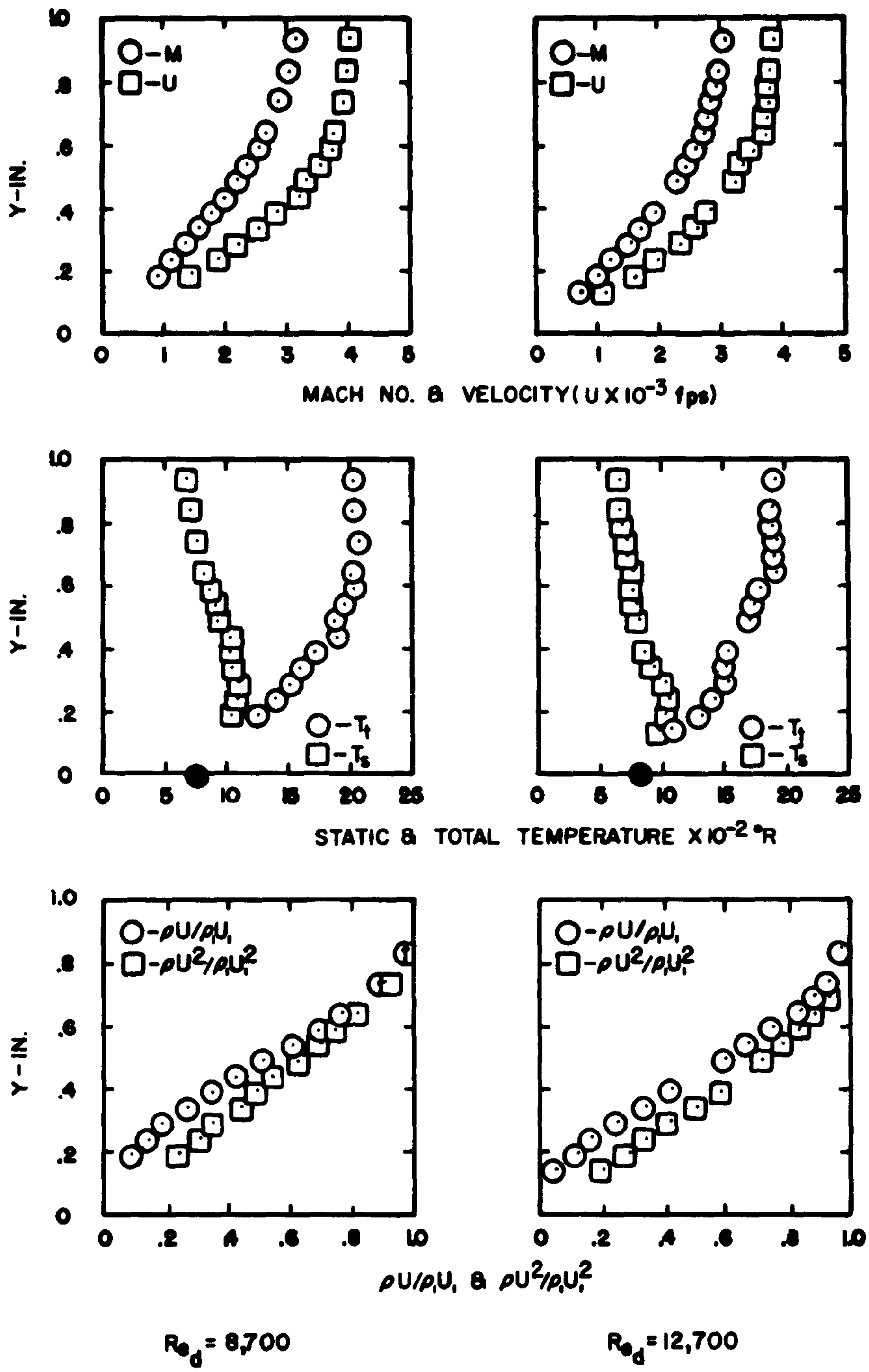

FIG. 19. EFFECT OF MACH NUMBER 12,14 ON BOUNDARY LAYER ($\alpha = 0°$) AT S/D = 16.4

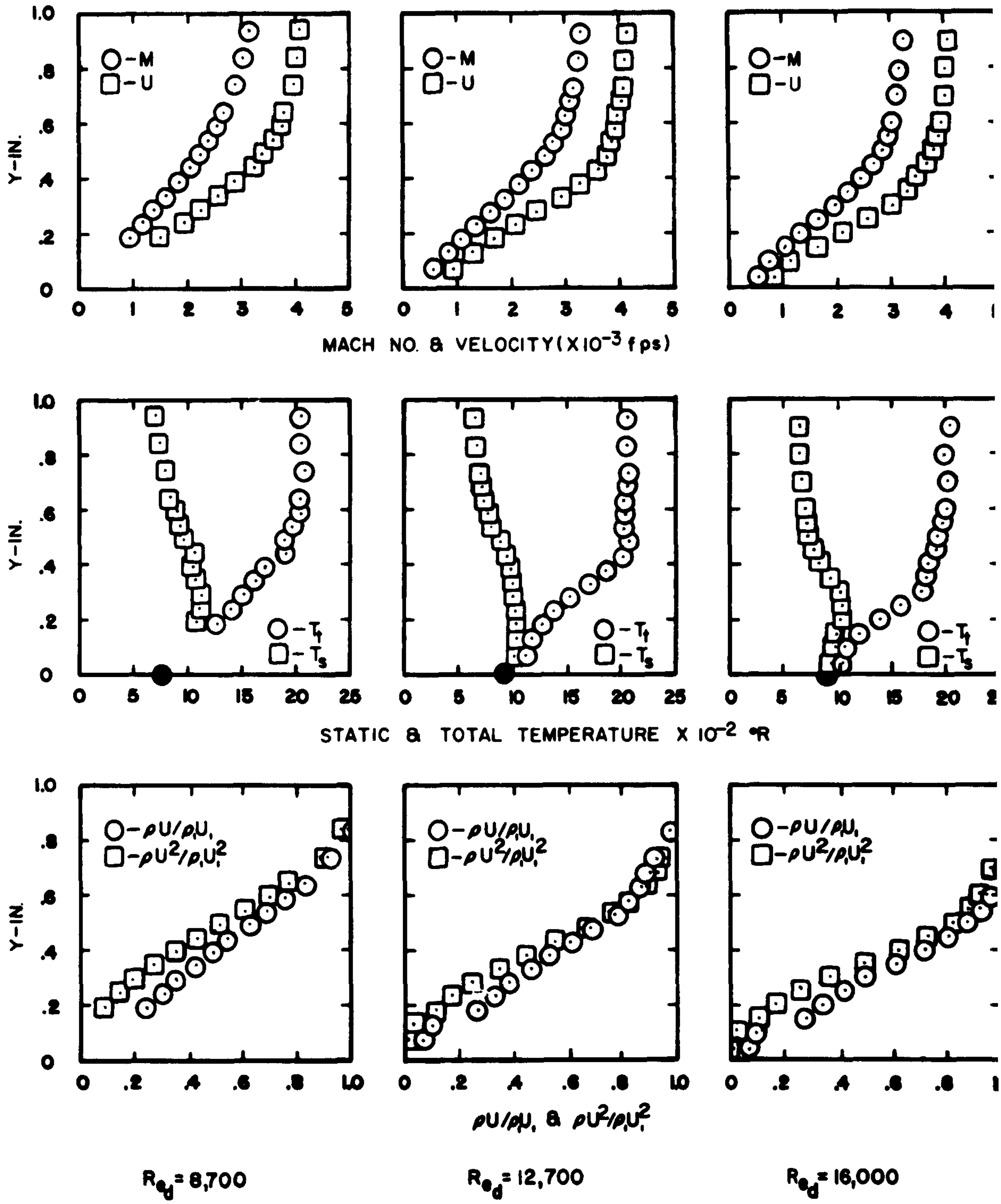

FIG. 20. EFFECT OF REYNOLDS NUMBER ON BOUNDARY LAYER AT M_∞ = 12, α = 0° AND S/D = 16.4

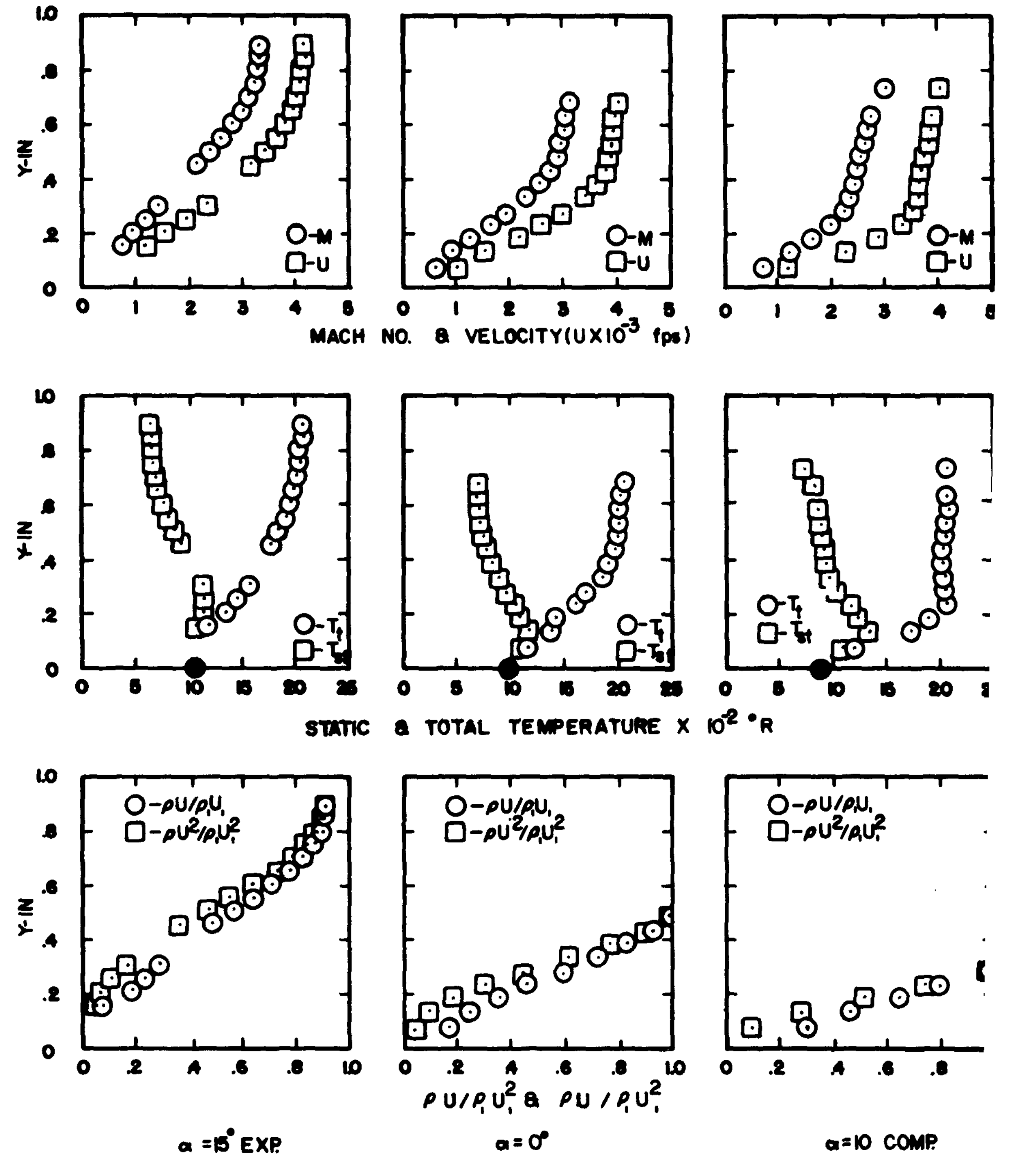

FIG. 21. EFFECT OF ANGLE OF ATTACK ON BOUNDARY LAYER AT M=7, S/D=16.4 AND Re_D =6,900

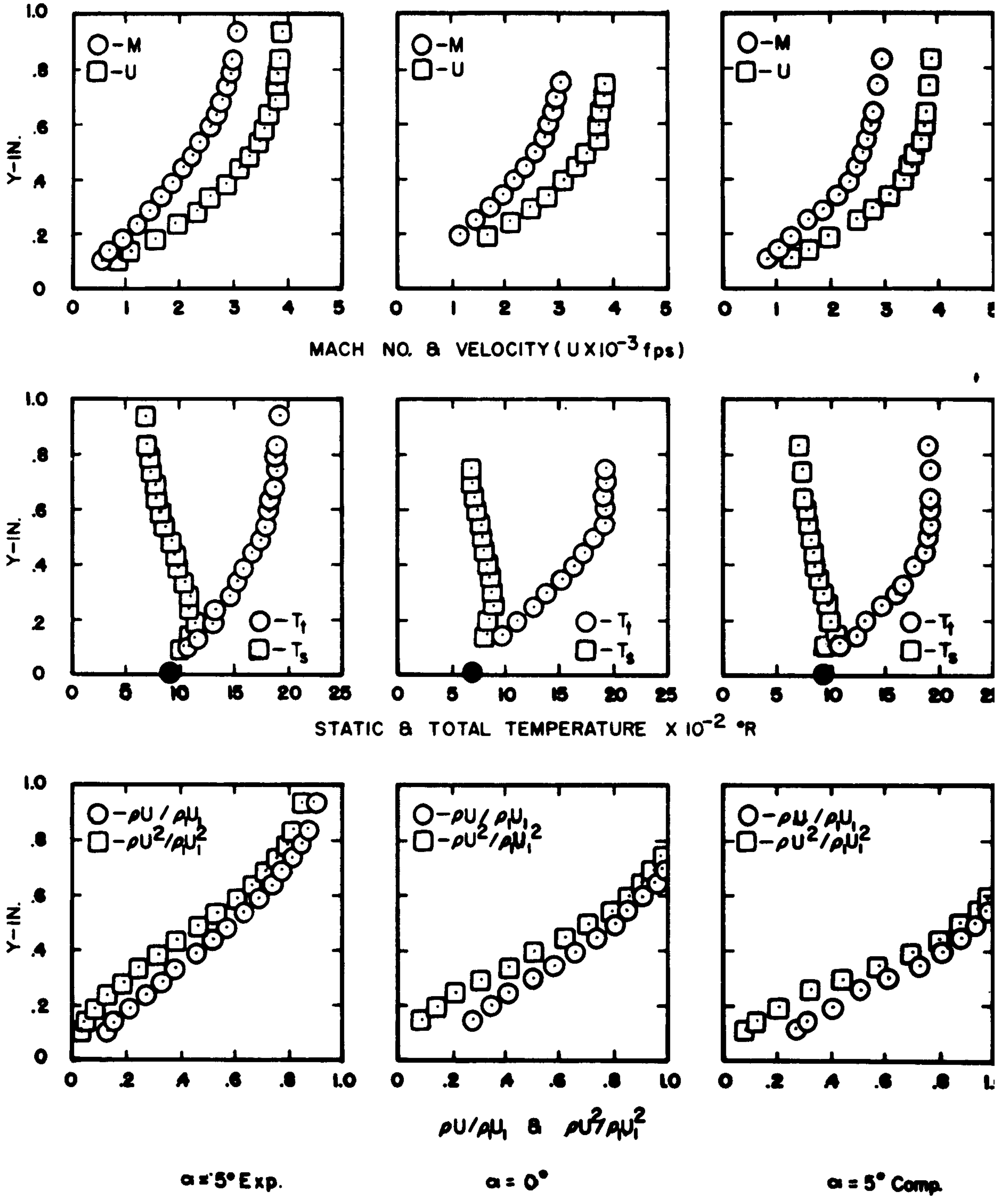

FIG. 22. EFFECT OF ANGLE OF ATTACK ON BOUNDARY LAYER AT $M = 14$, $S/D = 16.4$ AND $Re_D = 16{,}100$

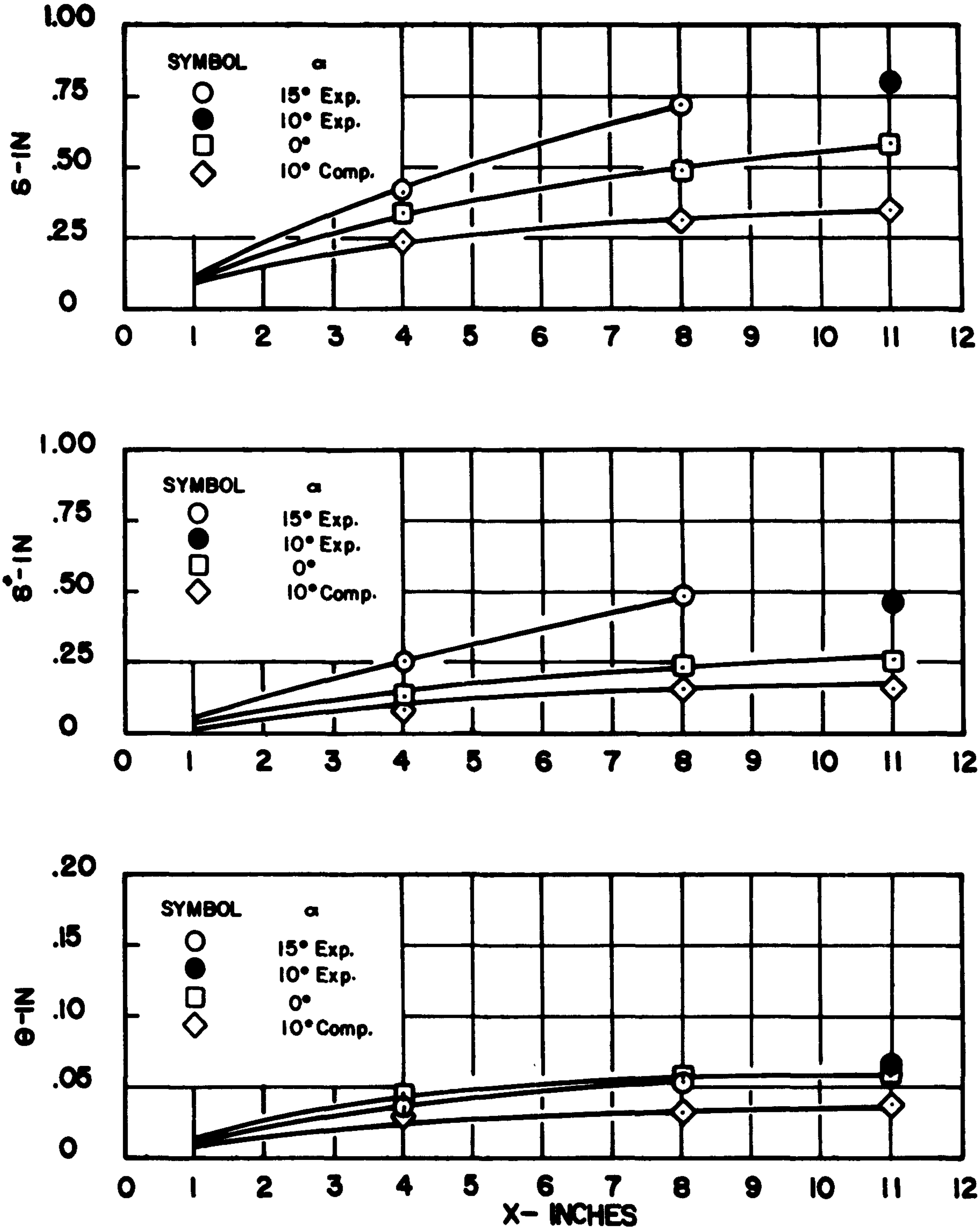

FIG. 23. BOUNDARY LAYER THICKNESSES, $M_\infty = 7$

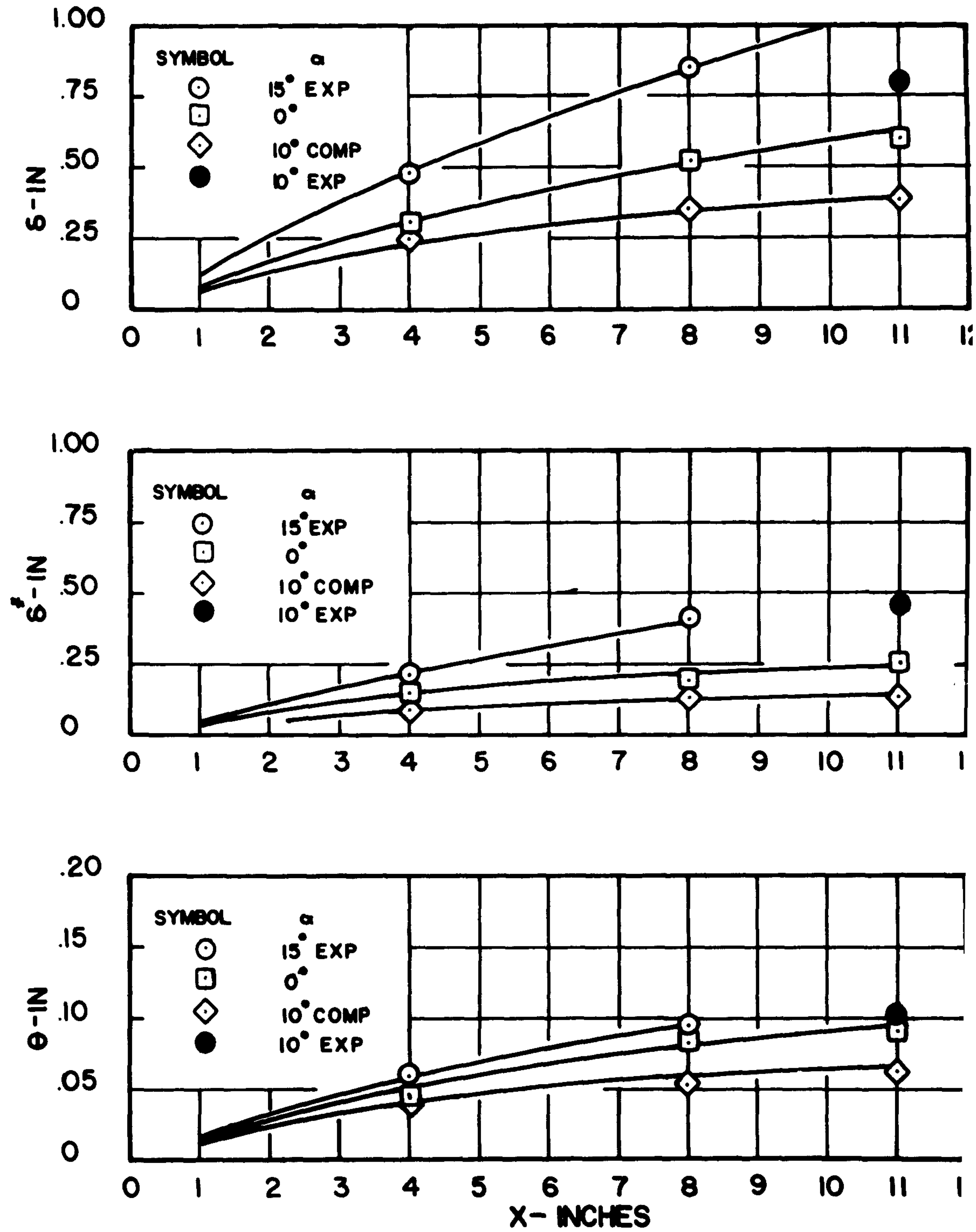

FIG. 24. BOUNDARY LAYER THICKNESSES, $M_\infty = 10$

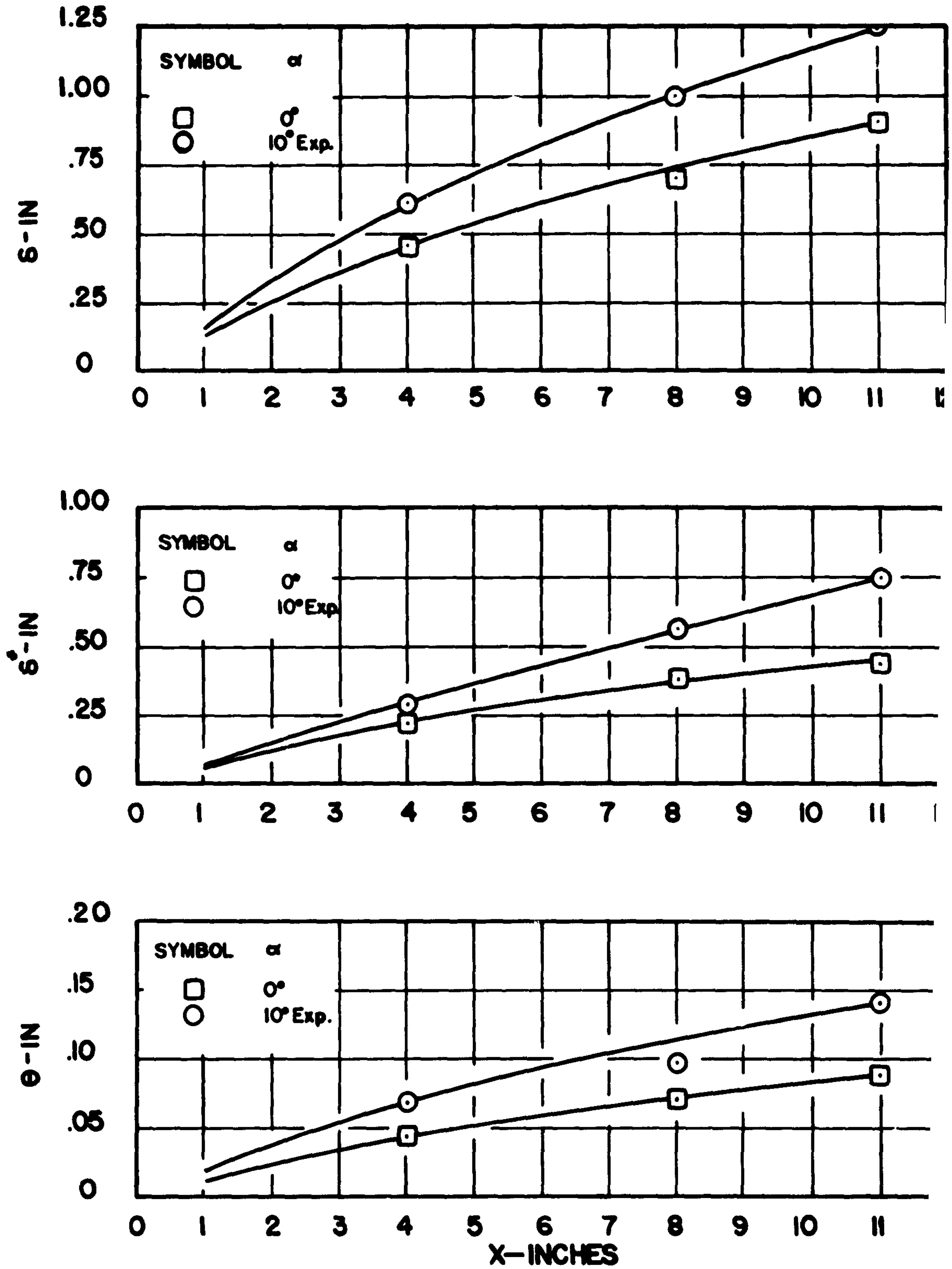

FIG. 25. BOUNDARY LAYER THICKNESSES, $M_\infty = 12$

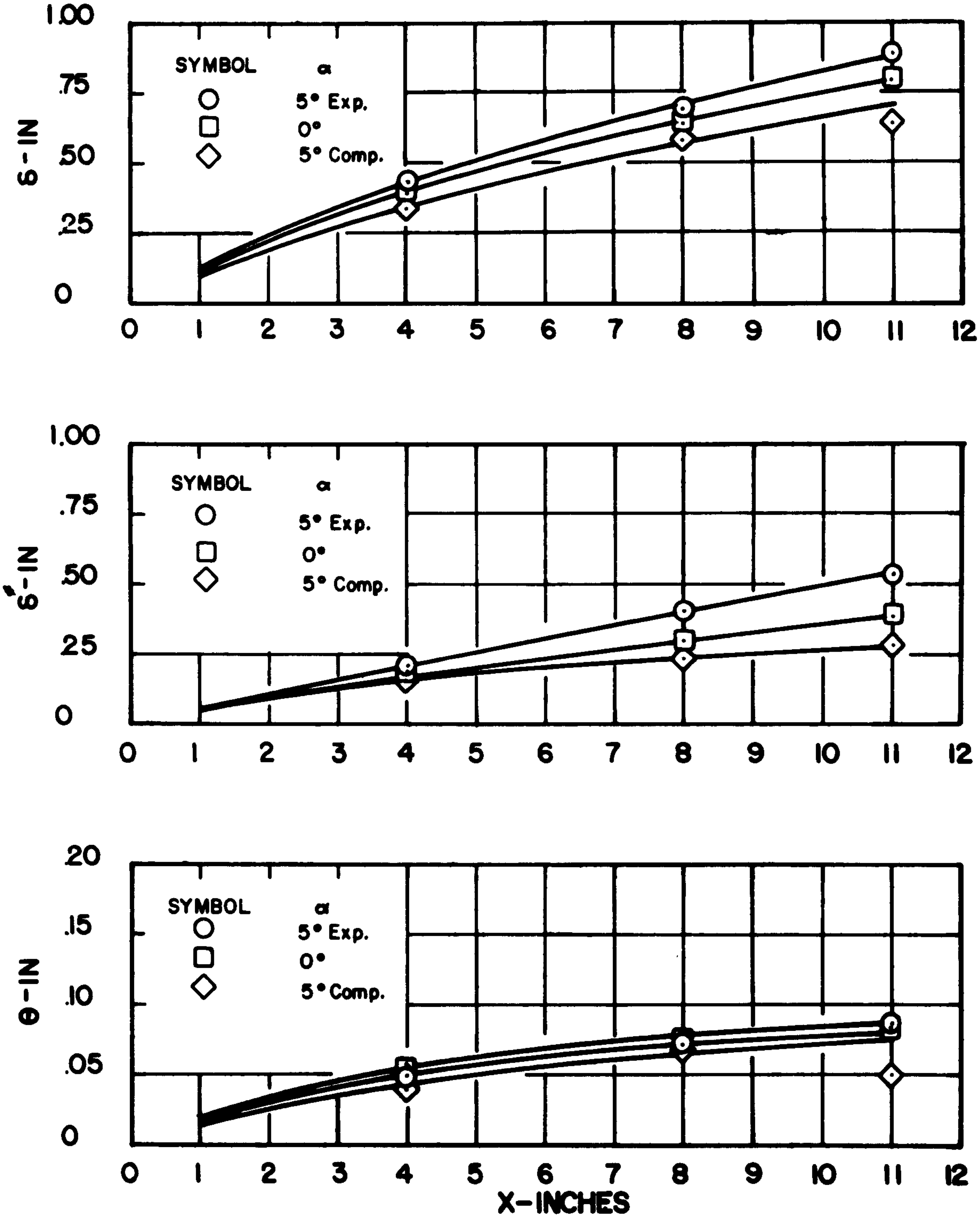

FIG. 26. BOUNDARY LAYER THICKNESSES, $M_\infty = 14$

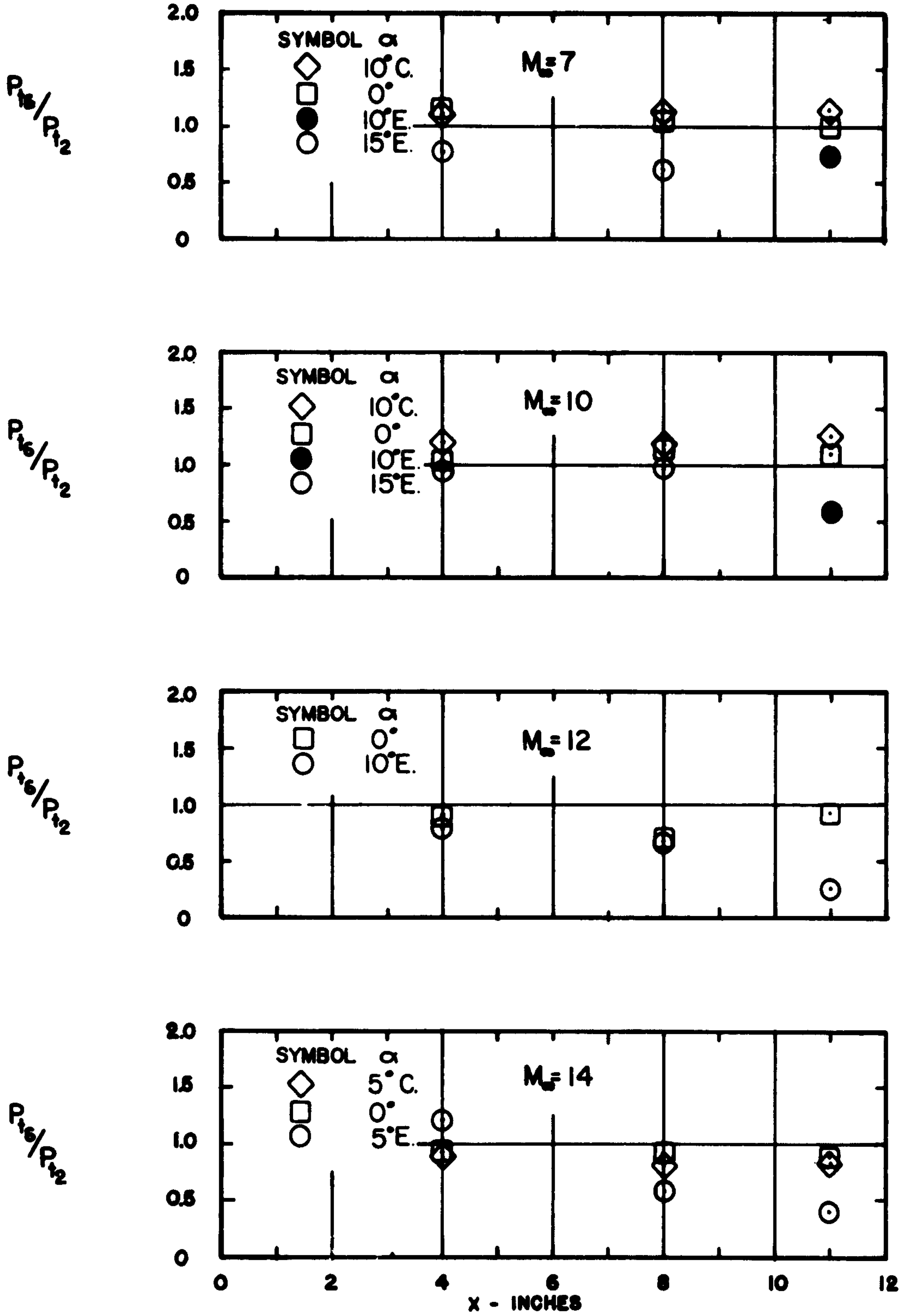

FIG. 27. STAGNATION PRESSURE RATIO VS. X

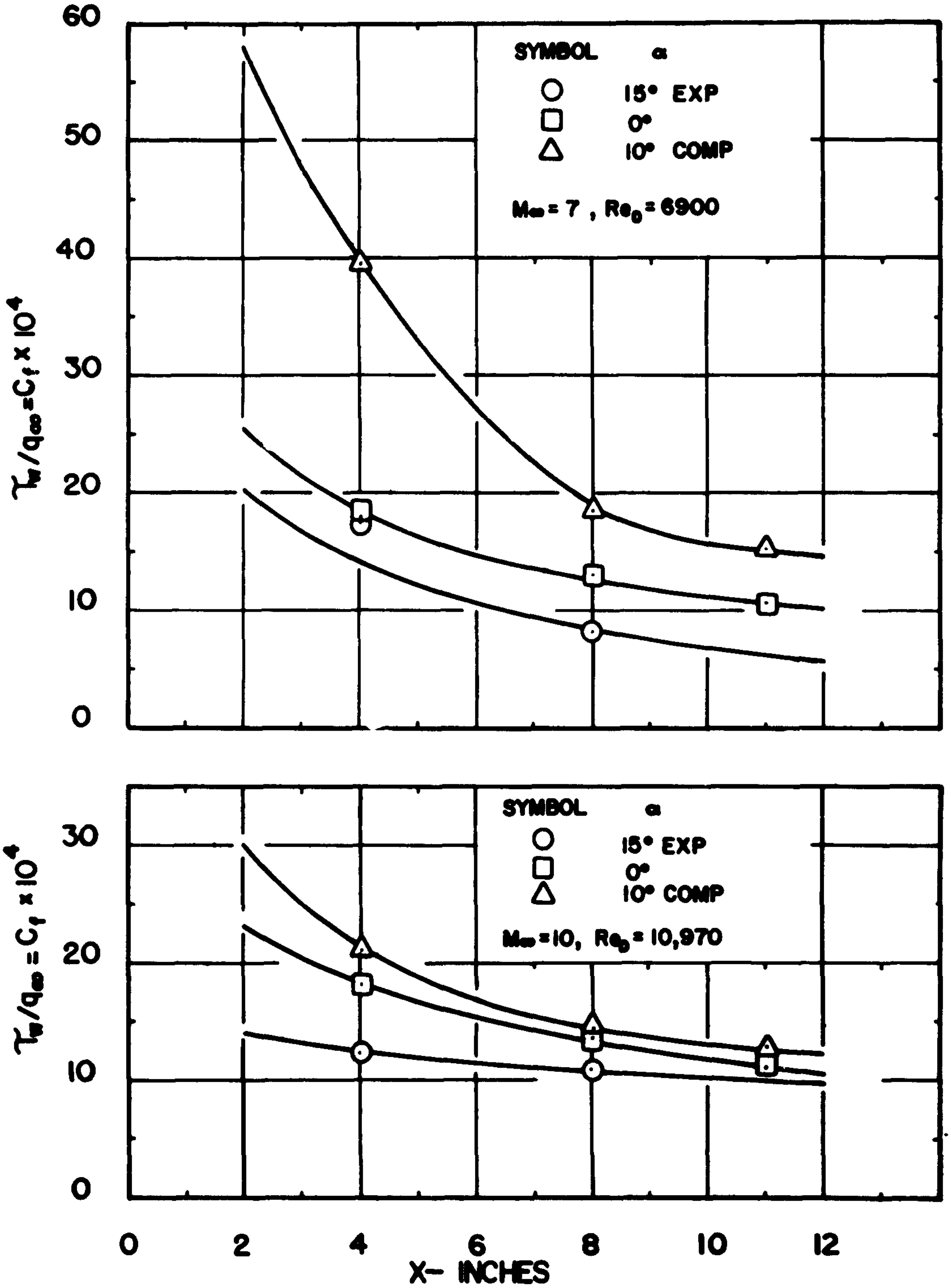

FIG. 28. SKIN FRICTION COEFFICIENT VS. X

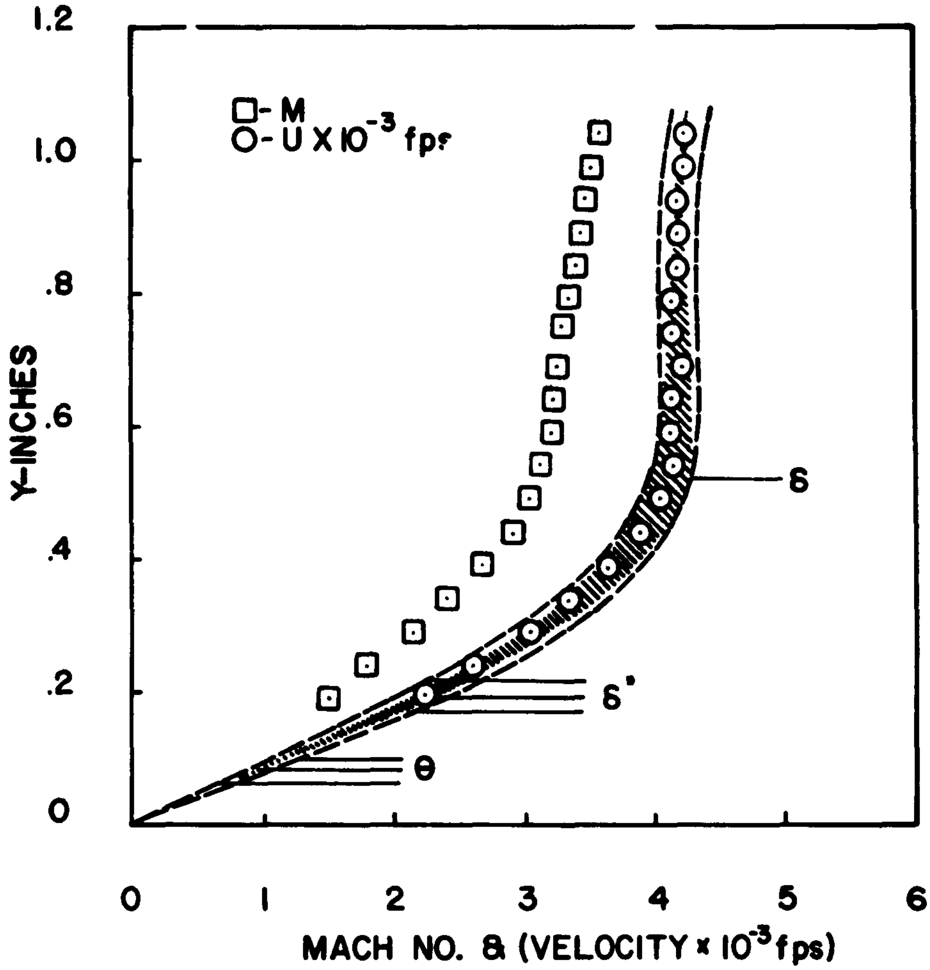

FIG. 29. ERROR ANALYSIS—MACH NO. & VELOCITY

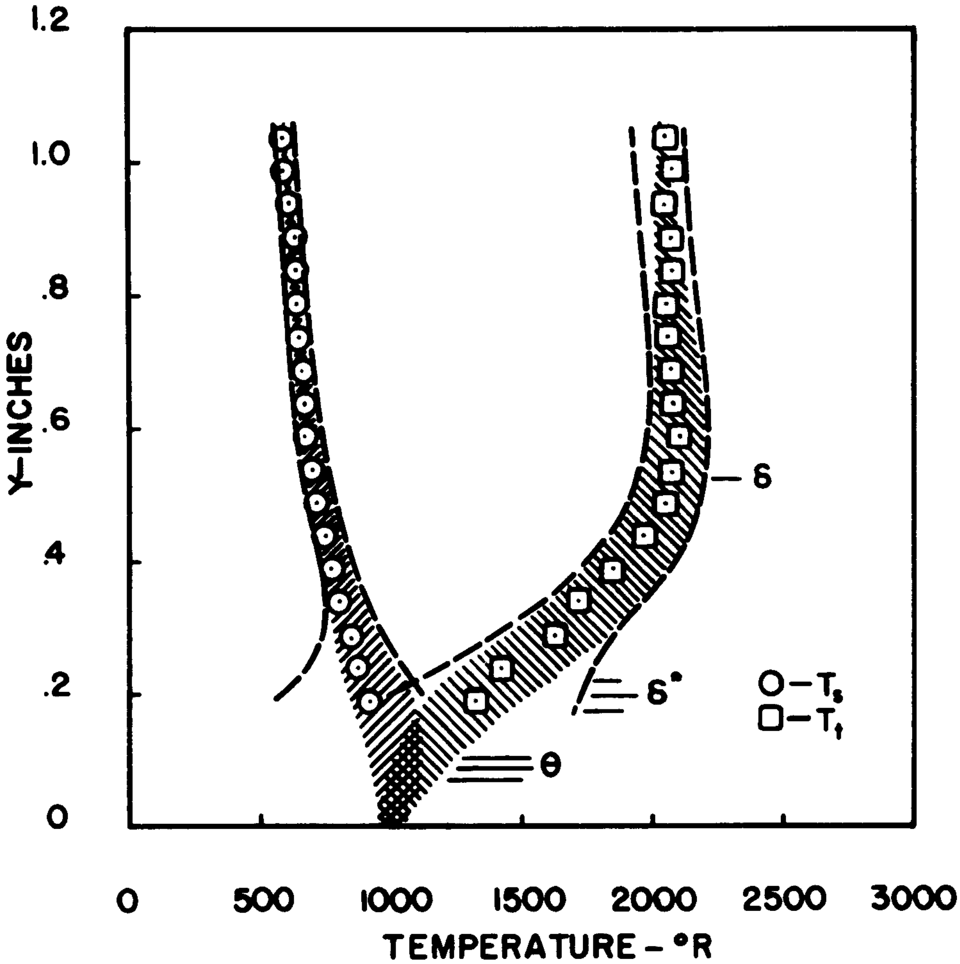

FIG. 30. ERROR ANALYSIS — STATIC & TOTAL TEMPERATURE

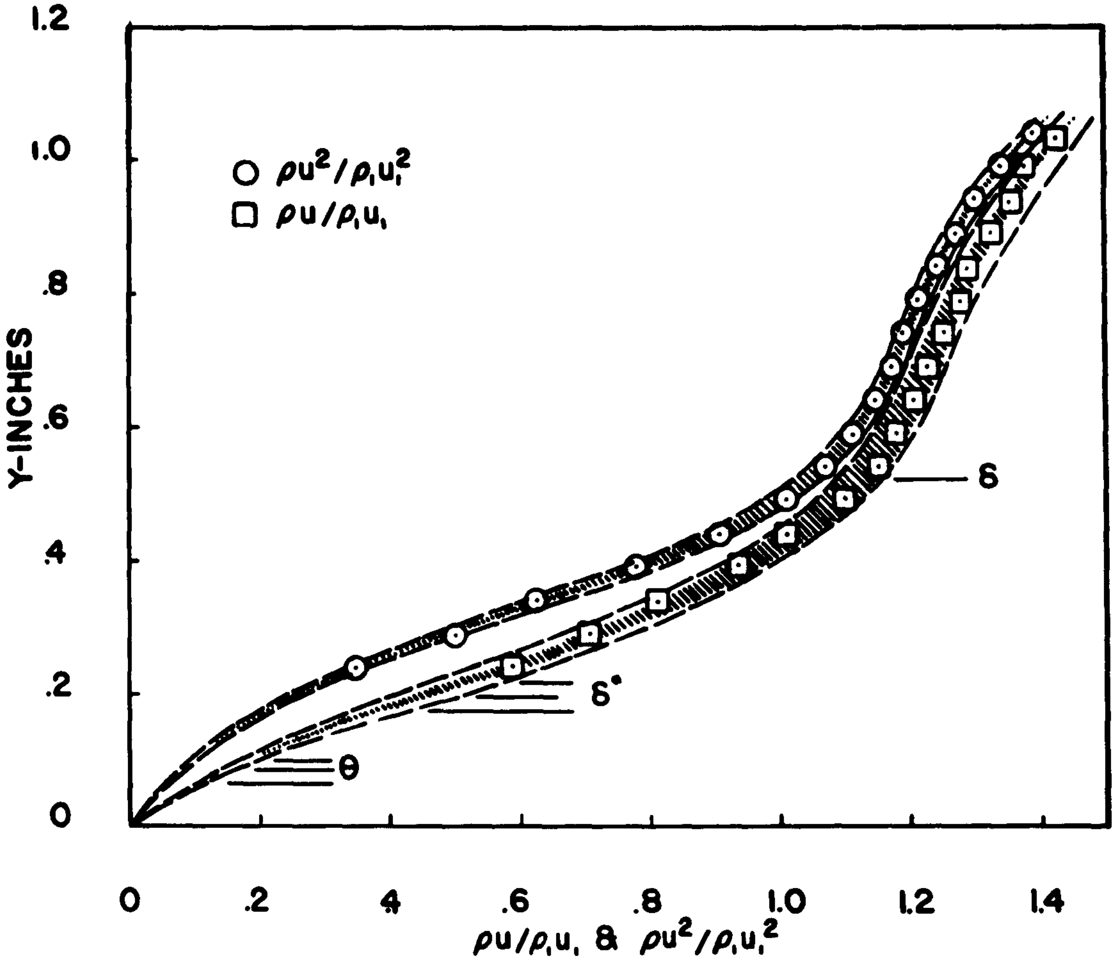

FIG. 31. ERROR ANALYSIS— $\rho u/\rho_1 u_1$ & $\rho u^2/\rho_1 u_1^2$

Aeronautical Systems Division, Dir/Aeromechanics, Flight Dynamics Lab, Wright-Patterson AFB, Ohio. Rpt Nr ASD-TDR-62-792, Vol II. AN EXPERIMENTAL INVESTIGATION OF THE SURFACE PRESSURE AND THE LAMINAR BOUNDARY LAYER ON A BLUNT FLAP PLATE IN HYPERSONIC FLOW: Laminar Boundary Layer Profiles on the Flat Plate. Final report, Mar 63, 107p. incl illus., tables, 7 refs.

Unclassified Report

The laminar boundary layer on unswept, 1/2-inch thick, cylindrically-blunted flat plate was examined at Mach numbers of 7, 10, 12 and 14; at Reynolds numbers from 9000 to 21,300, based on the plate thickness; and at angles-of-attack of 0°, 10° (compression) and 15° (expansion). The layer was probed at three stations, S/D = 8, 16 and 22 using a pitot probe and a sonic-pneumatic total temperature probe. The tests were conducted in the 12-inch

(over)

continuous hypersonic wind tunnel of The Ohio State University Aerodynamic Laboratory. The two probe outputs, together with the static pressure at the wall, were processed through an analogue computer and the results, i.e., Mach number, velocity, temperature, etc., are tabulated as functions of distance from the surface. Integrations were performed to obtain displacement and momentum thicknesses. Skin friction was also obtained, through the measurement of the velocity gradient at the wall. The results are presented in tabulated form, while typical data are plotted to illustrate the trends established by Mach number, Reynolds number and angle-of-attack.

1. Hypersonic boundary layer
2. Compressible flow
3. Hypersonic wind tunnels
4. Laminar boundary layer

I. AFSC Project 1366, Task 136606
II. Contract AF 33(616)-7827
III. Ohio State University, Columbus, Ohio
IV. G. M. Gergorek, T. C. Mark, J. D. Lee
V. Aval fr OTS
VI. In ASTIA collection

Aeronautical Systems Division, Dir/Aeromechanics, Flight Dynamics Lab, Wright-Patterson AFB, Ohio. Rpt Nr ASD-TDR-62-792, Vol II. AN EXPERIMENTAL INVESTIGATION OF THE SURFACE PRESSURE AND THE LAMINAR BOUNDARY LAYER ON A BLUNT FLAP PLATE IN HYPERSONIC FLOW: Laminar Boundary Layer Profiles on the Flat Plate. Final report, Mar 63, 107p. incl illus., tables, 7 refs.

Unclassified Report

The laminar boundary layer on unswept, 1/2-inch thick, cylindrically-blunted flat plate was examined at Mach numbers of 7, 10, 12 and 14; at Reynolds numbers from 9000 to 21,300, based on the plate thickness; and at angles-of-attack of 0°, 10° (compression) and 15° (expansion). The layer was probed at three stations, S/D = 8, 16 and 22 using a pitot probe and a sonic-pneumatic total temperature probe. The tests were conducted in the 12-inch

(over)

continuous hypersonic wind tunnel of The Ohio State University Aerodynamic Laboratory. The two probe outputs, together with the static pressure at the wall, were processed through an analogue computer and the results, i.e., Mach number, velocity, temperature, etc., are tabulated as functions of distance from the surface. Integrations were performed to obtain displacement and momentum thicknesses. Skin friction was also obtained, through the measurement of the velocity gradient at the wall. The results are presented in tabulated form, while typical data are plotted to illustrate the trends established by Mach number, Reynolds number and angle-of-attack.

1. Hypersonic boundary layer
2. Compressible flow
3. Hypersonic wind tunnels
4. Laminar boundary layer

I. AFSC Project 1366, Task 136606
II. Contract AF 33(616)-7827
III. Ohio State University, Columbus, Ohio
IV. G. M. Gergorek, T. C. Mark, J. D. Lee
V. Aval fr OTS
VI. In ASTIA collection